

# Development of Delaware's First "Smart Bridge"

by

NICOLE READER  
MICHAEL J. CHAJES  
HARRY W. SHENTON, III

Department of Civil and Environmental Engineering  
College of Engineering  
University of Delaware

October 2007

Delaware Center for Transportation  
University of Delaware  
355 DuPont Hall  
Newark, Delaware 19716  
(302) 831-1446



# **Development of Delaware’s First “Smart Bridge”**

**By**

**Nicole Reader  
Michael J. Chajes  
Harry W. Shenton, III**

**Department of Civil and Environmental Engineering  
College of Engineering  
University of Delaware**

**DELAWARE CENTER FOR TRANSPORTATION  
University of Delaware  
Newark, Delaware 19716**

*This work was sponsored by the Delaware Center for Transportation and was prepared in cooperation with the Delaware Department of Transportation. The contents of this report reflect the views of the authors who are responsible for the facts and accuracy of the data presented herein. The contents do not necessarily reflect the official views of the Delaware Center for Transportation or the Delaware Department of Transportation at the time of publication. This report does not constitute a standard, specification, or regulation.*

The Delaware Center for Transportation is a university-wide multi-disciplinary research unit reporting to the Chair of the Department of Civil and Environmental Engineering, and is co-sponsored by the University of Delaware and the Delaware Department of Transportation.

### **DCT Staff**

Ardeshir Faghri  
*Director*

Jerome Lewis  
*Associate Director*

Ellen M. Pletz  
*Assistant to the Director*

Lawrence H. Klepner  
*T<sup>2</sup> Program Coordinator*

Matheu J. Carter  
*T<sup>2</sup> Engineer*

Sandra Wolfe  
*Secretary*

### **DCT Policy Council**

Robert Taylor, Co-Chair  
*Chief Engineer, Delaware Department of Transportation*

Michael Chajes, Co-Chair  
*Dean, College of Engineering*

The Honorable Tony DeLuca  
*Chair, Delaware Senate Transportation Committee*

The Honorable Richard Cathcart  
*Chair, Delaware House of Representatives Transportation Committee*

Timothy K. Barnekov  
*Dean, College of Human Resources, Education and Public Policy*

Harry Shenton  
*Chair, Civil and Environmental Engineering*

Ralph A. Reeb  
*Director of Planning, Delaware Department of Transportation*

Stephen Kingsberry  
*Director, Delaware Transit Corporation*

Shannon Marchman  
*Representative of the Director of the Delaware Development Office*

Roger Roy  
*Representative, Transportation Management Association*

Jim Johnson  
*Executive Director, Delaware River & Bay Authority*

*Delaware Center for Transportation  
University of Delaware  
Newark, DE 19716  
(302) 831-1446*

# Development of Delaware's First "Smart Bridge"

by Nicole Reader, Michael Chajes, and Harry Shenton



October 2007

## **Executive Summary**

Bridges are a vital link in the nation's highway system. They also represent a tremendous investment for the owner. Therefore, it is necessary to have a system for maintaining and ensuring the reliability of these important structures. The Federal Highway Administration's Long-Term Bridge Performance Program (LTBPP), still in the planning phase at the time of this report, will consist of efficient maintenance and structural health monitoring (SHM) strategies for bridges across the nation. One of the SHM technologies being implemented in the program is permanently instrumented bridges. The project discussed in this paper is Delaware's first permanently instrumented bridge, and it provides a prototype for future permanently instrumented bridges for the LTBPP. This project also serves as a building block for a larger permanent instrumentation system that will be installed on the replacement Indian River Inlet Bridge.

For this project, which was the master's thesis work for a student at the University of Delaware, a three-span continuous slab-on-girder composite bridge was permanently instrumented with 61 gages. The gages consisted of foil and vibrating wire strain gages, accelerometers, string pots, resistance temperature detectors (RTDs), and thermocouples.

The body of this report is the student's thesis. It is organized as follows:

Chapter 1 provides the motivation for the project, explains the Long-Term Bridge Performance Program, and describes the Indian River Inlet Bridge, which is planned to incorporate a long-term structural health monitoring system to aid DelDOT in maintenance and operation of the signature structure. The plan is for the system to monitor the response in the bridge both during construction and under normal operation.

Chapter 2 provides background information on long-term monitoring systems and provides a brief review of the literature on projects where such systems have been implemented.

Chapter 3 discusses selection of the bridge to be instrumented and provides details about the bridge. Located on I-495 over Edgemoor Road north of Wilmington, Bridge 1-821 was chosen as the best candidate for Delaware's first "Smart Bridge." This slab-on-steel-girder bridge is similar to many of the bridges in Delaware and throughout the nation and therefore serves as a good prototype for other instrumented bridges. The ADT and ADTT are relatively high on Bridge 1-821 and will give substantial amounts of data. There is a service road that runs along Edgemoor Road under the bridge, which allowed for easy access when instrumenting the bridge. Bridge 1-821 is also located less than twenty miles from the University of Delaware, which makes maintenance and monitoring of the system easy.

Chapter 4 discusses the diagnostic tests, which included a static test and an ambient vibration test conducted during the preliminary planning for the permanent instrumentation. It was important to test the bridge prior to instrumentation to better understand its response, to calibrate a numerical model, and to make final decisions on sensors and sensor locations. A static diagnostic test was run in the summer of 2004, and a dynamic diagnostic test was run in the summer of 2006.

Chapter 5 discusses the finite element model. Having an accurate finite element model of the bridge has been useful in several aspects of the project thus far and will also be of value in the future. Numerical approximation of the static and dynamic characteristics of the bridge enabled identification of types of gages and their locations for optimum results. Estimations on what the strain gages should be reading could be quantified from the calibrated model. The model can also provide predictions of what the new gages should be reading in case they are tested on the bridge in a location where there is no existing gage.

Chapter 6 provides information about instrumentation and installation of the SHM system. Phenomena to be captured with the permanent instrumentation of the bridge include, for ambient traffic, dynamic characteristics, transverse load distribution, and girder deflections and rotations. Long-term data include strains and displacements to provide insight into how the bridge reacts to daily and seasonal temperature changes, as well as how the behavior might change over the lifetime of the bridge. To obtain the necessary information to quantify these behaviors, two different types of data are being recorded: event data and monitored data.

Chapter 7 provides details about the current status of the project and plans for future work. Although there were some minor setbacks during the project, a large portion of the work has been completed. A calibrated finite element model was created and compared to diagnostic test results, which is a key element in the process. The LTBPP recommendations on which types of gages will be used on permanently instrumented bridges were followed, and the majority of the gages were installed on the prototype bridge. Only WIM sensors and weather-related gages were not included in the Delaware bridge. Detailed records of instrumentation costs and hours of work associated with installation were recorded and presented. All work completed in this portion of the first permanent instrumented Delaware bridge can be replicated and used on future long-term instrumented bridges.

Future work will include diagnostic tests and analysis of the real-time data to verify that the system is functioning properly. Organized data retrieval and reporting methods also need to be developed in order to quantify the bridge's behavior and sustainability.

**DELAWARE'S FIRST LONG TERM INSTRUMENTED BRIDGE:  
A PROTOTYPICAL INSTRUMENTATION & INSTALLATION PLAN**

by

Nicole Reader

A thesis submitted to the Faculty of the University of Delaware  
in partial fulfillment of the requirements for the degree of Master of Civil  
Engineering

Spring 2007

Copyright 2007 Nicole Reader  
All Rights Reserved

**DELAWARE'S FIRST LONG TERM INSTRUMENTED BRIDGE:  
A PROTOTYPICAL INSTRUMENTATION & INSTALLATION PLAN**

by

Nicole Reader

Approved: \_\_\_\_\_  
Michael J. Chajes, Ph.D.  
Professor in charge of thesis on behalf of the Advisory  
Committee

Approved: \_\_\_\_\_  
Harry W. Shenton III, Ph.D.  
Professor in charge of thesis on behalf of the Advisory  
Committee

Approved: \_\_\_\_\_  
Michael J. Chajes, Ph.D.  
Chair of the Department of Civil and Environmental Engineering

Approved: \_\_\_\_\_  
Eric W. Kaler, Ph.D.  
Dean of the College of Engineering

Approved: \_\_\_\_\_  
Carolyn A. Thoroughgood, Ph.D.  
Vice Provost for Research and Graduate Studies

## **ACKNOWLEDGMENTS**

I would like to thank my advisor, Michael J. Chajes, for his outstanding leadership and direction that he has given me in the past two years as a graduate student and even the four years as an undergraduate student here.

I would also like to thank Dr. Harry "Tripp" Shenton for his advisement and assistance with my research project and being an excellent professor through my undergraduate and graduate years at the university.

I would like to thank Gary Wenczel and Danny Richardson for the many hours of work contributed towards my research project to work.

I would like to thank the rest of the faculty and staff at the University of Delaware for always helping out whenever possible.

I would finally like to thank my family and close friends, who are like family to me, for providing me with constant encouragement and care to keep me moving forward. I wouldn't have been able to do it without them. I would especially like to thank my Dad and Stepmom for their unconditional love and support throughout all the years of my education.

## TABLE OF CONTENTS

LIST OF TABLES .....	vi
LIST OF FIGURES.....	vii
ABSTRACT .....	xi
1. INTRODUCTION .....	1
1.1 Motivation .....	1
1.2 Long-Term Bridge Performance Program .....	2
1.3 Indian River Inlet Bridge.....	4
2. BACKGROUND .....	7
3. INSTRUMENTED BRIDGE .....	11
3.1 Bridge Selection .....	11
3.2 Bridge Description .....	12
4. DIAGNOSTIC TESTS .....	17
4.1 Static Test .....	17
4.1.1 Static Test Results .....	21
4.2 Ambient Vibration Test .....	25
4.2.1 Ambient Vibration Test Results.....	26
4.3 Summary of Diagnostic and Ambient Vibration Test Results ....	31
5. FEM MODEL.....	32
5.1 Model Description .....	32
5.2 Parametric Studies & Model Calibration .....	35
5.3 Eigenvalue Finite Element Analysis.....	45
5.4 Summary of FEM results .....	51
6. INSTRUMENTATION & INSTALLATION .....	53
6.1 Sensors.....	54

6.1.1 Strain Gages .....	53
6.1.2 Displacement Gages .....	56
6.1.3 Acceleration Gages.....	59
6.1.4 Temperature Gages.....	63
6.2 Data Acquisition System .....	66
6.3 Wiring.....	69
6.4 Data Logger Programming .....	74
6.5 Installation .....	86
6.6 Costs.....	91
7. CURRENT STATUS & FUTURE WORK.....	97
APPENDIX A. SAMPLE POWER AND CROSS SPECTRA .....	101
APPENDIX B.....	111
APPENDIX C. SAMPLE CR9000 BASIC CODE .....	118
APPENDIX D. ADDITIONAL PHOTOGRAPHS .....	138
REFERENCES.....	145

**LIST OF TABLES**

Table 3.1 Summary of old and new cross sections along the length of the bridge.....13

Table 4.1 Summary of peak strains from 2004 static diagnostic test .....21

Table 4.2 Summary of phase angles with respect to gage three .....29

Table 5.1 Comparison of ABAQUS and experimental natural frequencies .....48

Table 6.1 Sample Gage Designations .....53

Table 6.2 Anticipated Schedule for Future Bridge Instrumentation .....91

Table 6.3 Summary of total costs for permanent instrumentation of Bridge 1-821 .....93

Table 6.3 continued.....94

Table B.1 South Junction Box Trunk Cable Wire Pair Designations ..... 112

Table B.1 continued..... 113

Table B.2 North Junction Box Trunk Cable Wire Pair Designations..... 113

Table B.2 continued..... 114

Table B.3 Cost of Instrumentation ..... 115

Table B.3 continued..... 116

Table B.3 continued..... 117

**LIST OF FIGURES**

Figure 3.1 AutoCAD plan of Bridge 1-821 .....14

Figure 3.2 AutoCAD sketch of cross-section one detail .....14

Figure 3.3 AutoCAD sketch of cross section two detail.....14

Figure 3.4 AutoCAD sketch of cross section three detail .....15

Figure 3.5 AutoCAD sketch of cross section four detail .....15

Figure 4.1 AutoCAD plan of strain gage locations for 2004 static diagnostic test .....18

Figure 4.2 AutoCAD drawing of pass one of 2004 static diagnostic test .....18

Figure 4.3 AutoCAD drawing of pass two of 2004 static diagnostic test .....19

Figure 4.4 AutoCAD drawing of pass three of 2004 static diagnostic test .....19

Figure 4.5 AutoCAD drawing of pass four and five of 2004 static diagnostic test .....20

Figure 4.6 AutoCAD sketch of truck weights and dimensions .....20

Figure 4.7 Typical plot of strain vs. time for midspan gages during pass one of 2004 diagnostic test (Burrell, 2004) .....22

Figure 4.8 Strain vs. time plot for quarter span top and bottom flange gages during pass 4 (Burrell, 2004) .....24

Figure 4.9 AutoCAD plan of accelerometer locations for 2006 dynamic diagnostic test.....26

Figure 4.10 Gage (1) power spectrum from 2006 dynamic test .....27

Figure 4.11 Cross spectrum for gage five with respect to gage three .....28

Figure 4.12	Basic sketch of modes one through three .....	30
Figure 5.1	Transverse distribution for original load placement comparison to actual 2004 test data.....	36
Figure 5.2	Load placement #1 for load position parametric study .....	37
Figure 5.3	Load placement #2 for load position parametric study .....	37
Figure 5.4	Load placement #3 for load position parametric study .....	38
Figure 5.5	Load placement #4 for load position parametric study .....	38
Figure 5.6	Transverse distribution with different load positions in FEM.....	39
Figure 5.7	Zoomed view of transverse distribution with different load positions .....	40
Figure 5.8	Transverse distribution plot for varying concrete moduli .....	41
Figure 5.9	Zoomed in version of transverse distribution plot for varying concrete moduli .....	42
Figure 5.10	Transverse distribution comparison for pass one .....	44
Figure 5.11	ABAQUS mode one shape for original FEM.....	46
Figure 5.12	ABAQUS mode two shape for original FEM.....	46
Figure 5.13	ABAQUS mode three shape for original FEM .....	47
Figure 5.14	ABAQUS mode one shape for pinned FEM.....	49
Figure 5.15	ABAQUS mode two shape for pinned FEM.....	49
Figure 5.16	ABAQUS mode three shape for pinned FEM .....	50
Figure 6.1	AutoCAD plan of all gage layouts .....	55
Figure 6.2	Vishay Micromeasurements LWK-Series weldable foil strain gage <i>courtesy of Vishay Micromeasurements</i> .....	54
Figure 6.3	Vishay Micromeasurements MR1-350-130 bridge completion module <i>courtesy of Vishay Micromeasurements</i> .....	54

Figure 6.4	Geokon 4100 vibrating wire strain gage <i>courtesy of Geokon</i> .....	56
Figure 6.5	AutoCAD plan of bridge with strain gage locations & designations .....	57
Figure 6.6	Unimeasure Inc. HX-P510 Series – analog position string pot <i>courtesy of Unimeasure Inc.</i> .....	56
Figure 6.7	AutoCAD plan of bridge displacement gage locations and designations .....	58
Figure 6.8	Dimensions of Crossbow accelerometers <i>courtesy of Crossbow</i> .....	60
Figure 6.9	LF Series Crossbow accelerometer <i>courtesy of Crossbow</i> .....	60
Figure 6.10	AutoCAD plan of bridge with accelerometer locations and designations .....	62
Figure 6.11	Vishay Micromeritics weldable temperature sensor <i>courtesy of Vishay Micromeritics</i> .....	64
Figure 6.12	Dimensions of bondable surface thermocouple <i>courtesy of Omega</i> .....	65
Figure 6.13	AutoCAD plan of bridge with temperature gage locations and designations .....	66
Figure 6.14	Campbell Scientific CR9000X Measurement Control System <i>courtesy of Campbell Scientific</i> .....	68
Figure 6.15	Photo of platform & fiberglass enclosure .....	69
Figure 6.16	Photograph of south junction box interior.....	72
Figure 6.17	PC9000 program generator main screen .....	76
Figure 6.18	PC9000 program generator configure logger specification window .....	77
Figure 6.19	PC9000 program generator scan control window .....	78
Figure 6.20	PC9000 program generator output table specification window .....	79

Figure 6.21 PC9000 program generator thermocouple specification window .....	81
Figure 6.22 PC9000 program generator bridge specification window for foil strain gages.....	82
Figure 6.23 PC9000 program generator bridge specification window for RTD's.....	83
Figure 6.24 PC9000 program generator bridge specification window for accelerometers.....	84
Figure 6.25 PC9000 program generator voltage specification window for string pots.....	85
Figure A.1 Gage (2) power spectrum .....	102
Figure A.2 Gage (3) power spectrum .....	103
Figure A.3 Gage (4) power spectrum .....	104
Figure A.4 Gage (5) power spectrum .....	105
Figure A.5 Gage (6) power spectrum .....	106
Figure A.6 Cross spectrum for gage (1) with respect to gage (3) .....	107
Figure A.7 Cross spectrum for gage (2) with respect to gage (3) .....	108
Figure A.8 Cross spectrum for gage (4) with respect to gage (3) .....	109
Figure A.9 Cross spectrum for gage (6) with respect to gage (3) .....	110
Figure D.1 Interior of main fiberglass box.....	140
Figure D.2 Laptop with field monitor .....	141
Figure D.3 Foil strain gage with bridge completion module .....	141
Figure D.4 Protective gage enclosure .....	142
Figure D.5 Steel coupon with attached gages .....	142
Figure D.6 Thermocouple (TD35) grouted into deck .....	143
Figure D.7 Accelerometer epoxied to beam.....	143

Figure D.8 Enclosed vibrating wire and foil strain gages.....	144
Figure D.7 String pot mount.....	144

## **ABSTRACT**

Bridges are vital links in transportation systems, and represent a tremendous economic investment for their owners. Therefore, it is necessary to have a reliable process for maintaining them and ensuring their reliability. The Federal Highway Administration (FHWA) awarded a contract to the University of Delaware’s Center for Innovative Bridge Engineering (CIBrE) to develop specifications for a long-term bridge performance program (LTBPP). The LTBPP is intended to create a quantitative database of bridge condition and performance that can be used to understand why bridges deteriorate. The program will use structural health monitoring (SHM) technologies to collect some of the desired data. These SHM technologies will be implemented on hundreds of permanently instrumented bridges throughout the country. The research presented in this thesis describes Delaware’s first permanently instrumented bridge, a potential prototype for the LTBPP. The SHM system used on this bridge will also serve as a prototype for a more extensive SHM system that is being planned for the 1,000 foot Indian River Inlet Bridge.

The SHM system developed consists of sixty one sensors and was installed on a three-span continuous slab on girder composite bridge on I-495 in New Castle County, Delaware. The thesis presents the planning that led up to the actual instrumentation, including diagnostic static and dynamic tests used to establish baseline behavior, design details of the SHM system, and programming aspects related to the data acquisition system. An extensive finite element model of the bridge was also created and calibrated based on the diagnostic test data. Detailed cost and labor summaries associated with the instrumentation are also discussed. Finally, recommendations for remaining work are presented.

## **Chapter 1**

### **INTRODUCTION**

#### **1.1 Motivation**

It is impossible to imagine today's society without a functional highway transportation system. It is also impossible for the highway system to be functional without bridges. Whether it is a long-span signature bridge or a simply supported highway overpass, these bridges serve as vital links within the nation's highway system. Bridges also represent a significant investment for the owner, most of whom are Departments of Transportation. In order to maintain the nation's infrastructure there are various existing and emerging methods to sustain the durability and integrity of these vital structures. In order to more effectively maintain bridges, it is essential that we understand how they deteriorate. By permanently monitoring selected bridges using structural health monitoring (SHM) technologies, we can accomplish that goal. Taking advantage of the information gathered by SHM systems can enable bridge owners to prevent catastrophic disasters, address problems at early stages, and focus rehabilitation costs. (Lauzon and DeWolf, 2004)

## **1.2 Long-Term Bridge Performance Program**

The use of long term bridge health monitoring is being considered for use in the Federal Highway Administration's (FHWA) Long-Term Bridge Performance Program (LTBPP). This program, whose framework was worked on by researchers at the University of Delaware's Center for Innovative Bridge Engineering (CIBrE), is intended to yield a quantitative database that can be used to better understand why bridges deteriorate. It is hoped that the database will enable the development of better bridge models, and will shed light on the effectiveness of different construction and maintenance strategies. This information will help bridge owners allocate their limited resources for the most efficient management. In order to obtain the needed data, there are three methods of data collection that are expected to be implemented in the LTBPP. These methods are in-depth visual inspections, forensic autopsying of decommissioned bridges, and long term monitoring of instrumented bridges. Long term monitoring in this case means collecting data for twenty or more years. The instrumented bridges can also provide a test bed for verification of any future structural health monitoring techniques that may be developed.

Based on the expected LTBPP budget and the goals of the program, it is expected that about fifty bridges across the nation will be permanently instrumented. These fifty bridges will represent ten percent of the anticipated 500 bridges that will be selected for detailed inspections. The fifty bridges that are chosen to be instrumented are expected to include a representative subset of the bridges that are chosen for detailed

inspection. The bridges selected will consist of very common types that are seen frequently through out the nation's infrastructure.

The final LTBPP will incorporate rigid specifications and protocols regarding the instrumentation of permanently instrumented bridge, and the data to be collected. The data collected is likely to include the following:

- Structural parameters (strain, displacement, rotation, acceleration, and force)
- Environmental parameters (temperature, humidity, UV, wind speed and direction, and precipitation)
- Traffic (video and WIM)

Two different types of data can be collected from permanently instrumented bridges, event data and monitor data. Event data is data that is collected during a specific loading event, such as a truck pass, earthquake excitation, or wind gust. Event data is Scaptured at a high frequency (100 Hz or more) to properly quantify the bridge's behavior during the dynamic loading event. Monitor data does not require as fast a scan rate. This data is collected at specified intervals, such as every hour, in order to quantify long-term effects in the structure due to daily or seasonal environmentally induced responses.

The LTBPP is likely to implement a variety of sensors. For example, strain might be measured using foil gages, vibrating wire gages,

or fiber-optic transducers. The selection of gage type shall be based on performance characteristics, such as sensitivity, durability, ease of installation, etc. The performance characteristics must satisfy the necessary demands for proper acquisition of data. The sensors also need to be durable enough to endure the environmental conditions at the bridge site, which can sometimes be quite harsh. Specifications are also made for the data acquisition system. The system must be able to scan fast enough and support the necessary number of gages to be implemented.

When considering all individual components of the instrumented bridge, cost is a very important factor. The LTBPP includes estimates of how much a single instrumented bridge should cost. The estimated instrumentation cost includes direct cost for equipment, labor, travel, and any indirect costs associated with labor and travel. AC power is assumed to be available at the site, however this most likely will not be the case. The estimation is based on a average rate of \$2,000 per sensor/channel. The average cost of a typical instrumented bridge is estimated to be \$250K with an additional \$25K per year for maintenance and data reporting costs. (Chajes, McNeil, et.al., 2006)

### **1.3 Indian River Inlet Bridge**

Another application of long term bridge monitoring that will be implemented in the near future in Delaware is on the replacement Indian River Inlet Bridge. The bridge is located in southern Delaware just below Dewey Beach and connects portions of Delaware State Route (SR) 1. The bridge spans the Indian River Inlet and currently has two sets of piers

located in the inlet. The piers have been subjected to serious scour. After failing attempts to mitigate the scour, a new structure is being designed that will span the entire length of the inlet. The proposed structure is a cable-stayed bridge and will represent a significant investment for the Delaware Department of Transportation (DelDOT). The Center for Innovative Bridge Engineering (CIBrE) at the University of Delaware is developing a long term monitoring structural health monitoring system for the new structure to aid DelDOT in maintenance and operation of the signature structure. The system will monitor the response in the bridge both during construction and under normal operation. (Chajes, Shenton, et al., 2006)

The bridge discussed in this thesis represents a prototype for a permanently instrumented slab on steel girder bridge. This project focused on the planning and installation for Delaware's first permanently instrumented bridge. The permanent instrumentation procedures and protocols serve as a sample for future permanently instrumented bridges for the LTBPP. The project also serves as a stepping stone for the larger and more involved instrumentation of the Indian River Inlet Bridge. The same data acquisition and sensors will be used in that project, but on a larger scale and with additional types of sensors. This thesis will highlight steps that occurred prior to the instrumentation, such as selection of the bridge and static and dynamic diagnostic tests to establish base line bridge behavior. The main portion of the thesis details the instrumentation plan and its installation.

The work conducted includes selecting which sensors should be used in order to best characterize the bridge behavior, and selecting the optimal sensor locations. A calibrated finite element model was created in order to estimate the bridge's static and dynamic behavior. The wiring scheme to accommodate all of the instrumented gages was created. A standard gage designation system was also developed to provide an easy and organized way to keep track of all the gages. AutoCAD drawings of all gage locations and wire layouts were also created to assist in the field deployment. The data acquisition system was programmed to collect data from the gages to provide monitored and event data. After preliminary instrumentation planning took place, installation of the system on the bridge began and occurred in two phases. Detailed records of man-hours required for installation along with associated costs were kept through out the project.

## Chapter 2

### BACKGROUND

Long term instrumentation as a form of structural health monitoring has been implemented on a variety of bridges all over the world. Many bridge owners invest in long term monitoring systems for long span signature bridges since the instrumentation cost represents a small fraction of the total cost of the structure. Japan's Akashi Kaikyo bridge, the world's longest bridge, has an extensive and technologically advanced long term monitoring system. Some other long span bridges that have permanent monitoring systems include the Commodore Barry Bridge in Pennsylvania, the Hamilton Bridge in Ohio, and a number of bridges in Hong Kong, China. A. Emin Aktan (2002) from Drexel University has developed a detailed model guide for monitoring major bridges. He discusses the monitoring systems for the long span bridges mentioned above, along with numerous other larger bridges that have been instrumented. Although Aktan's bridge monitoring guide focuses on larger bridges, the recommendations can also be translated to smaller scale bridges. Aktan's report is helpful in providing information on sensor requirements and recommendations, data acquisition systems and networking, and economic considerations for any type of instrumented bridge.

Along with monitoring long span bridges, there has also been extensive work conducted involving permanently instrumented shorter span bridges. Hani Nassif et.al. (2006) from Rutgers University has permanently instrumented the Doremus Avenue Bridge located in northern New Jersey. The instrumented bridge is a three-span, continuous structure and has ten steel composite girders that support four lanes of traffic. The sensors used consist of strain gages, accelerometers, linear variable displacement transformers (LVDT's), and weigh-in-motion (WIM) sensors. Finite element analysis was used to provide information on optimal gage placement. The specific objectives set for the Doremus Avenue project are as follows:

- Develop a truck live load model based on actual truck weight data received from the WIM system
- Develop a fatigue load model to estimate remaining life of the bridge
- Verify LRFD-AASHTO girder distribution factors, dynamic load amplification, and multiple presence events
- Verify New Jersey's deflection limits
- Evaluate substructure dynamics

Although the Doremus Bridge project had detailed goals set, other similar monitoring projects of smaller, more typical bridges have had more general scopes. For example, John T. DeWolf and Robert G. Lauzon (2004) from the University of Connecticut has been working with the Robert G. Lauzon of the Connecticut DOT to install permanent monitoring

systems on a variety of bridges in Connecticut. The systems are intended to help the Connecticut DOT assess the behavior and condition of the in-service highway bridges. The goals of this project are similar to the goals set forth by the LTBPP for long term instrumented bridges. The two primary objectives of the Connecticut bridge monitoring program are to provide a reliable enhancement to the current inspection procedure and to better understand the behavior of bridges.

The monitoring systems on the bridges in Connecticut are comprised of tiltmeters, accelerometers, strain gages, and thermocouples, which are all types of sensors that fall under the data collection recommendations of the LTBPP. Three different bridges in Connecticut have been equipped with permanent monitoring systems. The bridges consist of the following:

- A curved, three-span, continuous cast-in-place concrete multibox-girder bridge
- A ten-span, continuous precast concrete single cell girder bridge
- A curved, three-span, continuous steel dual-box girder bridge

Given that the monitoring of more typical shorter span bridges is fairly new, the benefits are still forthcoming. However, it is known that continuous monitoring of bridges will provide valuable information on a bridge's health and integrity. Continuous monitoring may also help to refine design criteria, provide data to allow the determination of accurate deterioration rates, and more efficient bridge maintenance programs. (Lauzon and DeWolf, 2004)

Although Delaware's first long term instrumented bridge shares similar characteristics and monitoring techniques with the previously mentioned projects, it also has its own unique features. The instrumented bridge in Delaware is intended to serve as an economical prototype for future instrumented bridges throughout the nation. It is not specific to one certain type of bridge, or to one category of data. The project also provides a detailed breakdown of instrumentation costs and person-hours associated with implementing a long term instrumentation system, whereas projects in the past have not emphasized these important features.

## Chapter 3

# INSTRUMENTED BRIDGE

### 3.1 Bridge Selection

Different factors were considered when choosing Delaware's first permanently instrumented bridge. These factors consisted of type of bridge, average daily traffic (ADT) and average daily truck traffic (ADTT), accessibility to the bridge, and location relative to the University of Delaware. The search for the best candidate took place in the summer of 2003 when Mamie Lynch (2003), an NSF-REU student, investigated about 180 bridges in New Castle County, Delaware. Bridge 1-821, located on I-495 over Edgemoor Road, was chosen as the best candidate for Delaware's first Smart Bridge. This bridge is a slab on steel girder bridge, which is similar to many of the bridges in Delaware and throughout the nation, and therefore serves as a good prototype for other instrumented bridges in the future. The ADT and ADTT are relatively high on Bridge 1-821 and will give substantial amounts of data. There is a service road that runs along Edgemoor Road under the bridge, which allowed for easy access when instrumenting the bridge. Bridge 1-821 is also located less than twenty miles from the University of Delaware, which makes maintenance and monitoring of the system easy. The original bearings were also replaced by elastomeric pad bearings in the fall of 2006. During the replacement

the entire superstructure was lifted by hydraulic jacks, and could have damaged any instrumentation. Therefore, it is important to choose a bridge that has had the bearings replaced or will not see a replacement. An additional factor to consider when choosing steel girder bridges as a prototype is when the bridge was painted or will be re-painted. Harsh sand blasting and painting could easily damage the delicate sensor equipment. Therefore, it is best to choose a bridge that was recently painted. Bridge 1-821 had been recently painted and will only see small touch up jobs in the time the bridge is instrumented, once again making it an excellent candidate. Another factor to consider when selecting to be instrumented bridges is the height of the bridge above the ground. Girders that are located high above the ground and are not easily accessible without a lift. This can be good and bad. The good part is that the instrumentation system will be protected from vandalism. However, the bad part is that there is the need for a lift to access the girders, which becomes an additional cost when instrumenting. Furthermore, accessing the sensors in the future will also require a lift. One downfall to Bridge 1-821 is that there are high-tension power lines running adjacent to the bridge. These power lines can cause a large amount of unwanted noise in data. Therefore, it is recommended that future bridges that are chosen to be instrumented are not located near large power lines.

### **3.2 Bridge Description**

Bridge 1-821 is a four span bridge with one simply supported span and three continuous spans running in the North and South

directions. The only portion that was instrumented is the three northbound continuous spans and, therefore, spans two through four are the only portions that are considered throughout the paper. A plan of the continuous portion can be seen in Figure 3.1.

### BRIDGE 1-821 PLAN

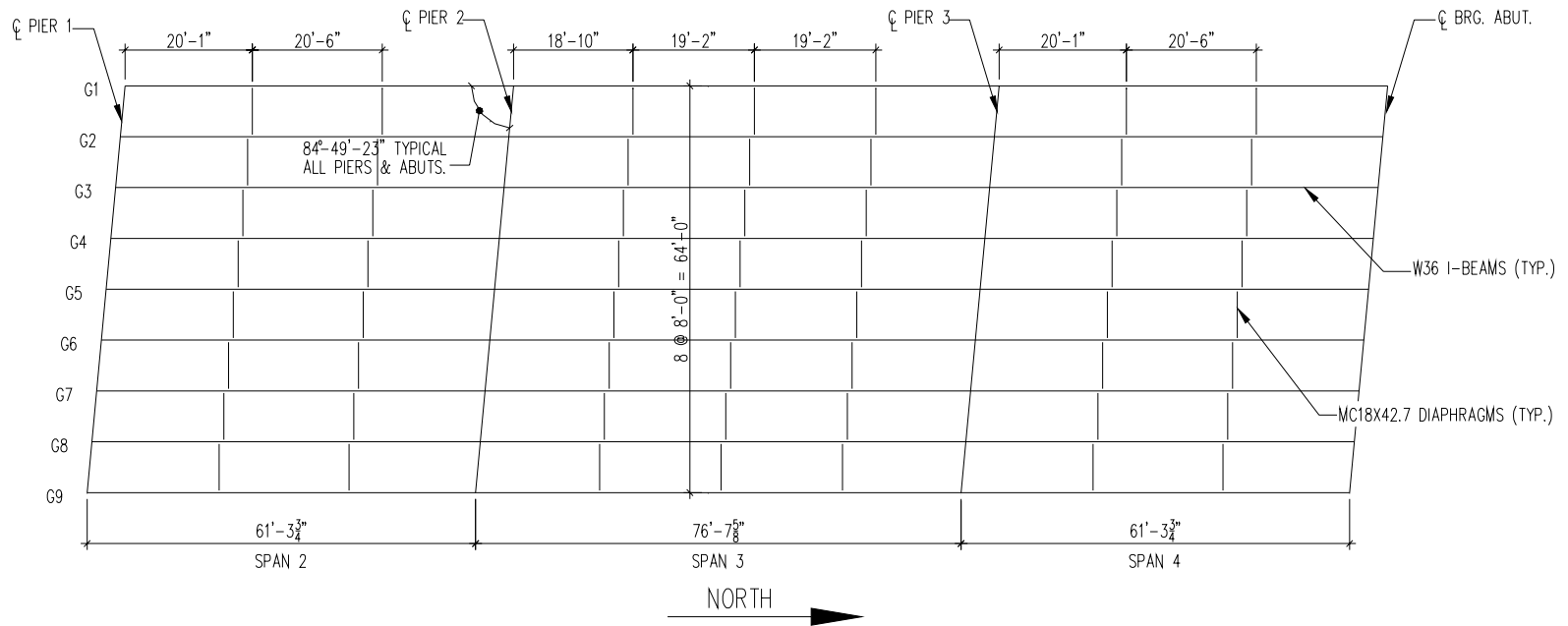


Figure 3.1 AutoCAD plan of Bridge 1-821

Concrete piers support spans two, three, and the left end of the fourth span. A sloped abutment supports the right end of the fourth span. The bottom of the steel girders sit about 50'-0" above ground level at the non-sloped areas under the bridge. The bridge is at a slight skew of 5.2°. The total length of the continuous portion is about 200'-0". The center span is 76'-7<sup>5</sup>/<sub>8</sub>" and the outside spans are 61'-3<sup>3</sup>/<sub>4</sub>" each. There is a composite slab supported by nine equally spaced steel girders. When the bridge was originally constructed it only consisted of seven equally spaced composite girders sustaining three lanes of traffic. However, in order to allow for four lanes of traffic, two girders were added to the east side of the bridge, and are referred to as G8 and G9 on the plan shown in Figure 3.1. All nine girders are spaced 8'-0" center to center. The slab spans 69'-6" transversely and has a parapet on each side.

The entire bridge is comprised of four different cross sections. The original seven girders vary longitudinally between three different cross sections due to the negative bending regions located at the piers. The two new girders only vary between two different cross sections. Cross section one of girders one through seven consists of a W36x135 steel beam with an 8" composite concrete slab on top. Cross section two consists of a W36x150 steel beam with an 8" composite concrete slab on top. Cross section three consists of a W36x150 steel beam with 0.688"x10" cover plates on both the top and bottom flanges. The concrete deck is supported by the beam in cross section three but not considered to take any load because it is located in the negative bending region. The cross sections of

the two added girders consist of the W36x150 composite cross section existing in the old girders and a W36x210 in the negative bending regions. A summary of the old cross sections and the cross sections of the two added girders is shown in Table 3.1. AutoCAD drawings of the four different cross sections can be seen in Figures 3.2 – 3.5.

**Table 3.1 Summary of old and new cross sections along the length of the bridge**

<i>Old X-Section</i>	Distance (ft)	Cross Section #	<i>New X-Section</i>	Distance (ft)	Cross Section #
<b>Span 2</b>	0.0' - 44.3'	1	<b>Span 2</b>	0.0' - 44.3'	2
	44.3' - 52.3'	2		44.3' - 61.3'	4
	52.3' - 61.3'	3	<b>Span 3</b>	61.3' - 78.3'	4
61.3' - 70.3'	3	78.3' - 120.94'		2	
70.3' - 78.3'	2	120.94' - 137.94'		4	
<b>Span 3</b>	78.3' - 120.94'	1	<b>Span 4</b>	137.94' - 154.94'	4
	120.94' - 128.94'	2		154.94' - 199.24'	2
	128.94' - 137.94'	3			
<b>Span 4</b>	137.94' - 146.94'	3			
	146.94' - 154.94'	2			
	154.94' - 199.24'	1			

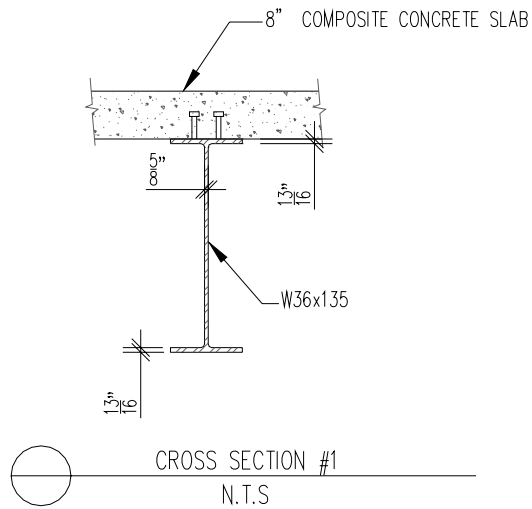


**Figure 3.2 AutoCAD sketch of cross-section one detail**

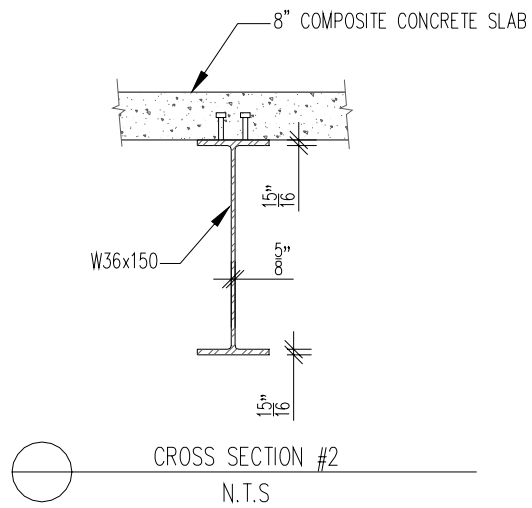


**Figure 3.3 AutoCAD sketch of cross section two detail**

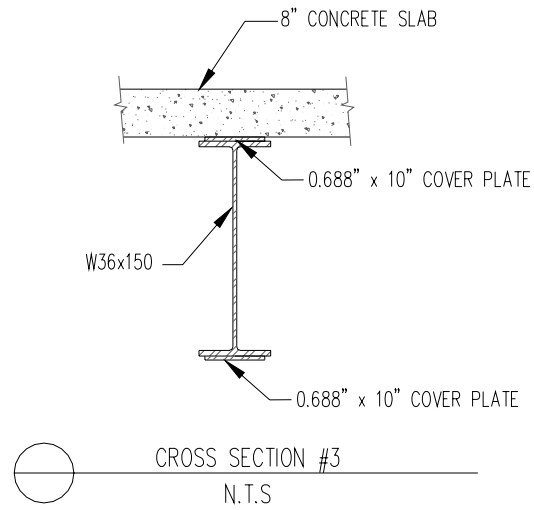


**Figure 3.4 AutoCAD sketch of cross section three detail**

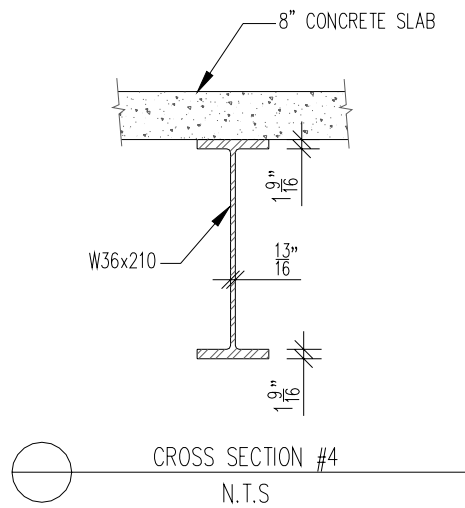


**Figure 3.5 AutoCAD sketch of cross section four detail**

There are also intermediate MC18x42.7 diaphragms located along the length of the bridge. The locations of the diaphragms can be seen in the bridge plan located in Figure 3.1.

## **Chapter 4**

### **DIAGNOSTIC TESTS**

Two diagnostic tests have been conducted on Bridge 1-821 during the preliminary planning for the permanent instrumentation. It was important to test the bridge prior to instrumentation to better understand the bridge's response, to calibrate a numerical model, and to make final decisions on sensors and sensor locations. A static diagnostic test was run in the summer of 2004 and a dynamic diagnostic test was run in the summer of 2006. It is important to note that the diagnostic tests were run while the original bearings were still supporting the bridge, as apposed to the current in place elastomeric bearing pads. The following sections summarize the tests and their results.

#### **4.1 Static Test**

In the summer of 2004 an NSF-REU student, Geoff Burrell (Burrell, 2004), conducted a controlled static load test on the bridge. The bridge was instrumented with a total of twenty eight strain gages. The gage layout is shown in Figure 4.1.

STRAIN GAGE LOCATIONS FOR STATIC DIAGNOSTIC TEST

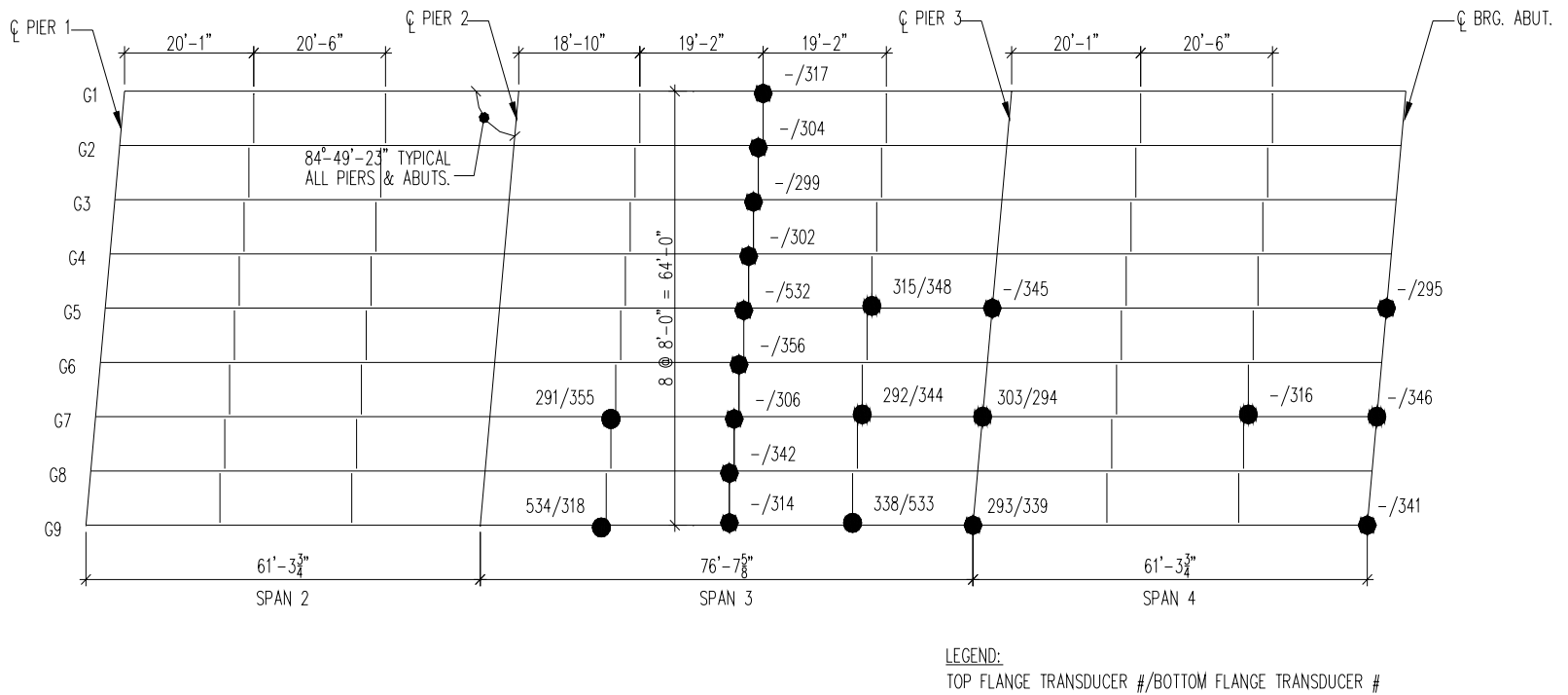
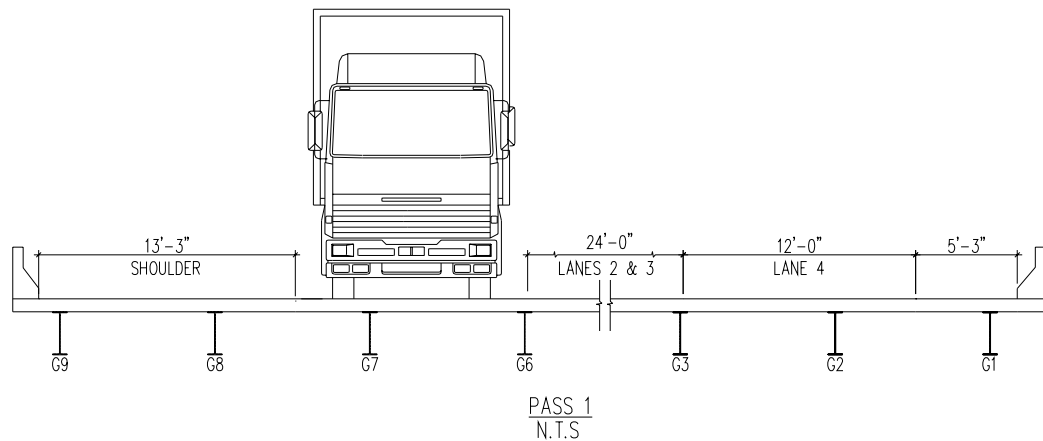
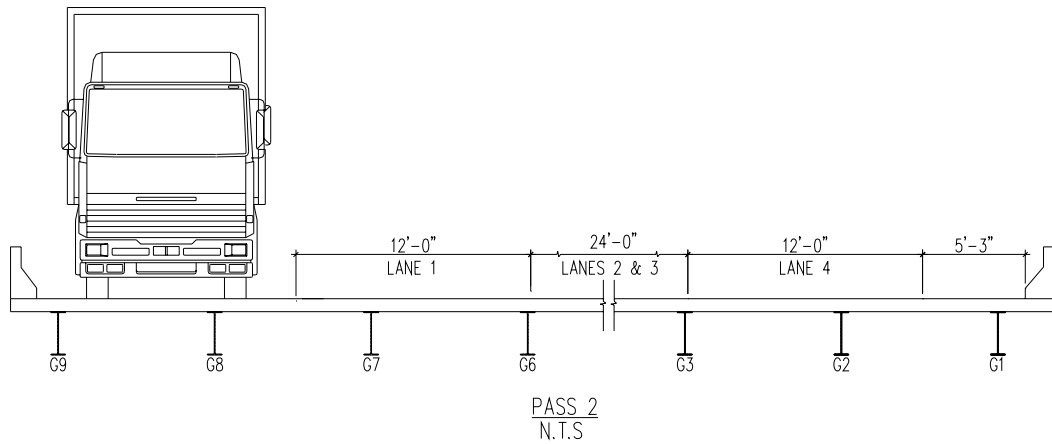


Figure 4.1 AutoCAD plan of strain gage locations for 2004 static diagnostic test

Two loaded dump trucks made five passes at about five mph across the bridge and the resulting strains were recorded using an on-site data acquisition system. Ambient traffic strains were also recorded for three minutes. In truck passes one and two, one truck would cross and the next truck would drive onto the bridge once the first truck was off the bridge. The reason for one truck following a distance behind the other is to test the repeatability of the bridge response. The location of the truck(s) for the truck passes can be seen in Figures 4.2 – 4.5. The detailed truck weights and dimensions from the test can be seen in Figure 4.6.



**Figure 4.2 AutoCAD drawing of pass one of 2004 static diagnostic test**



**Figure 4.3 AutoCAD drawing of pass two of 2004 static diagnostic test**

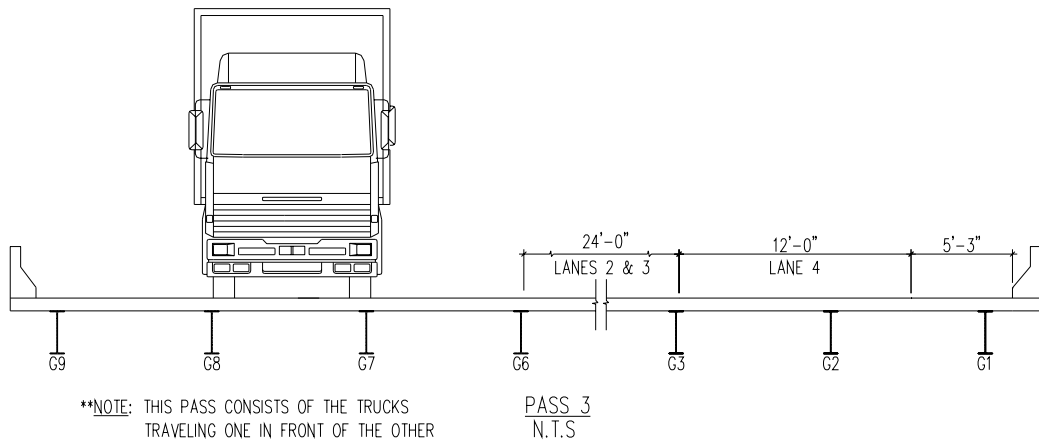


**Figure 4.4 AutoCAD drawing of pass three of 2004 static diagnostic test**

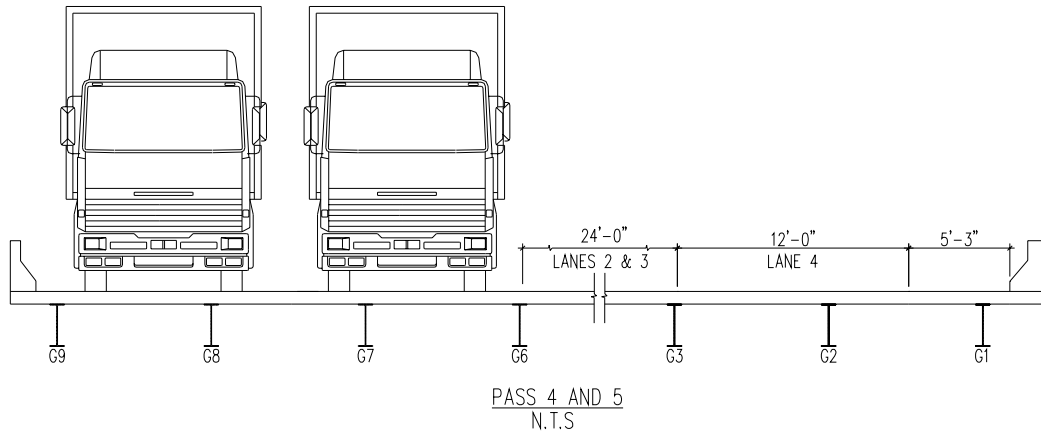


**Figure 4.5 AutoCAD drawing of pass four and five of 2004 static diagnostic test**

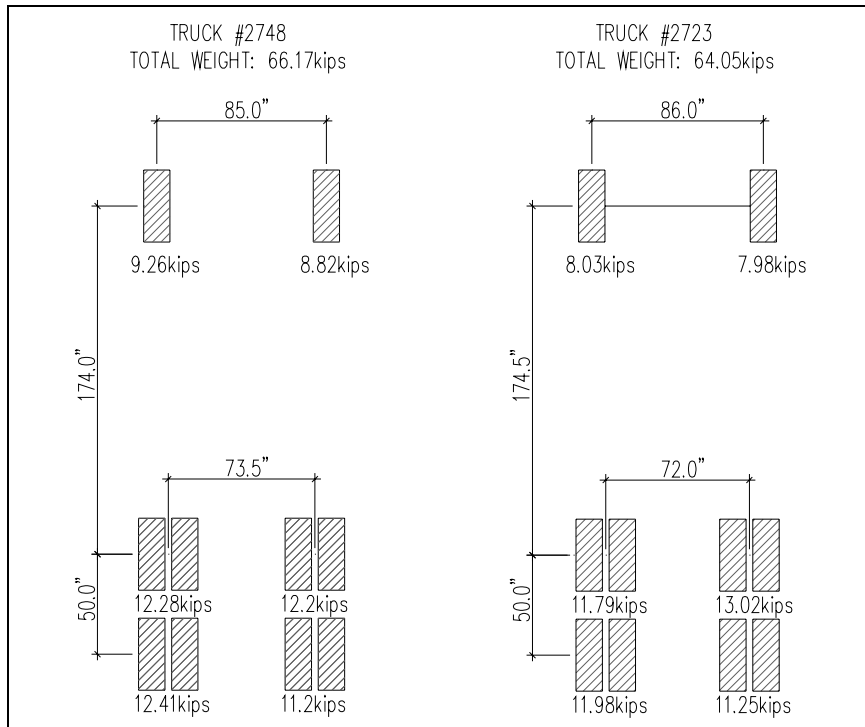


**Figure 4.6 AutoCAD sketch of truck weights and dimensions**

#### 4.1.1 Static Test Results

The overall response of the bridge to the semi-static loads was consistent with what would be expected for a three span continuous bridge. The peak tensile strain occurred at the midspan of the bridge (span 3) where maximum the positive bending would be expected to occur. Likewise, the maximum compressive strain occurred over pier two in the negative bending region. A summary of peak strains for each pass are shown in the table below.

**Table 4.1 Summary of peak strains from 2004 static diagnostic test**

	Peak Strain (Microstrain)					
	Pass 1	Pass 2	Pass 3	Pass 4	Pass 5	Ambient
Tension (Midspan)	152.5	141.6	160.4	209.8	205.2	205.1
Compression (Pier 2)	-41.2	-32.5	-56.9	-58.1	-58.1	-40.1

Strain versus time response showed that there was good repeatability of the data when the trucks passed one after other consecutively. (Burrell, 2004) The response also showed that the girder at midspan goes into negative bending when the truck is on an adjacent span and then goes into positive bending once the truck is on the midspan. A typical plot of strain versus time from a midspan transducers for pass is shown in Figure 4.7.

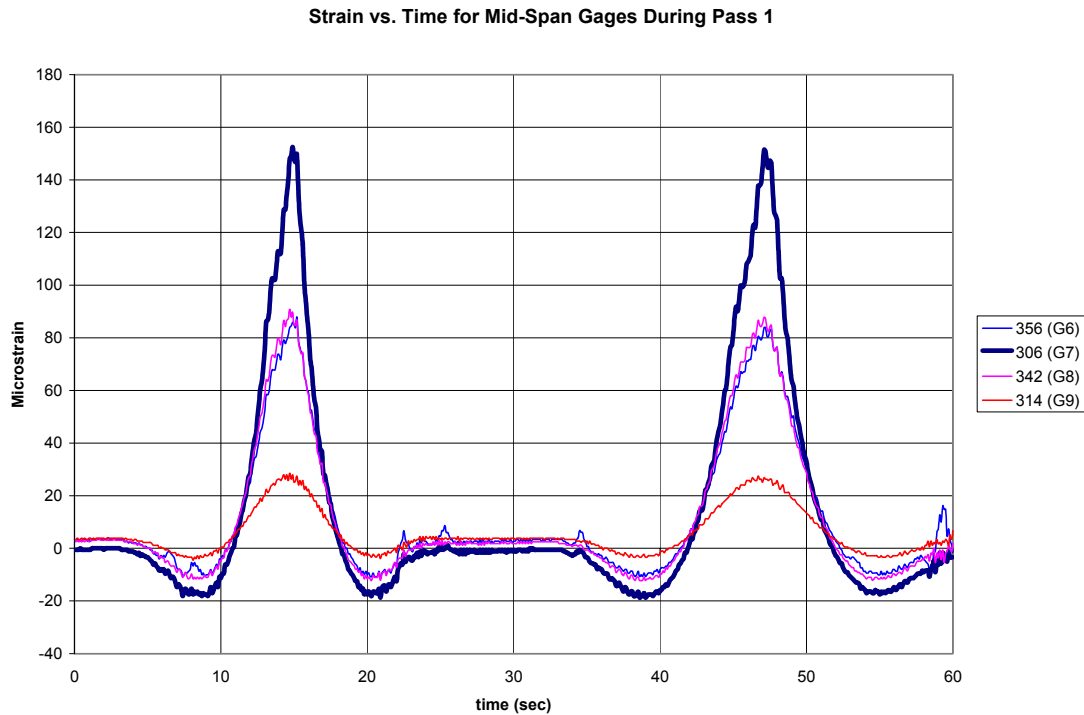


**Figure 4.7 Typical plot of strain vs. time for midspan gages during pass one of 2004 diagnostic test (Burrell, 2004)**

Using the recorded response, the measured transverse load distribution of the bridge was compared to values calculated using AASHTO Standard Specifications for Highway Bridges (2002). According to AASHTO the distribution factors are as follows:

$$DF = S / 7 \text{ (Single Truck)} \quad (\text{Eq. 4.1})$$

$$DF = S / 5.5 \text{ (Side-By-Side Trucks)} \quad (\text{Eq. 4.2})$$

where S is the span between girders in feet. According to AASHTO calculations the transverse distribution factors for a single truck pass and side-by-side truck pass are 1.14 and 1.45, respectively. To calculate a

distribution factor based on the recorded load test data, the following formulas are used:

$$DF = \text{Peak } \varepsilon / (\Sigma \text{ all transverse } \varepsilon)/2 \text{ (Single Truck)} \quad (\text{Eq. 4.3})$$

$$DF = \text{Peak } \varepsilon / (\Sigma \text{ all transverse } \varepsilon)/2 \text{ (Side-By-Side Trucks)} \quad (\text{Eq. 4.4})$$

The calculated distribution factor for a single truck was 0.86 and it was 1.4 for a side-by-side truck pass. Burrell also calculated the distribution factor by assuming every other girder was sensed in order to see what the accuracy would be. The percent difference for a single truck was 16 percent and about 5 percent for side-by-side trucks. Due to the large percent difference in distribution factor for a single truck pass, it was recommended that every girder should be instrumented for accurate representation of transverse load distribution.

Composite action of the bridge was also demonstrated from the data. A plot of strain versus time of two strain gages, one located on the top flange and one on the bottom flange, is shown in Figure 4.8.

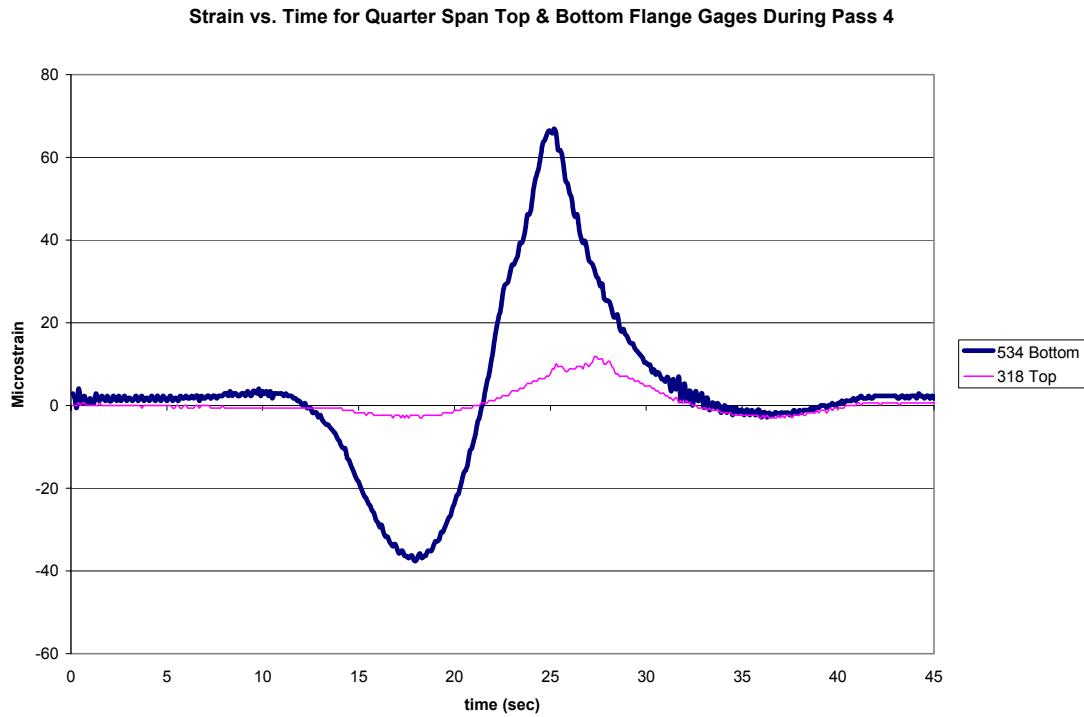


**Figure 4.8 Strain vs. time plot for quarter span top and bottom flange gages during pass 4 (Burrell, 2004)**

As the truck passes, both the top and bottom flanges go into tension at the same time, leaving the deck to take the compression due to bending. Based on the recorded response, it is clear that composite action exists between the deck and girders since the deck and beams shared the bending stresses.

A final parameter that was analyzed from the recorded data was the percent fixity at the bearings. Any pin or roller joint is considered to rotate freely, or in other words to have zero fixity. However there may be some restraint to rotation due to the nature of the bearings. The percent

fixity was calculated by taking the ratio of the strain on the bottom flange at the abutment to the strain on the bottom flange at midspan. The percent fixity of the bridge was calculated to be 26 percent. Due to the presence of fixity at the supports, it was determined that there be permanent gages installed on the top and bottom flanges at the abutments.

Comprehensive details and results of the diagnostic test can be found in Burrell's (2004) report.

#### **4.2 Ambient Vibration Test**

In the summer of 2006 an ambient vibration test was conducted on Bridge 1-821 by Katie Wehrum, an NSF-REU student. (Wehrum, 2006) Six single axis accelerometers were placed on the steel girders of Bridge 1-821 to measure vertical acceleration in the bridge due to ambient traffic. Three accelerometers were placed at midspan of the center span, two were placed at quarter and three-quarter span of the center span, and one accelerometer was placed at quarter span of the span three. A schematic of the six accelerometers can be seen in Figure 4.9. Two ten minute windows of ambient traffic data were recorded at 40 Hz. The data was recorded by a Keithley DATPAT data acquisition system.

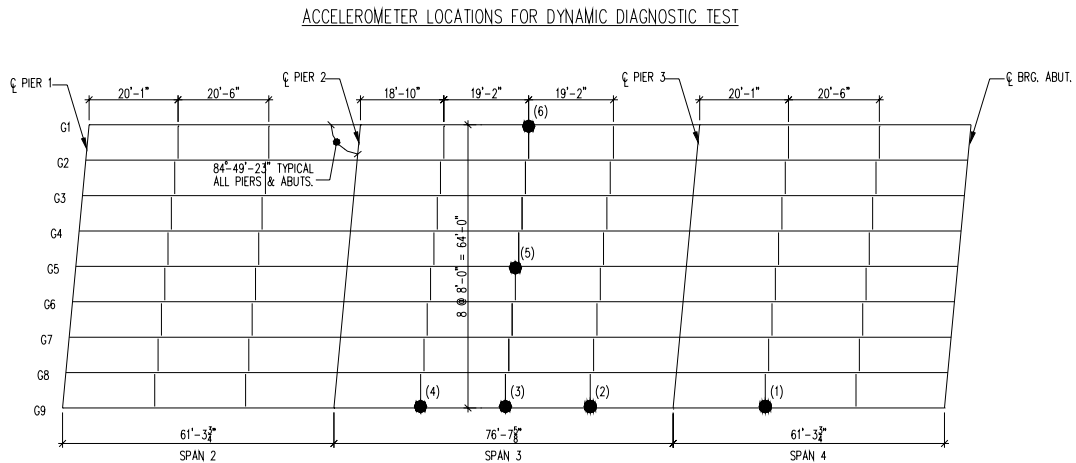


**Figure 4.9 AutoCAD plan of accelerometer locations for 2006 dynamic diagnostic test**

#### 4.2.1 Ambient Vibration Test Results

One of the recorded data sets was used to analyze the dynamic properties of the bridge. The data was sorted by a MATLAB program that produced power spectrum for each gage. The power spectrum results in plots of frequencies and corresponding amplitudes for the different modes of the structure. The power spectra can be used to determine the natural frequencies for the bridge. A sample power spectrum for gage (1) is shown in the Figure 4.10.

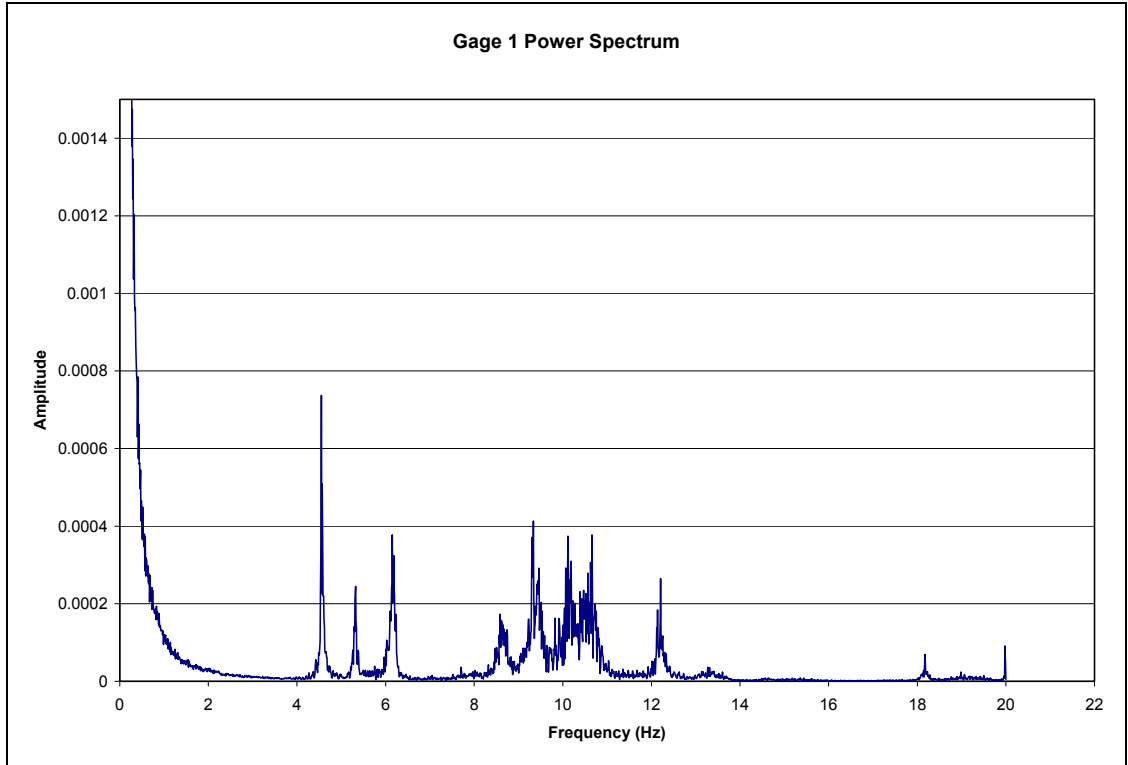


**Figure 4.10 Gage (1) power spectrum from 2006 dynamic test**

Similar power spectra for the other five gages produced from the dynamic test data are shown in Appendix A. The different peaks in amplitude correspond to the natural frequencies for the different modes. Modes one through three have natural frequencies of about 4.6 Hz, 5.3 Hz, and 6.1 Hz respectively.

The MATLAB program also generated cross spectra vectors relative to the data from gage three. The relative cross spectra vectors represented the phase angles for each gage in each mode and helped in identifying the mode shapes for each mode. A sample cross spectrum for gage five with respect to gage three is shown in Figure 4.11.

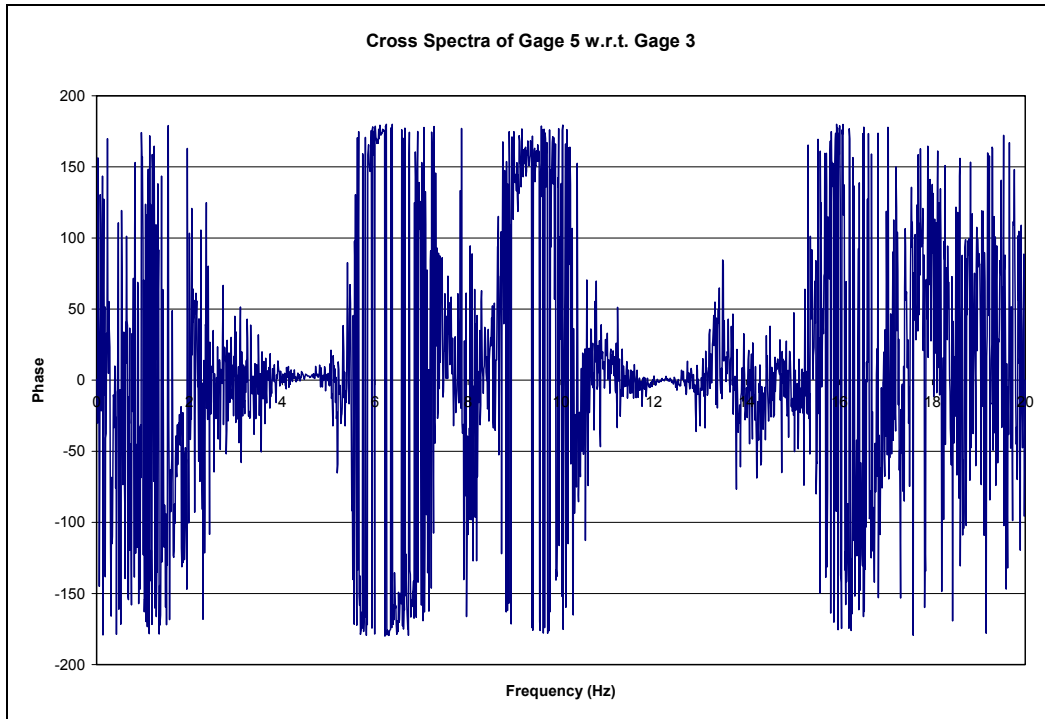


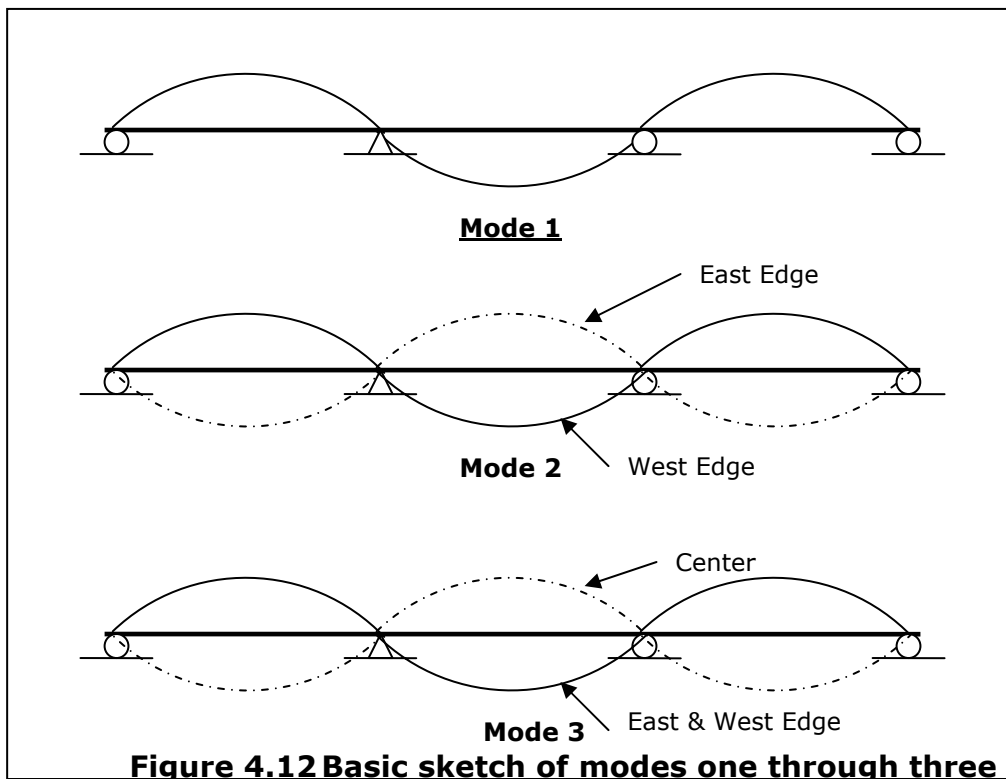
**Figure 4.11 Cross spectrum for gage five with respect to gage three**

A phase angle of zero degrees means that the two gages being considered are in phase with each other and a phase angle  $180^\circ$  means that the two gages are out of phase. Gage five was in phase in modes one and two and out of phase in mode three (See Figure 4.11). The remaining four cross spectra can be seen in Appendix A. Table 4.2 summarizes whether each gage was in or out of phase with gage three for modes one through three.

**Table 4.2 Summary of phase angles with respect to gage three**

	Mode 1	Mode 2	Mode 3
Frequency	4.6 Hz	5.3 Hz	6.1 Hz
Gage 1	Out of Phase	Out of Phase	Out of Phase
Gage 2	In Phase	In Phase	In Phase
Gage 4	In Phase	In Phase	In Phase
Gage 5	In Phase	N/A	Out of Phase
Gage 6	In Phase	Out of Phase	In Phase

Basic sketches of modes one through three look like are provided in Figure 4.11.



Mode one was a basic waving motion of the entire bridge with the entire transverse cross section moving in phase, whereas, mode two was the same waving motion, but with torsional effects taking place transversely. As can be seen in Figure 4.12, the longitudinal centerline of the bridge was not moving at all because of the torsional effects taking place. This same phenomena explains why there is not a mode two frequency spike on the cross spectrum for gage five, which was placed along the longitudinal centerline. Again, mode three had the same waving motion longitudinally, but in this mode, the center was out of phase with the edges.

Comprehensive details and results from the ambient vibration test can be found in Wherum's (2006) final report.

#### **4.3 Summary of Diagnostic and Ambient Vibration Test Results**

The maximum positive and negative strains seen during the static diagnostic test were +209.8 and -58.1 microstrain. The maximum positive strain was seen at midspan and the maximum negative strain was seen over pier two. Both maxima occurred during pass four of the diagnostic test, which was corresponded to the two trucks traveling side by side across the bridge. The distribution factors calculated from the measured data for a single truck and side-by-side truck pass are 0.86 and 1.4, respectively. The first three natural frequencies measured from the ambient vibration test are 4.6 Hz, 5.3 Hz, and 6.1 Hz.

## Chapter 5

### FEM MODEL

Having an accurate finite element model of the bridge has been useful in several aspects of the project thus far, and will also be of value in the future. By numerically approximating static and dynamic characteristics of the bridge, types of gages and their locations for optimum results were identified. Estimations on what strain gages should be reading could be quantified from the calibrated model. The model also can provide predictions of what the new gages should be reading in case they are tested on the bridge in a location where there is no existing gage.

#### 5.1 Model Description

The finite element model mesh of the bridge was created using a computer program called FEMAP (2006) and then analyzed using ABAQUS (2006). FEMAP is a more user-friendly code generating program than ABAQUS. The geometry of the bridge was laid out in FEMAP and then meshed to the desired tolerance. Material properties, boundary conditions, and load scenarios were all specified in FEMAP. Once an input file was complete with all necessary model specifications, it was analyzed using ABAQUS. Only a linear analysis was performed.

The beams, cover plates, and concrete deck and parapets were all modeled using two-dimensional 4-noded standard shell elements with a

specified thickness. The diaphragms were modeled as one-dimensional 2-noded beam elements with a cross section representative of an MC18x42.7. The beams and cover plates were meshed to a tolerance of 3" x 3" elements. The deck and parapets consisted of 12" x 12" elements. Jian Liu (2006) showed that modeling parapets should not be ignored due to their stiffening of the outside girders and attracting more load. Although the added stiffness of the parapets is ignored in design, it should be taken into account in a finite element model to ensure accurate representation of the system. The diaphragm beam elements were 3" long elements. The geometry of the beams was set at the appropriate y-coordinate so that the top surface of the cover plates and flanges were flush with each other. By providing an even surface at the tops of the beams, there were no interfering elements between the beams and composite concrete deck. The flanges and webs of the beams shared common nodes at the intersection in order to ensure continuity in the beam. Since the spans were continuous the nodes at the changing cross section interface were merged to a tolerance of 0.25". In order to account for the minor skew in the bridge, each adjacent girder was set twelve inches behind the other. Each girder then had an eight foot section of slab above it. By offsetting the girders and slabs by a distance of twelve inches, the nodes of the twelve inch elements in the deck could then line up and merge correctly to ensure continuity of the deck.

Cover plates and the concrete deck were connected to the beams via rigid links. The rigid links in ABAQUS function on the basis of a

master-slave system. The link does not have any material or section properties but is a means of transferring load effects. By slaving a node to a particular master node, the slaved node is restrained to displace in all six degrees of freedom as the master node. When slaving the cover plates to the beam flanges it was not crucial as to whether the cover plate node or the flange node was the slave since the cover plates were not taking considerable load. However, when linking the beams and the concrete deck, it was more important to consider what was governing the deflection when the loads are applied. The steel beams are the primary load carrying system and the deck serves more as a distributor of the load amongst the girders. Therefore, the deck was slaved to the corresponding nodes on the steel beams. Rigid links also connected the parapets to the deck, where the parapet nodes were slaved to the corresponding deck node. The bridge was modeled, left to right, as roller, pin, roller, roller supports.

The steel material properties were specified as having a Modulus of Elasticity of 29,000 ksi and Poisson's ratio equal to 0.3. The concrete was assumed to have an elastic modulus of 3,605 ksi, which is based on the formula of  $57,000\sqrt{f'c}$ , where  $f'c$  is 4 ksi. The Poisson's ratio of the concrete was set equal to 0.2. The entire model mesh consisted of 173,710 elements and 177,548 nodes. The analysis used full (non-reduced) integration. ABAQUS computes strains at two integration points through the thickness of the elements. The strains reported from the model are the strains at the top of the element.

## **5.2 Parametric Studies & Model Calibration**

Given that there was a static diagnostic test conducted on the bridge, there was actual data to compare the finite element results to. Therefore, the model could be calibrated accordingly to represent the real bridge more closely. The first truck pass that was compared was pass four, which consisted of both trucks driving across the bridge. The wheel loads were placed at mid-span of the bridge in the model and the strain values at midspan of each girder were compared to the diagnostic strain results at a time when the maximum strain was recorded. All strain values taken from the model are assumed to be taken at the same location at which the gages were placed on the bridge. The wheel loads were placed at an initial position which was thought to represent the wheel loads at midspan from pass four. Figure 5.1 shows the strain vs. transverse span distance for pass four from the model and the actual load test.

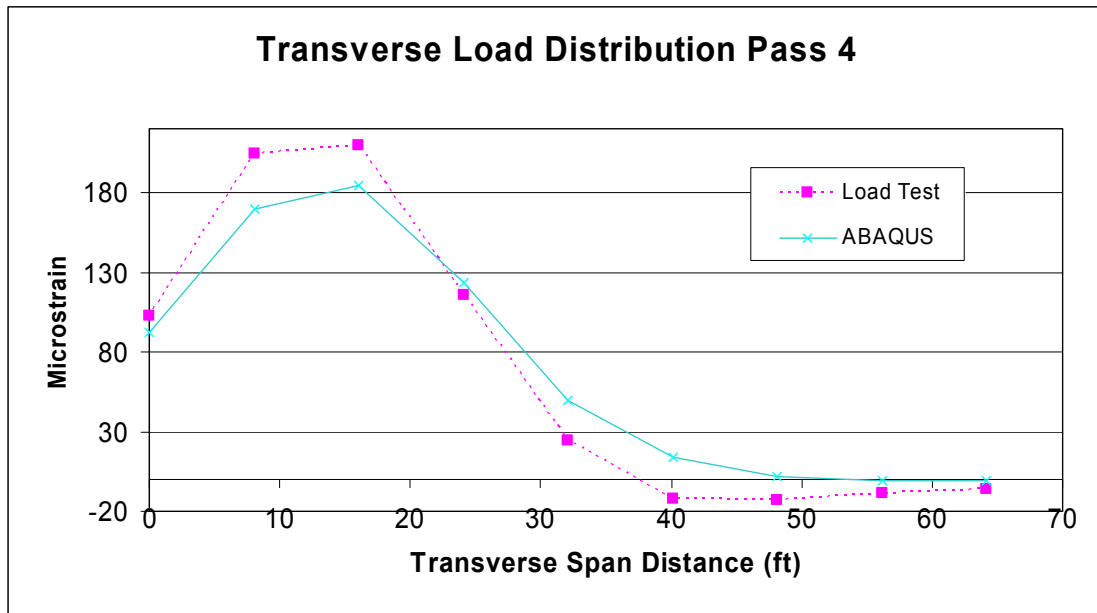


**Figure 5.1 Transverse distribution for original load placement comparison to actual 2004 test data**

The results of the transverse distribution plot shown in Figure 5.1 showed a difference in the distribution trend near the loaded region between the actual load test and the ABAQUS model. Due to the discrepancy in transverse distribution, there was a need to investigate the effects of load position in the model. Although pass four of the test called for one truck to be in lane one and the other in the shoulder, the exact locations of the trucks varied slightly as they drove across the bridge. By varying the wheel locations in the finite element model by one foot increments, the load distribution patterns were noticeably changed in the loaded regions. The variation in load location was limited to one foot increments since the deck was made up of twelve inch elements and the

loads must be placed at nodes. Figures 5.2 – 5.5 show the different load locations with respect to the girders that were analyzed.

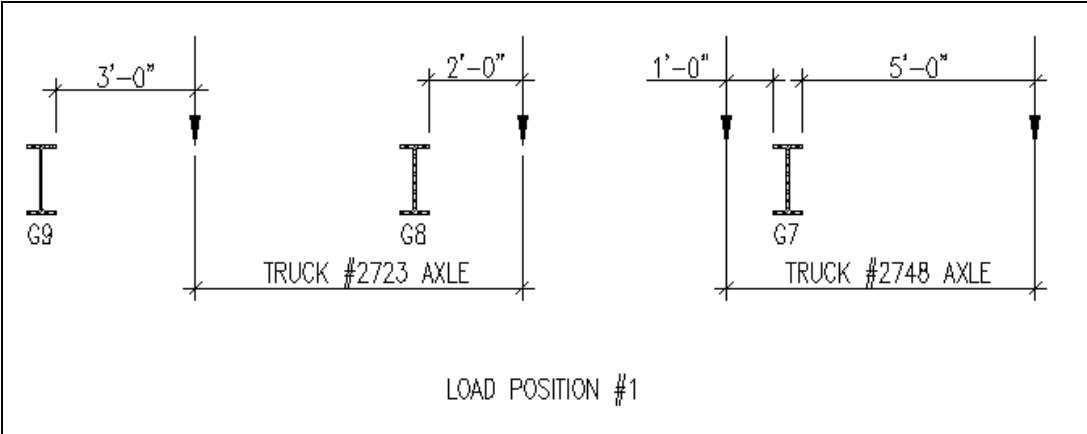


**Figure 5.2 Load placement #1 for load position parametric study**

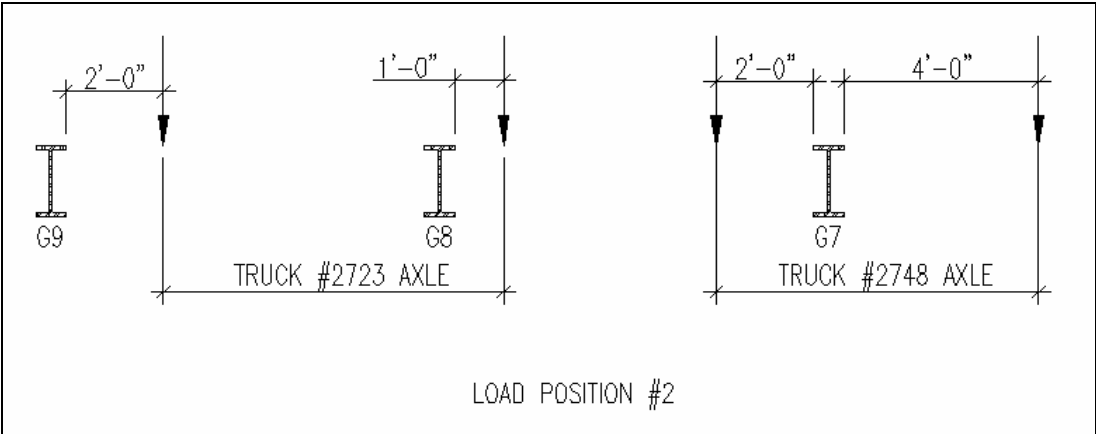


**Figure 5.3 Load placement #2 for load position parametric study**

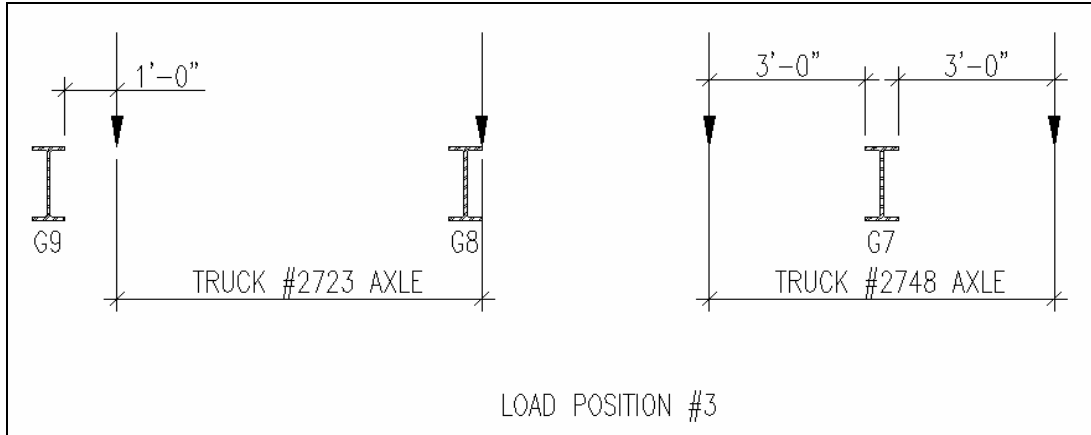


**Figure 5.4 Load placement #3 for load position parametric study**

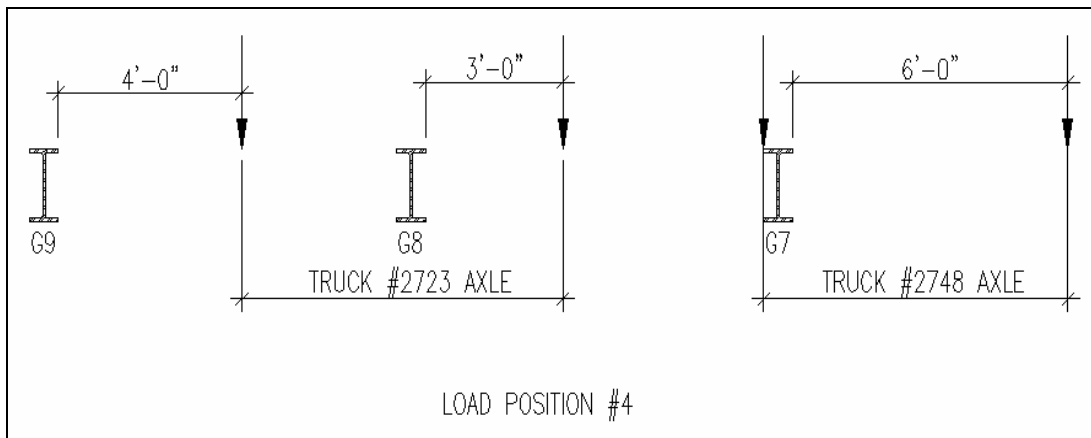


**Figure 5.5 Load placement #4 for load position parametric study**

After the four analyses were run in ABAQUS, the strains at midspan for each girder were plotted versus the distance transversely across the bridge. The transverse strain distribution from pass four of the diagnostic test (corresponding to the analysis) was also plotted on the

same graph. The results are shown in Figure 5.6, with an enlarged plot that better shows the results in the region of the loading (See Figure 5.7).

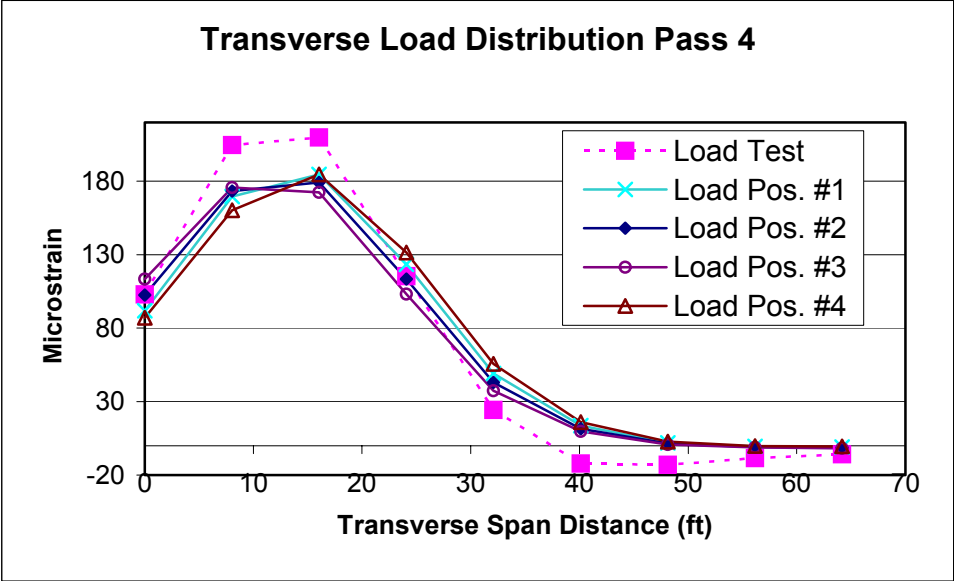


**Figure 5.6 Transverse distribution with different load positions in FEM**

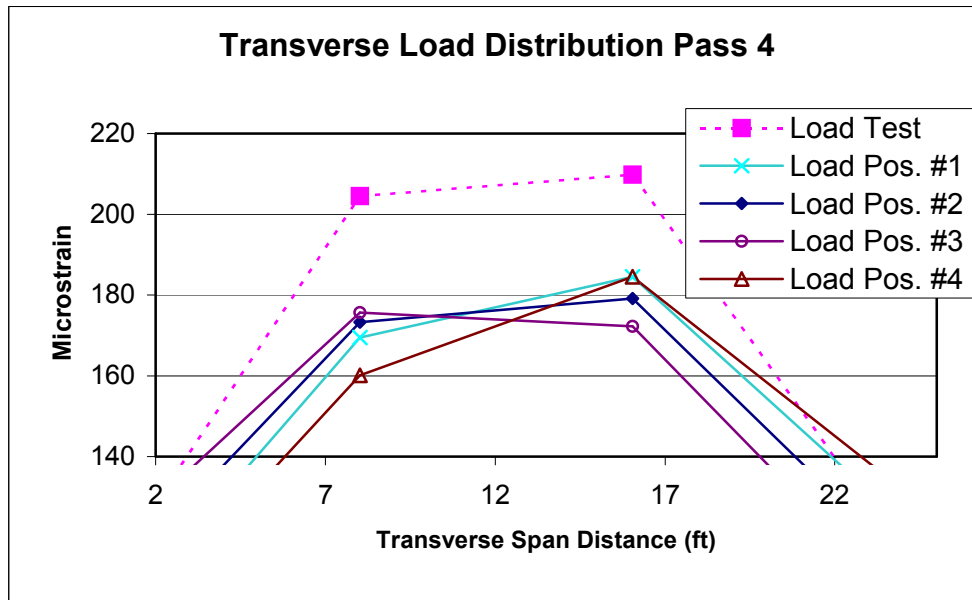


**Figure 5.7 Zoomed view of transverse distribution with different load positions**

As can be seen in the plots, especially in the zoomed in version, load position two most closely matches the distribution that actually occurred during the load test. In load positions one and four the wheel loads are placed such that too much load is being transferred to girder seven with respect to girder eight. In load position one the opposite is occurring, where too much load is being transferred to girder seven and not enough to girder eight. Therefore, load position two was the load case used to conduct the remaining parametric studies.

In order to investigate the effect that varying concrete stiffness had on the model, a parametric study was run with varying concrete moduli. The parametric study was conducted and again compared to data from truck pass four. The original concrete modulus was assumed to be

3605 ksi. The analysis was run with the elastic modulus of the deck and parapets equal to  $\frac{1}{3}E$ ,  $\frac{2}{5}E$ ,  $\frac{1}{2}E$ ,  $E$ , and  $2E$ . Figure 5.8 shows the transverse load distribution for the actual test compared to distributions with varying concrete moduli. A zoomed in version of this plot is shown in Figure 5.9 in order to more closely show the comparisons.

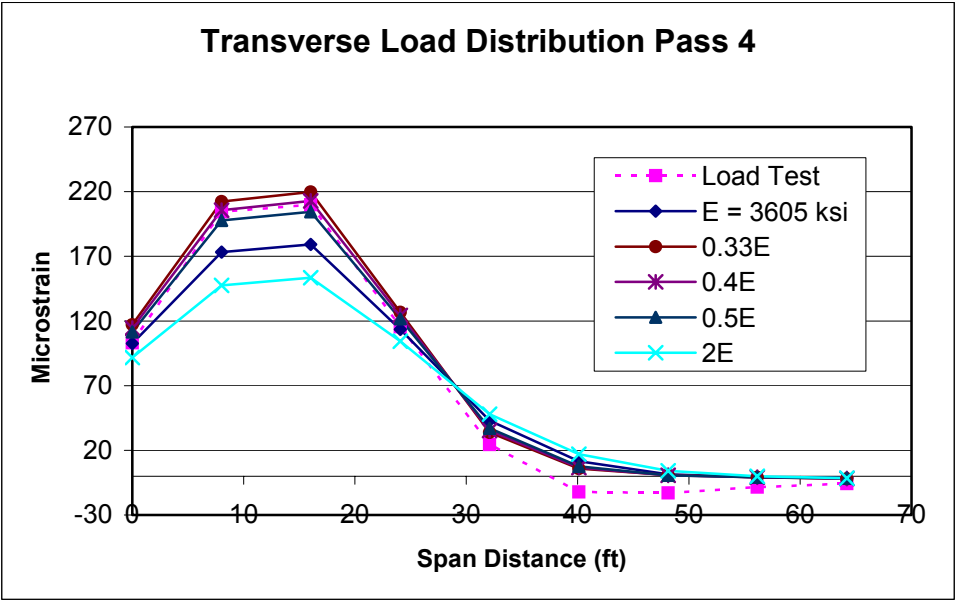
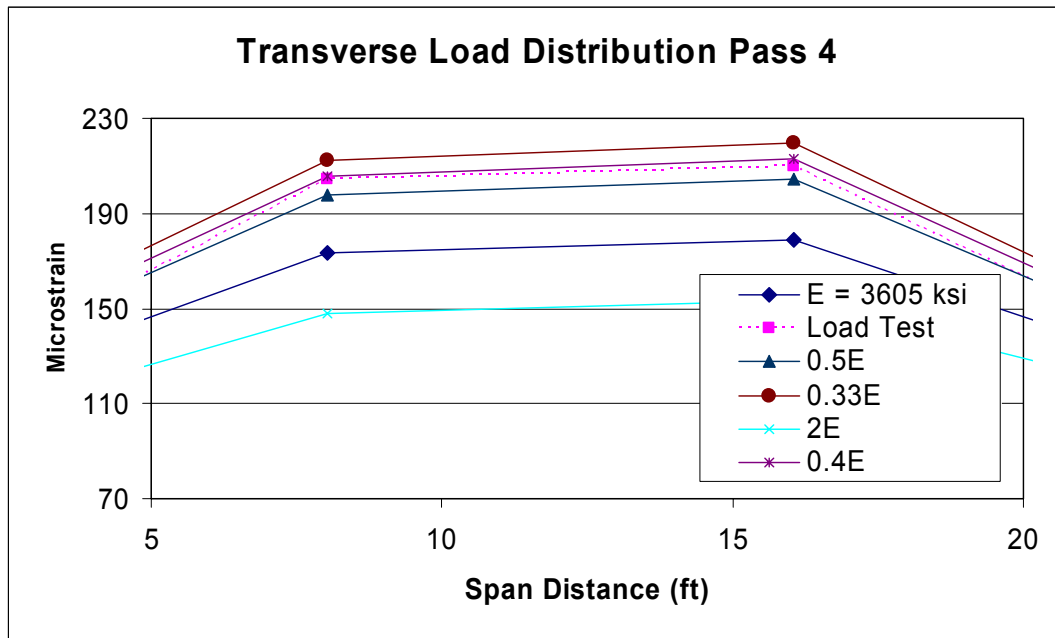


Figure 5.8 Transverse distribution plot for varying concrete moduli



**Figure 5.9 Zoomed in version of transverse distribution plot for varying concrete moduli**

The plot shows that as the elastic modulus of the concrete was decreased from the original modeled value of  $E = 3605$  ksi, the strains in the regions of loading are increased. This is expected because the strains are based on the stiffness of the composite section, which is based on the stiffness of the steel and the concrete. While the reduced stiffness increases the strains in regions close to the load, it also decreases the strains in the beams located further away from the load due to the decreased ability of the concrete to transfer the load (notice change in slope beyond 18 feet). However, the reduction in strain in the girders located away from the load is not as significant as the increase in strain in the girders near the load. When the elastic modulus was increased to two

times the original modeled value, the strains were reduced as would be expected. The strains located in the region near the load were smaller than actual strains due to the added stiffness of the concrete. Conversely, in regions located away from the load, the strains increased due to the added ability to transfer the load transversely to the adjacent girders.

When the modulus was reduced to forty percent of 3605 ksi, the modeled data matched the test data quite well. It is most likely not the case that the concrete in the field has a modulus of 1442 ksi. There are multiple factors that make up the stiffness of the bridge, and it is not easy to capture all of these effects in a numerical model. The boundary conditions and effects of non-structural elements are just some of the items that are difficult to account for in the model. Furthermore, finite element models tend to be stiffer than the systems that they represent. It just so happens that by adjusting only the concrete stiffness by this amount leads to a model that compares well with the data. This agreement means that the model exhibits a realistic global stiffness. For verification purposes, pass one of the static load test was analyzed using the calibrated model ( $E = 0.4E$ ) and compared to the measured results. Figure 5.10 shows the comparison between the calibrated finite element model and the actual data recorded during the load test.

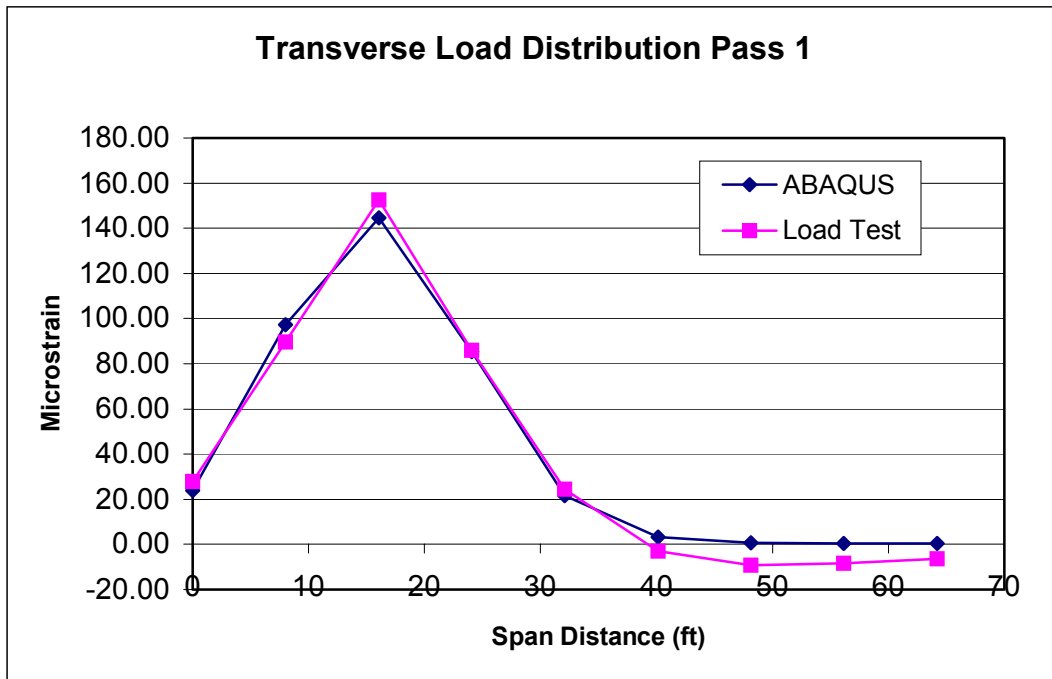


**Figure 5.10 Transverse distribution comparison for pass one**

As can be seen in the plot, there was excellent agreement between the finite element model and the actual load test results. The previous analyses and results show that the non-calibrated finite element model overestimates the stiffness of the system. As mentioned before, finite element models can be stiffer than the actual structure due to the finite number of degrees of freedom in a finite element model. In an actual structure there are an infinite number of degrees of freedom. However, when a structure is modeled, there needs to be a finite number of degrees of freedom. This will restrict the model from being what is exactly true in the actual structure. When comparing the results, one can see that there is also some negative bending in the girders furthest away

from the load (girders one through four) that occurred in the actual test and was not seen in the finite element analysis. This phenomenon that is not reflected in the analysis could also be a result of the additional stiffness in the model. This minor mismatch was not resolved by reducing the modulus of elasticity of the concrete.

### **5.3 Eigenvalue Finite Element Analysis**

ABAQUS was used to run a dynamic analysis of the bridge. Specifications were made in FEMAP for ABAQUS to calculate the natural frequencies and associated mode shapes for the first three modes of the bridge based on the finite element model. Although the calibration based on static results reduced the concrete modulus to 1442 ksi, the original modulus value of 3605 ksi was used for the dynamic analysis. When the model was run in ABAQUS, results were not what would be expected. The first mode shape was unusual at a fairly low frequency of 1.62 Hz. The second mode shape looked reasonable but occurred at a frequency of only 4.12 Hz. The third mode was at a frequency of 4.3 Hz and oddly resembled a shape that would be expected in the first mode. Figures 5.11 – 5.13 show the mode shapes for modes one through three for the original model.

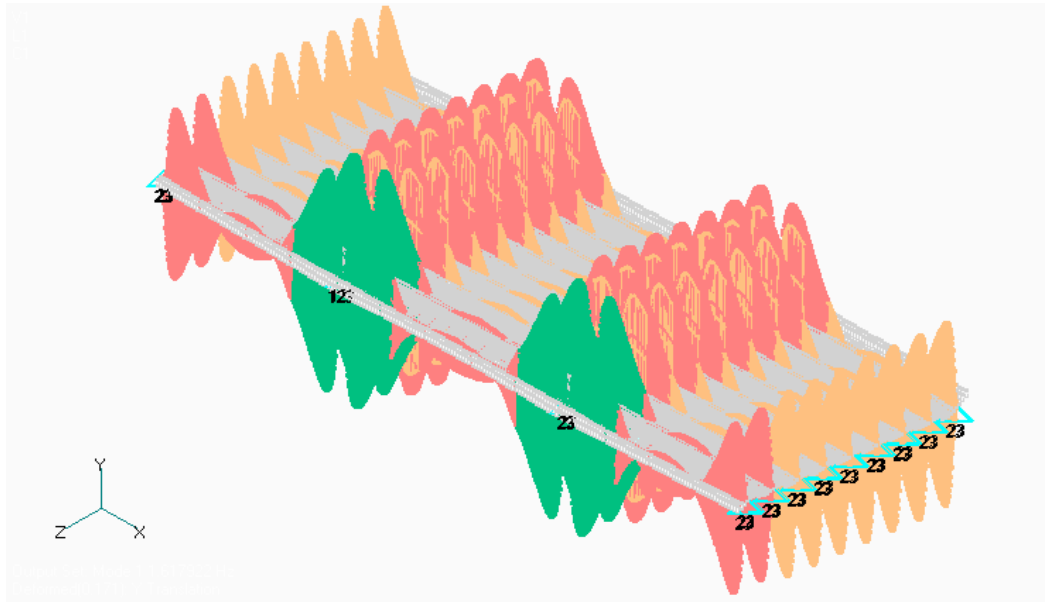


**Figure 5.11 ABAQUS mode one shape for original FEM**

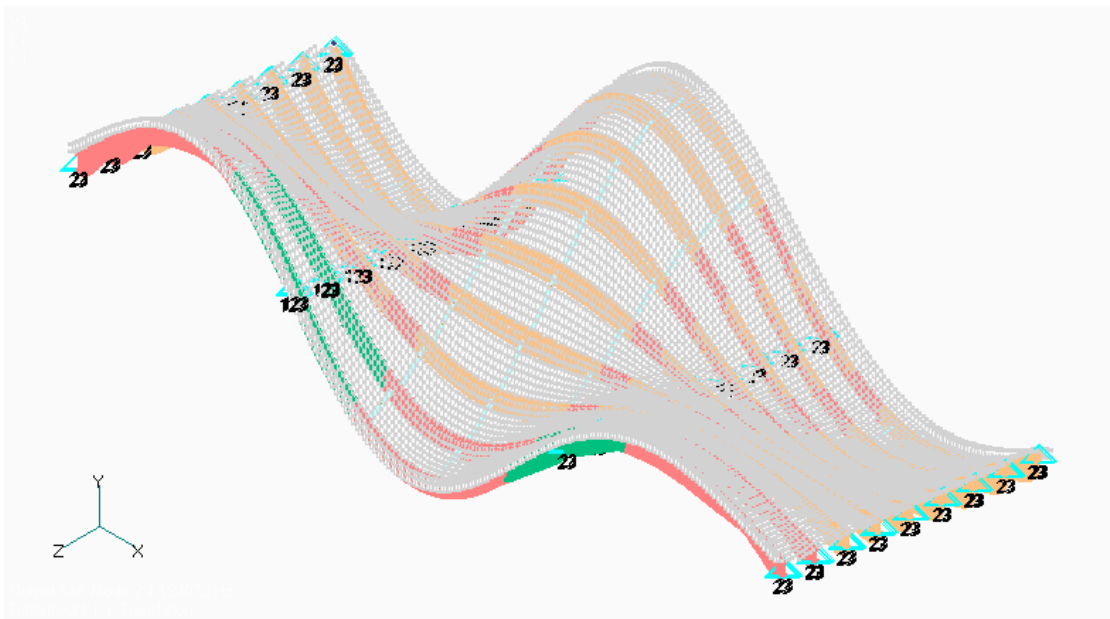


**Figure 5.12 ABAQUS mode two shape for original FEM**

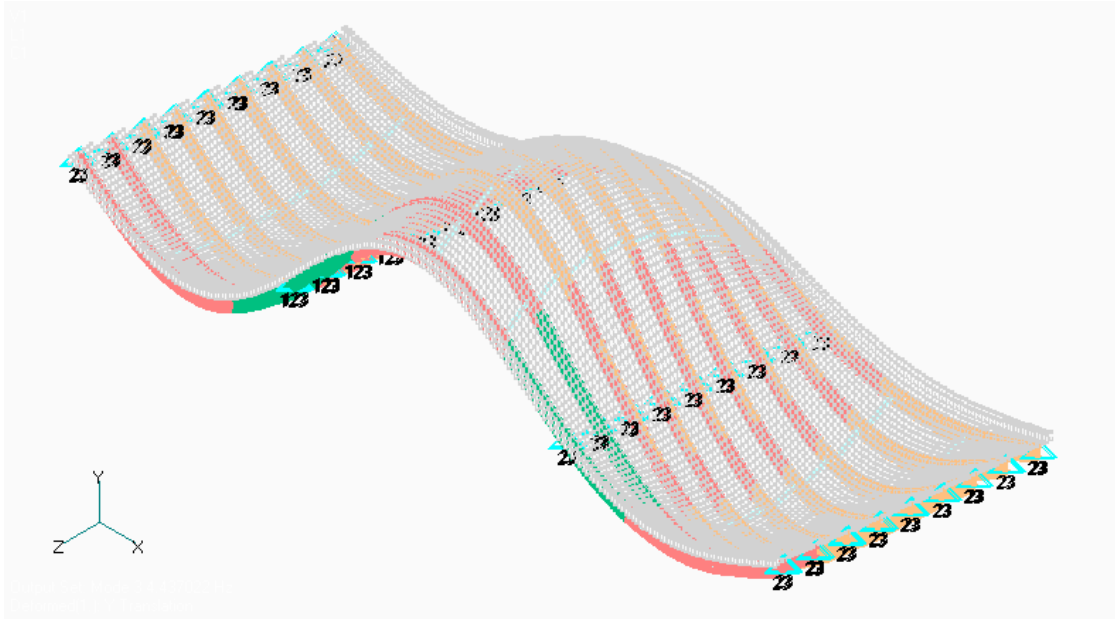


**Figure 5.13 ABAQUS mode three shape for original FEM**

The original model did not yield results that were consistent with the experimental results. The thought was that the low frequencies and strange mode shapes may have been a result of not enough lateral restraint on the deck. Thus, pin constraints were imposed at the two corners of the deck on the west side of the bridge. It should be noted that the added pin constraints did not change the static analysis results. The output from ABAQUS for the pinned deck model resembled the experimental data better. Using the adjusted model, the frequencies of modes one through three were found to be 4.61 Hz, 5.55 Hz, and 6.25 Hz respectively. Table 5.1 shows a comparison of the computed frequencies for the unpinned deck model (original), pinned deck model, and the actual frequencies that were computed based on the field test.

**Table 5.1 Comparison of ABAQUS and experimental natural frequencies**

	<i>ABAQUS un-pinned model</i>	<i>ABAQUS pinned model</i>	<i>Ambient Vibration Test</i>
	<b>Frequency (Hz)</b>		
<b>Mode 1</b>	1.62 (64.8%)	4.61 (0.2%)	4.6
<b>Mode 2</b>	4.12 (10.4%)	5.55 (4.7%)	5.3
<b>Mode 3</b>	4.44 (27.2%)	6.25 (2.5%)	6.1

\* Number in parentheses represents percent error

As can be seen in Table 5.1, the natural frequencies for the pinned deck model were very close to the actual frequencies, varying by no more than five percent, from those measured during the ambient vibration test. The mode shapes that ABAQUS output from the pinned deck model also matched the experimental data rather closely. Pictures of the mode shapes produced by ABAQUS for the first three modes can be seen in Figures 5.14 – 5.16.

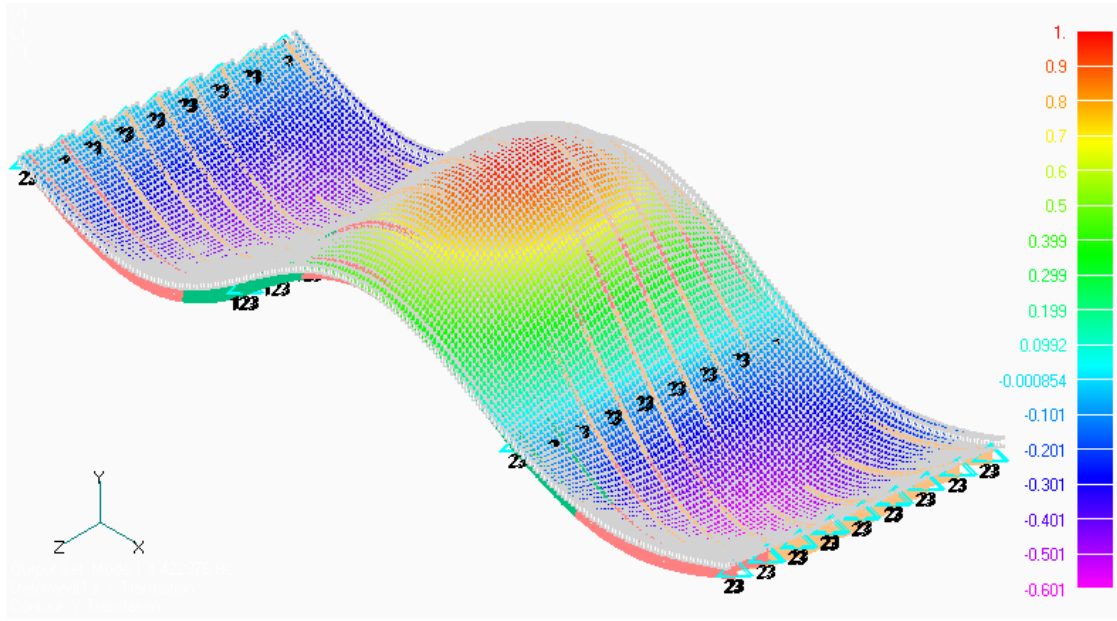


**Figure 5.14 ABAQUS mode one shape for pinned FEM**

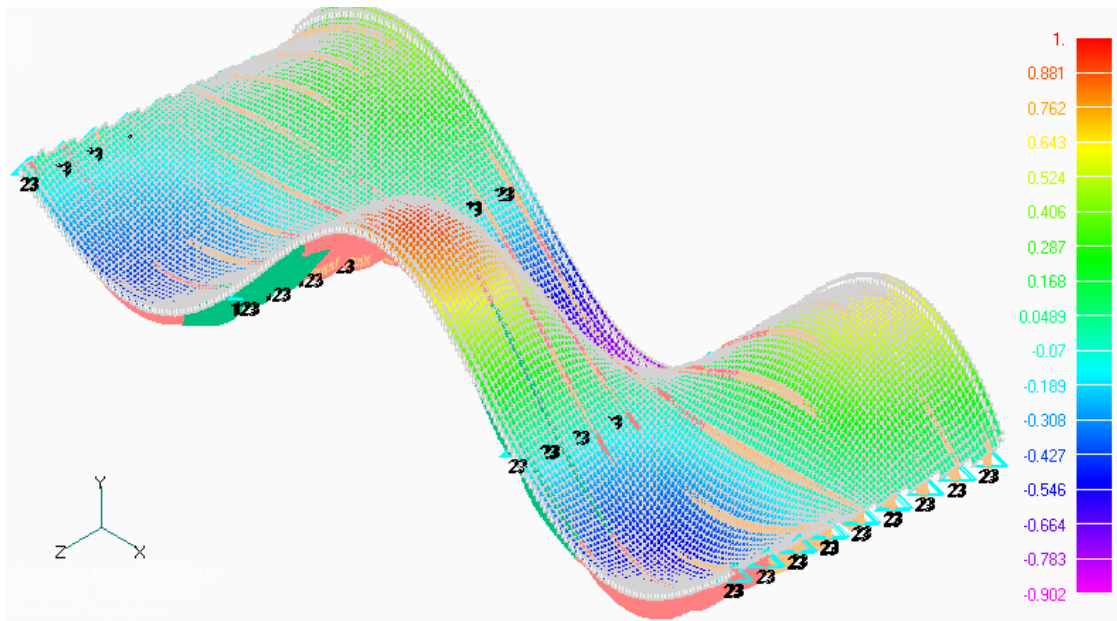


**Figure 5.15 ABAQUS mode two shape for pinned FEM**

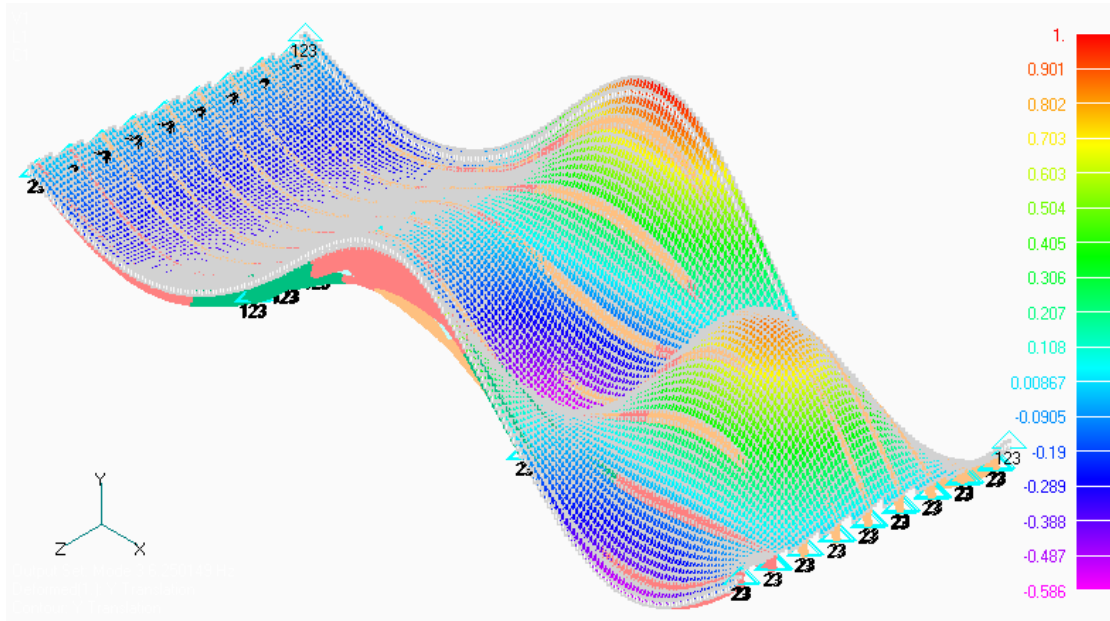


**Figure 5.16 ABAQUS mode three shape for pinned FEM**

The mode shapes from the analysis shown in Figures 5.14 – 5.16 are consistent with qualitative mode shapes that were extracted from the test data. The first mode shape is a basic waving motion of the entire bridge with the entire transverse cross section moving in phase and spans two and four out of phase with the center span. Mode two was the same waving motion, but with torsional effects taking place transversely. The east and west edges were out of phase within a span and spans two and four were out of phase with the center span. The third mode shape computed did not show as symmetric behavior between spans two and four, which was seen in modes one and two. The waving motion took place longitudinally, but in this mode the center was out of phase with the edges in spans three and four and the entire span two was in phase with

itself. Span two, the center of span three, and the edges of span four were all in phase. It is possible that this phenomenon was occurring during the ambient vibration test, but there were no accelerometers on span two to show that effect.

#### **5.4 Summary of FEM results**

The calibrated model with a concrete modulus equal to forty percent of the original modulus (3605 ksi) agreed well, in terms of transverse distribution, with the static diagnostic test data. It was seen that the FEM results were rather sensitive to the load placement and it is important to note when comparing future static test results. When computing dynamic characteristics, the concrete modulus elasticity was kept at the original value (3605 ksi). However, the original constraints of the model produced uncharacteristic mode shapes. Once the deck was pinned at the corners on the west side of the bridge, the mode shapes and frequencies were much closer to the frequencies calculated from the measured ambient vibration data. It is also important to note that the added deck restraint did not affect the static FEM results.



## Chapter 6

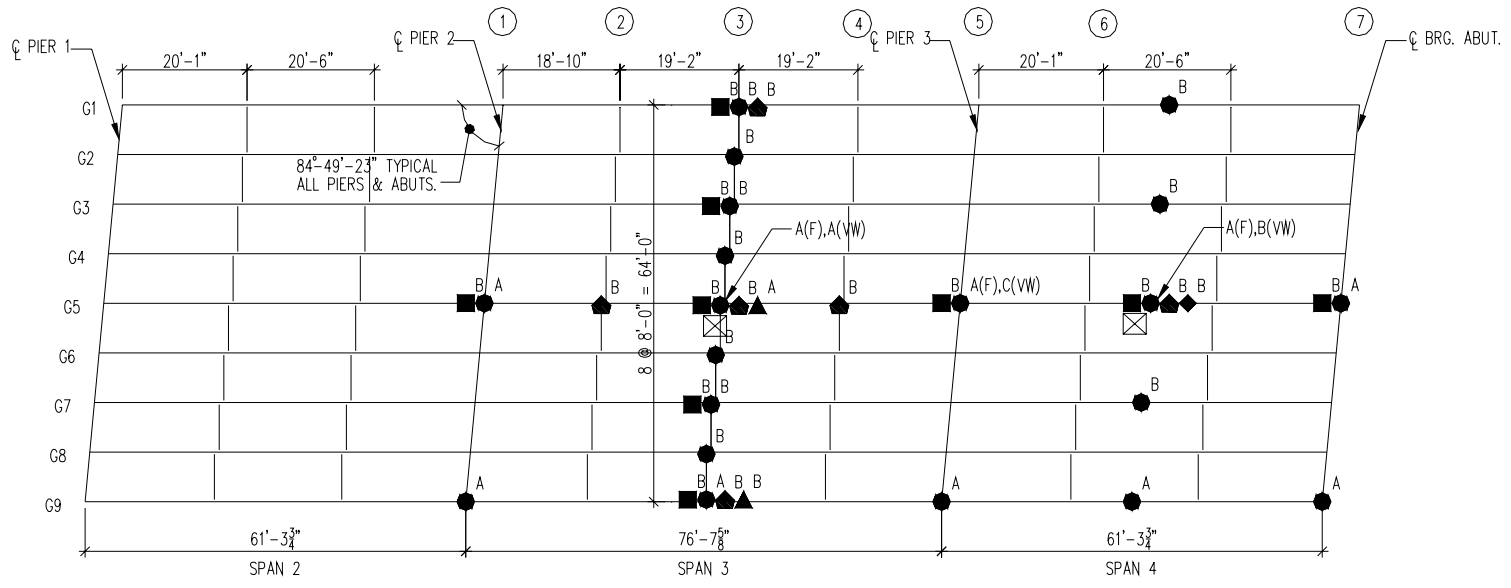
# INSTRUMENTATION & INSTALLATION

There are many phenomena intended to be captured with the permanent instrumentation of the bridge. For ambient traffic these phenomena include dynamic characteristics, transverse load distribution, and girder deflections and rotations. In terms of long-term data, we intend to monitor strains and displacements to provide insight into how the bridge reacts to daily and seasonal temperature changes, as well as how the bridge behavior might change through its lifetime. In order to obtain the necessary information to quantify these behaviors of the bridge, there are two different types of data that will be recorded. There is the data that will be recorded when a significant load is applied to the bridge, such as a truck driving across, which can be considered event data. Then there is the data that will be recorded at certain intervals to look at long-term changes in the structure not due to particular loading events, which can be considered monitored data. The following section describes the instrumentation protocols and installation processes necessary to capture the desired data and to characterize the structural behavior of the smart bridge.

## **6.1 Sensors**

Sixty one gages made up of six different types of sensors have been selected to monitor the bridge. The sensors are foil strain gages, vibrating wire strain gages, string pots, accelerometers, thermocouples, and resistance temperature detectors (RTD's). A simple grid system has been developed in order to designate all sixty one gages that were implemented on the bridge. The girders are numbered one through nine with one starting at the west side of the bridge. The girder numbers serve as a y-axis for the grid. There are also numbers running left to right (or south to north) at pier and diaphragm locations that serves as an x-axis for the grid. The grid number locations and all gages are shown in the bridge plan located in Figure 6.1.

BRIDGE 1-821 GAGE LAYOUT PLAN



\*\*NOTE: THERE WILL BE ONE ADDITIONAL PRECISION DUMMY STRAIN GAGE & ONE ADDITIONAL STRAIN & TWO TEMPERATURE GAGES ON A HANGING THERMAL COUPON NOT SHOWN ON THE ABOVE PLAN.

- STRAIN (31)
- DISPLACEMENT (9)
- ▲ ACCELERATION (6)
- ▲ SURFACE TEMPERATURE (3)
- ◆ AIR TEMPERATURE (1)

☒ BREAKOUT BOX

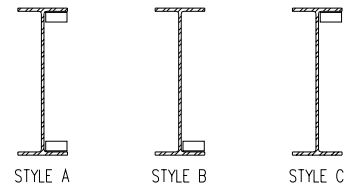


Figure 6.1 AutoCAD plan of all gage layouts

The gage designation is made up of four characters, however, the fourth character is not always necessary. The first character represents the first letter of what the gage is measuring with the exception to the vibrating wire strain gages and RTD's since they had to be differentiated from the foil strain gage (S) and thermocouples (T), respectively. For example the designation for a string pot begins with the letter "D" and the designation for a vibrating wire gage begins with the letter "V". The next two characters in the designation are the numbers that represent the grid location of the gage. For example the string pot located on pier 2 and girder 5 has the designation "D15". The next character can either be the letter "T" or "B" or "X" or "Y". The letters "T" or "B" describe if the gage is located on the top or bottom flange of the beam. The strain gages are the only gages that require the "T" or "B" designation since all other gages will be located on the bottom flange. Some strain gages will be located on the top flange if they are located in a negative bending region. The "X" and "Y" designates the wiring and output for accelerometers measuring in the lateral and vertical direction. Four gages fall outside of the standard designation labeling. The four gages are labeled SCOU, TCOU, SDUM, and TD35. SCOU, RCOU, and TCOU are a strain gage and temperature gages that are located on a steel coupon. SDUM is a dummy strain gage used to assess signal noise. TD35 is a temperature gage that is measuring deck temperature. The coupon and dummy gages took on other aliases since they fell outside the grid locations. The TD35 was at the same location of another thermocouple

and, therefore, needed to be differentiated. Sample designations for all six types of gages are shown in Table 6.1. The individual gages are further discussed in the following sections.

**Table 6.1 Sample Gage Designations**

<b>Gage Type</b>	<b>Designation</b>	<b>Location</b>
Foil Strain	S15T	Pier 2, Girder 5, Top Flange
Vibrating Wire	V35B	Span 3, Girder 5, Mid Span, Bottom Flange
Displacement	D31	Span 3, Girder 1, Mid Span, Bottom Flange
Accelerometer	A35X	Span 3, Girder 5, Mid Span, Bottom Flange (X-Axis)
Thermocouple	T39	Span 3, Girder 9, Mid Span, On Steel
RTD	R35	Span 3, Girder 5, Mid Span, On Steel

### **6.1.1 Strain Gages**

Both weldable foil and vibrating wire strain gages are being used to measure flexural strain in the beams. Thirty-two Vishay Micro-Measurements weldable foil strain gages are being used for capturing the flexural strain during an event. The foil gage can be read at much faster scan rates than the vibrating wire gage. The faster scan rates allows for the capturing of the event, such as a truck pass, in the short amount of time that it occurs. The foil gages used are the Vishay LWK-Series weldable strain gage. This model is made up of a nickel-chromium alloy grid and is encased in fiberglass-reinforced epoxy-phenolic. This gage has a strain range of  $\pm 5000$  microstrain and an operating temperature range of  $-320^{\circ}$  to  $+500^{\circ}$ F. The Vishay weldable strain gage requires minimal

surface preparation requirements and can be easily spot welded to the beam for permanent installation. The MR1-350-130 Vishay Micromeritics bridge completion module was used to complete the quarter bridge at the gage site. The module is covered with an environmental protection system to ensure long term durability. The module also provides a precision 350 ohm half bridge and a 350 ohm dummy gage for individual shunt calibrations. Pictures of the foil strain gage and the bridge completion module are shown in Figures 6.2 and 6.3.



**Figure 6.2 Vishay Micromeritics LWK-Series weldable foil strain gage**  
*courtesy of Vishay MicroMeasurements*

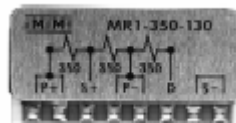


**Figure 6.3 Vishay Micromeritics MR1-350-130 bridge completion module**  
*courtesy of Vishay MicroMeasurements*

Of the thirty-two foil gages there is one dummy gage that is used to monitor noise and give a control value for a gage placed on a steel coupon. The gage on the steel coupon gives a base value for the other gages that characterizes the strain occurring based on temperature effects without other loading. The dummy gage will be read during an event and the coupon gage will only be read with the monitor data.

Four Geokon Model 4100 vibrating wire strain gages are being used to capture monitored flexural strain in the girders. This particular model is only 51 mm long and has a standard measurement range of 3000 microstrain. The gage also can withstand a temperature range from  $-20^{\circ}\text{C}$  to  $+80^{\circ}\text{C}$ , which is suitable for the conditions it will see on the smart bridge. The gages were able to be spot welded to the beam. While the vibrating wire gage requires a slower scan rate, it has better long-term accuracy. The enduring accuracy provides a better look at long-term effects that are occurring in the bridge, such as daily and seasonal changes, that will be captured in the monitored data. The picture in Figure 6.4 shows the Geokon 4100 vibrating wire gage that was used on the instrumented bridge.

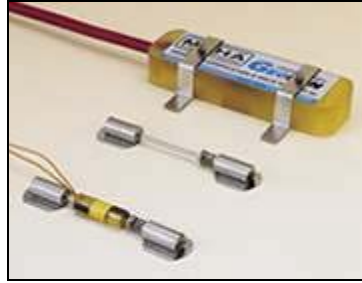
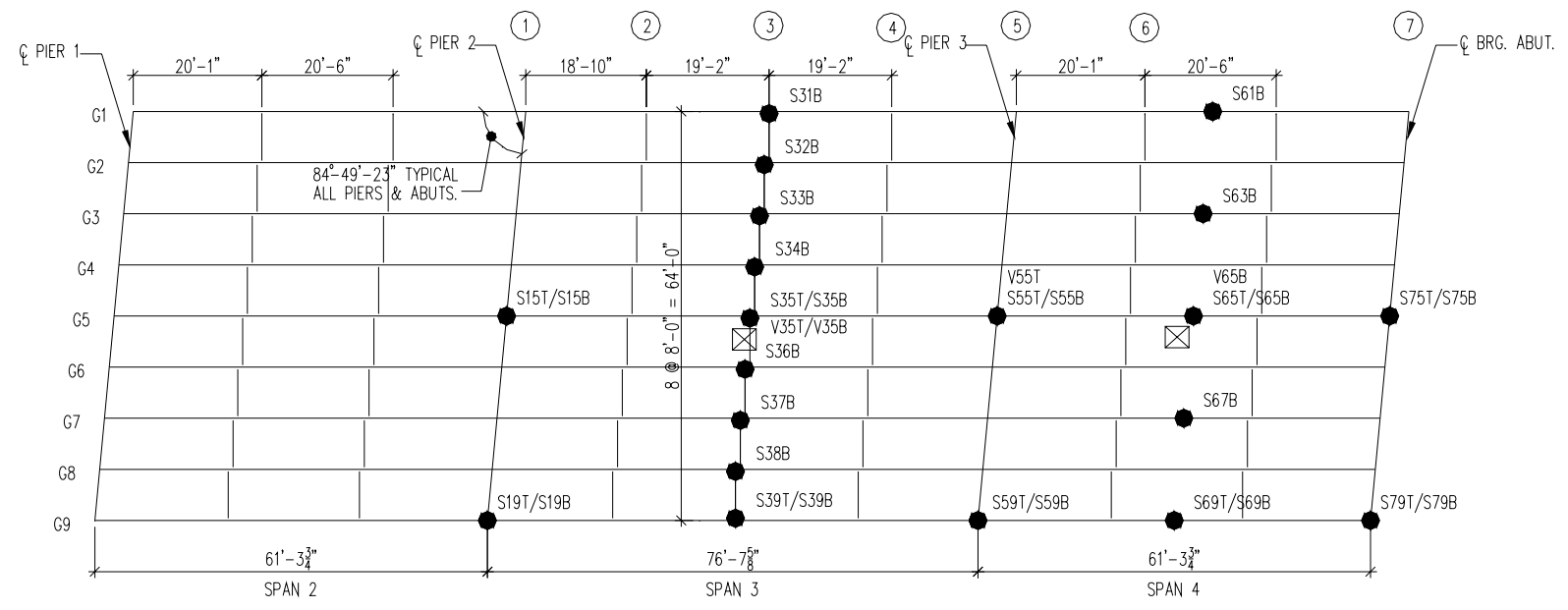


**Figure 6.4 Geokon 4100 vibrating wire strain gage** *courtesy of Geokon*

Both types of strain gages require a type of protective housing in order to protect them from moisture. The vibrating wire gages come with a stainless steel cover and appropriate sealants. However, the foil gages do not come equipped with gage protection. Therefore, an in house solution was made for the situation. A  $3\frac{1}{2}'' \times 2\frac{1}{2}'' \times 1\frac{1}{4}''$  deep rectangular plastic box with a small hole for exiting wires was placed over each foil gage and sealed with RTV. A plan of the bridge with all foil and vibrating wire strain gages, except for the coupon and dummy gages, is shown in Figure 6.5.

STRAIN GAGE LOCATIONS & DESIGNATIONS



\*\*NOTE: THERE WILL BE ONE ADDITIONAL PRECISION DUMMY STRAIN GAGE & ONE ADDITIONAL STRAIN & TWO TEMPERATURE GAGES ON A HANGING THERMAL COUPON NOT SHOWN ON THE ABOVE PLAN.

- STRAIN (31)
- ⊠ BREAKOUT BOX

**Figure 6.5 AutoCAD plan of bridge with strain gage locations & designations**

**6.1.2 Displacement Gages**

A Unimeasure Inc. HX-P510 series analog position string pot was chosen to measure vertical displacement and to calculate rotation of the beams. This series can function in a variety of environments including exposure to rain or wash down and can measure displacements in the range of zero to two inches. A photo of the string pot that is being used is shown in Figure 6.6.



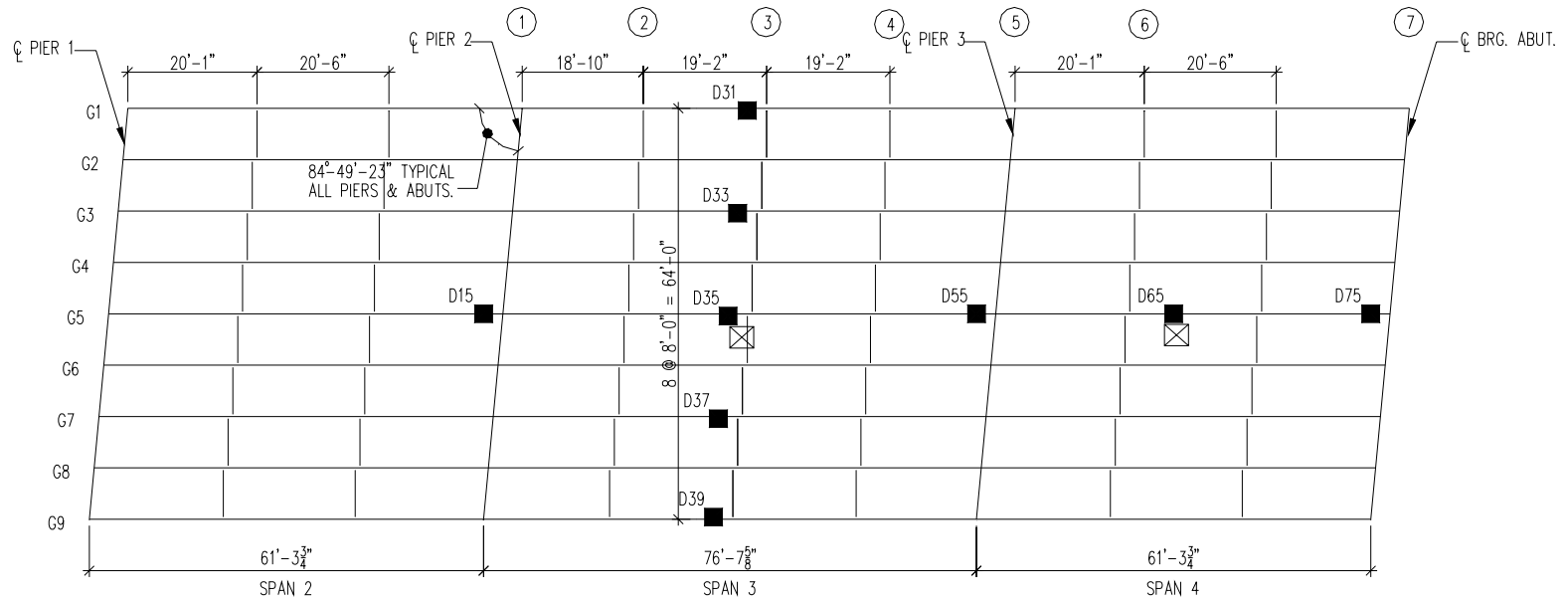
**Figure 6.6 Unimeasure Inc. HX-P510 Series – analog position string pot** *courtesy of Unimeasure Inc.*

The ring at the end of the string pot potentiometer cable pot was secured to a .063" diameter nylon coated stainless steel cable that was strung across the span and secured at the piers. The cable is low stretch and can take a tensile force of up to 270 lbs. At the piers the steel cable was hooked to a spring and the spring was attached to a turnbuckle that was embedded into the concrete pier. The spring will counteract any thermal expansion or contraction in the steel wire and the turnbuckle will

allow for manual tightening or loosening of the cable. The wire must remain taut enough to provide a stationary datum for the potentiometer cable. The base unit was bolted to aluminum plates and the plates were clamped to the beam. The end of the potentiometer cable remains stationary, while the entire base unit moves with the beam it is attached to. Vertical displacement of the beams is being measured during events and monitored over long term as well

There are a total of nine string pots instrumented on the bridge. The locations of these nine sensors can be seen in the gage layout plan shown in Figure 6.7.

DISPLACEMENT GAGE LOCATIONS & DESIGNATIONS



\*\*NOTE: THERE WILL BE ONE ADDITIONAL PRECISION DUMMY STRAIN GAGE & ONE ADDITIONAL STRAIN & TWO TEMPERATURE GAGES ON A HANGING THERMAL COUPON NOT SHOWN ON THE ABOVE PLAN.

■ DISPLACEMENT (9)

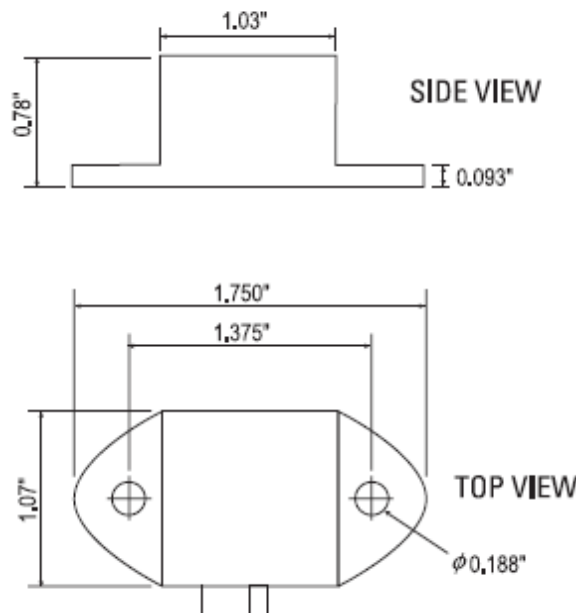
⊠ BREAKOUT BOX

Figure 6.7 AutoCAD plan of bridge displacement gage locations and designations

The string pots located at supports, D75, D55, and D15, will be placed about one foot away from the support and will be used to measure rotations. Assuming there is zero displacement at the support and measuring the displacement a specific distance away, the angle of rotation in the beam can be calculated through basic geometry.

### **6.1.3 Acceleration Gages**

Six crossbow accelerometers were installed on the bridge in order to capture dynamic effects during an event. Four of the six gages are single axis CXL01LF1 series gages measuring acceleration only in the vertical direction. The remaining two gages are tri-axial CXL01LF3 series accelerometers and are capturing vertical and any lateral movement, since the dynamic analysis showed lateral translation in the third mode. The tri-axial accelerometer is one unit but has three different wires for outputting accelerations in all three axes. Only two of the axes will be needed since only lateral and vertical accelerations are being measured. Both series of the accelerometers have an input range of  $\pm 1g$  and a sensitivity of 2 V/g. The accelerometers are encased in a nylon enclosure and can withstand a temperature range from  $-40^{\circ}C$  to  $+85^{\circ}C$ . Dimensions and a picture of the gage are shown in Figures 6.8 and 6.9.



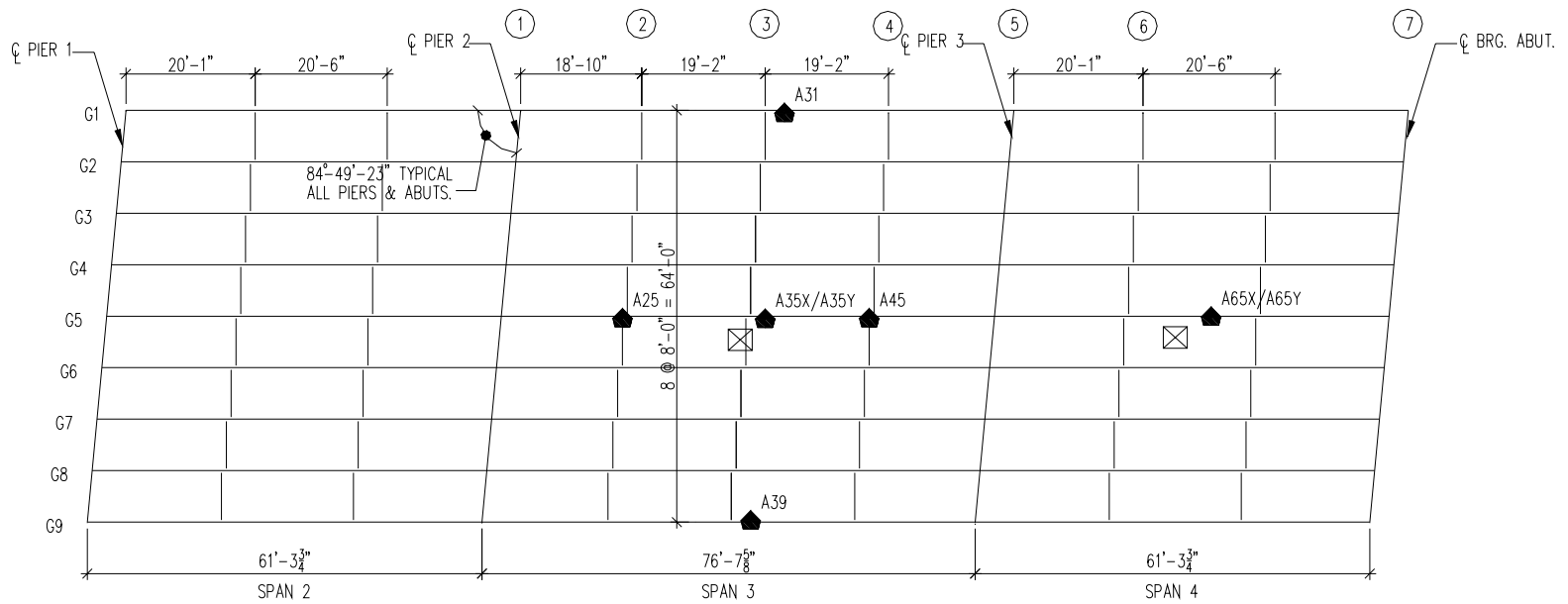
**Figure 6.8 Dimensions of Crossbow accelerometers** *courtesy of Crossbow*



**Figure 6.9 LF Series Crossbow accelerometer** *courtesy of Crossbow*

The accelerometer layout can be seen in Figure 6.10. The tri-axial accelerometers are denoted as A35 and A65, and are located at midspan of spans three and four, respectively.

ACCELERATION GAGE LOCATIONS & DESIGNATIONS



\*\*NOTE: THERE WILL BE ONE ADDITIONAL PRECISION DUMMY STRAIN GAGE & ONE ADDITIONAL STRAIN & TWO TEMPERATURE GAGES ON A HANGING THERMAL COUPON NOT SHOWN ON THE ABOVE PLAN.

⊠ BREAKOUT BOX

◆ ACCELERATION (6)

Figure 6.10 AutoCAD plan of bridge with accelerometer locations and designations

#### **6.1.4 Temperature Gages**

There are a total of eight temperature gages that were deployed on the bridge. Of the eight gages there are three resistance temperature detectors (RTD's), two standard thermocouples, and three surface temperature thermocouples. The RTD's are measuring steel temperature in three locations. One gage, RCOU, is measuring the material temperature of the steel coupon. The other two RTD's, R35 and R39, are measuring the steel temperature on the bottom flange of an interior and exterior girder, respectively. The purpose of the interior and exterior gage temperature measurements is to look at the temperature difference of the steel between a shaded and non-shaded girder and the effects the differential has on strain and deflection in the girder. The RTD's were purchased from Vishay-Micromeritics and can easily be spot welded to the steel to measure the temperature based on a resistance measurement. The gage outputs a resistance in microstrain and the microstrain is converted to a temperature. The conversion factor is ten microstrain per degree farenheight. A picture of an RTD temperature gage is shown in Figure 6.11 .

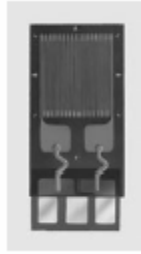


**Figure 6.11 Vishay Micromeasurements weldable temperature sensor** *courtesy of Vishay Micromeasurements*

Of the two standard thermocouples, T65 is reading general air temperature and the other, TD35, is reading deck temperature. The gage measuring deck temperature was grouted into a small hole that was drilled into the underside of the concrete deck. The purpose of installing a gage in the concrete deck is to examine the temperature gradient between the deck, which is directly exposed to sunlight, and the bottom of an interior steel girder, which is constantly shaded. The difference in temperature through the depth of the composite beam can induce bending stresses in the beam and these stresses can be quantified through the monitored strain data received from the vibrating wire gages.

The bondable surface thermocouples are located next to all the RTD's and are designated as TCOU, T35, and T39. The bondable surface thermocouples are a newer technology. The idea was to bond them near the RTD's, which are an older technology that has been tested and proven to work well, and compare the results. However, due to limitations on space in the data logger, which is discussed later in the wiring section of the paper, two of the bondable thermocouples were deployed and not

wired into the system. The bondable thermocouple on the steel coupon, TCOU, was wired into the system and will provide information on this type of gage's performance. A picture showing dimensions of the bondable thermocouple is located in Figure 6.12. All the temperature gage locations and designations are shown in Figure 6.13.

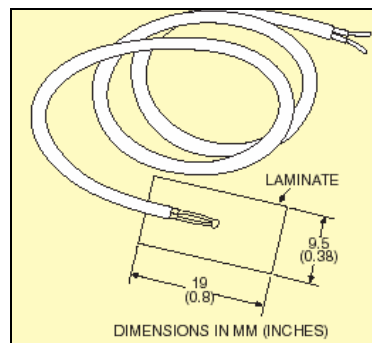
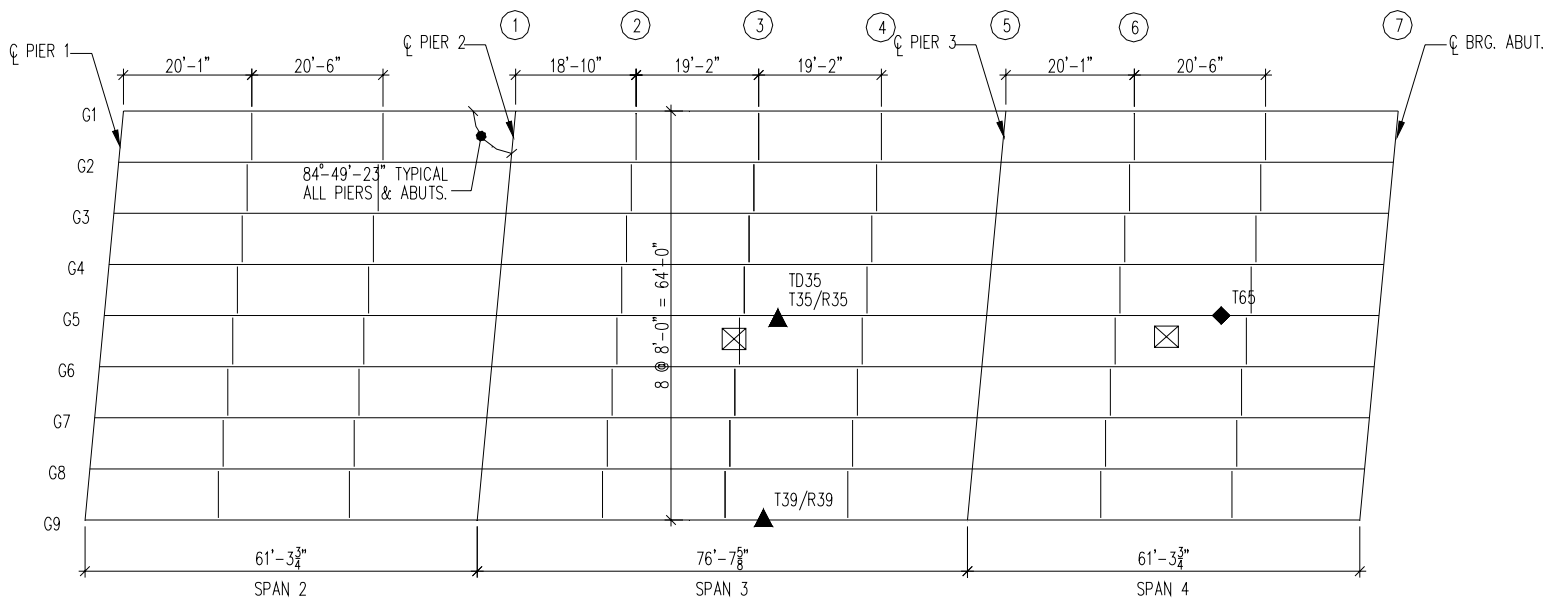


**Figure 6.12 Dimensions of bondable surface thermocouple** *courtesy of Omega*

TEMPERATURE GAGE LOCATIONS & DESIGNATIONS



\*\*NOTE: THERE WILL BE ONE ADDITIONAL PRECISION DUMMY STRAIN GAGE & ONE ADDITIONAL STRAIN & TWO TEMPERATURE GAGES ON A HANGING THERMAL COUPON NOT SHOWN ON THE ABOVE PLAN.

☒ BREAKOUT BOX

- ▲ SURFACE TEMPERATURE (5)
- ◆ AIR TEMPERATURE (1)

Figure 6.13 AutoCAD plan of bridge with temperature gage locations and designations

## **6.2 Data Acquisition System**

As discussed earlier in this section, two types of data are being recorded by the sensors, monitored data and event data. Monitored data is a scan of all displacement, vibrating wire, temperature gages, and the dummy and coupon strain gages every hour for about a two second period at a 0.45 Hz frequency. The low frequency is required for the slower reading vibrating wire gages. Event data is about a two second window of data that is triggered to record when there is an event, such as a truck driving over the bridge. The event data is read by all accelerometers, displacement gages, and foil strain gages except for the dummy and coupon gage. This data is recorded at a 100 Hz frequency. A 100 Hz scan rate is necessary to capture the trends data properly.

There is also the need for temporary data storage on the system and internet communication with the data logger. Ideally, monitored and event data will be recorded until temporary storage is full and the data will be retrieved via the internet to a permanent storage location to be processed and analyzed. Due to the previously mentioned data acquisition requirements, a high-speed data acquisition system with triggering, data storage, and internet capabilities is needed.

Mamie Lynch (2003), an NSF-REU student that worked on preliminary selection steps of the Smart Bridge project, researched various types of data acquisition systems. The Campbell Scientific CR9000X data logger was selected as the most suitable system for the requirements. The CR9000X is intended for applications requiring rapid scan rates, up to

4.5 kHz, and supports a large number of channels. There are 128 MBytes available for internal program and data storage, as well as an external PC Card memory option with various storage capacities. A 256 MByte PC Card was chosen for the Smart Bridge application. Nine available I/O modules can be configured with input or excitation boards based on the application. The CR9050 5 Volt Analog Input Module allows for fourteen input channels. One CR9060 Excitation Module can provide up to sixteen channels of 5 Volts excitation output. Of the sixteen channels there are six continuous and ten switched excitation channels. PC9000 Support Software, which is based on BASIC programming language, allows for straightforward program generation and also has different types of triggering capabilities. Communication with the CR9000X can either be done through a direct serial port connection or via the internet through an ethernet connection.



**Figure 6.14 Campbell Scientific CR9000X Measurement Control System** *courtesy of Campbell Scientific*

In order to house the CR9000X system, battery backup, any peripherals, and the modem for internet communication with the system, a 40" x 33" x 14" fiberglass enclosure was purchased. The fiberglass enclosure was secured to the concrete pier between spans three and four. A wooden platform with railings was also built near the enclosure for easy access to the system. A photo of the platform and enclosure setup is shown in Figure 6.15.



**Figure 6.15 Photo of platform & fiberglass enclosure**

Conduit was run underground from the nearest junction and up to the left side of the platform in order to house the electric and telephone line for power and internet connection to the data logger. Verizon is the internet service provider and Delmarva is the power supplier.

### **6.3 Wiring**

The basic wiring system for the smart bridge is comprised of standard gage wire soldered to the wire attached to the gage near the gage location and run to a junction box. At the junction box the gage wire strands are connected to wires in a trunk cable. From the junction box the trunk cables run to the CR9000X where the data from the gages is read. The only slight variation to this wiring scheme is that the vibrating wire

gages have their own gage wires running the entire length to the junction box where they are connected to the trunk cables like the rest of the gages.

Eight of the nine available I/O modules in the CR9000X were configured with input, excitation, and filter boards in order to accommodate the wires from the different gages. The nine available module compartments are filled with four CR9050 5 Volt Analog Input Modules three CR9060 Excitation Modules and one CR9052 Filter Module. There are fourteen available input channels per 9050 input module. Four input modules would thus support fifty-six gages. However, there are a total of sixty-one gages instrumented on the bridge. All gage wires were run to the CR9000 location, but three strain gages, S61, S63, and S67, and two surface thermocouples, T35 and T39, were not wired into the system. If, at a later time, information from the non-wired gages is desired, they can be swapped out with other gages. The strain gages that were not permanently wired into the system were gages that would provide information on transverse distribution in span four. There is already detailed information on transverse distribution in span three, so it was decided that these particular gages were not crucial for the desired information. The two surface thermocouples that were not wired into the system would be supplying the same information as the RTD's at the same location. Multiples of the same data from two different types of gages was therefore sacrificed due to the issue of channel availability in the logger system.

Seven trunk cables were run from the CR9000 to the two separate junction boxes located at mid span of spans two and three. The junction box at span three is denoted as the south junction box and span four's is denoted as the north junction box. Each trunk cable contains twenty-five wire pairs with unique color combinations. Three trunk lines run to the north junction box and four run to the south junction box. The junction boxes consist of 27" x 21" x 10" fiberglass enclosures that are secured to the bottom flange with metal frames and beam clamps. The trunk cables feed into the one side of the junction box and the gage wires feed into the opposing side of the box through nylon water tight pass throughs. Inside the junction box there are multiple terminal strips where the corresponding ends of the trunk cable wires and the gage wire ends are soldered together. A photo showing the interior of the south junction box is located in Figure 6.16.

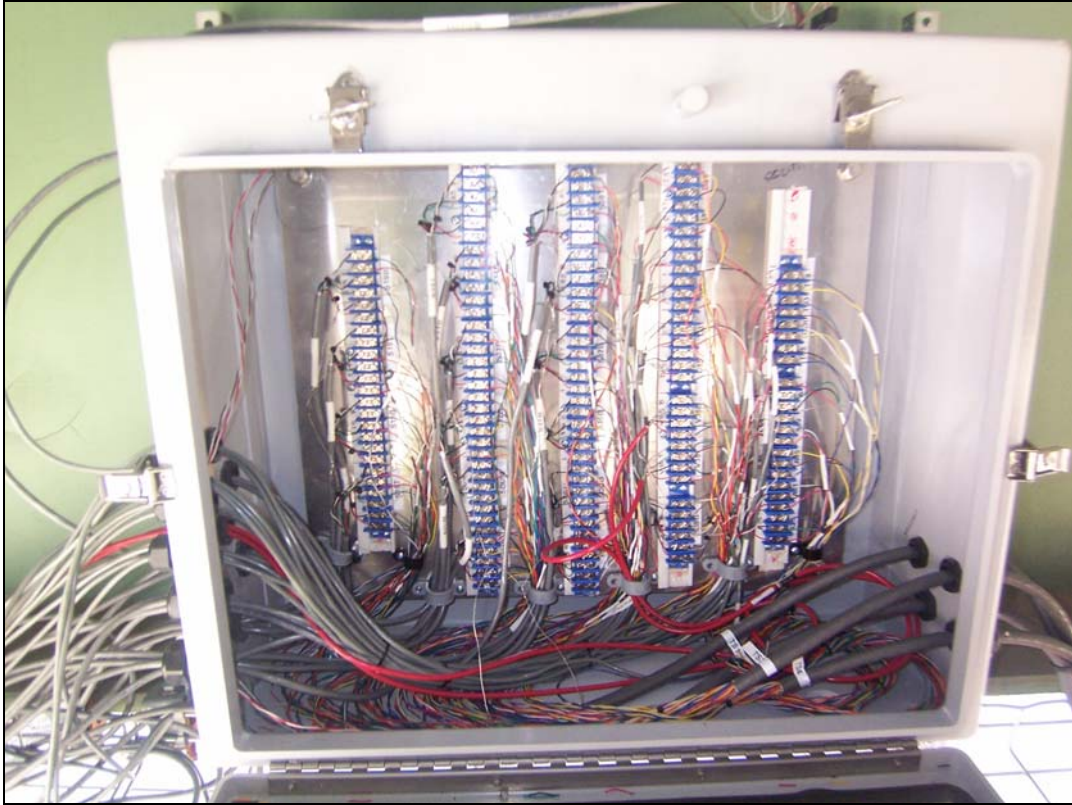


**Figure 6.16 Photograph of south junction box interior**

Six-conductor or three-conductor gage wire, depending on the gage type, was spliced to the trunk cable at the junction box and run to the gage location. The foil strain gages and RTD's are the only gages that require a six-conductor wire. Two of the wires are used for high and low input, two are used for excitation and ground, and the other two are used for shunt calibration, which only applies to the foil strain gages.

The string pots and single-axis accelerometers function similarly to each other and require three-conductor wire. Both types of gages have a red, white, and black wire coming from the gage. The red wire serves as

power, the white as input, and the black wire is ground. The excitation wire for the string pots plugs into a peripheral regulated 12 Volt excitation terminal located in the junction box. One key aspect is that the outside power source must be grounded to the same plane as the CR9000. Thus, a jumper was run from the ground terminal of the 12 Volt box to any ground terminal on the CR9000 system. The ground wire of the string pot can plug into either the ground of the outside power source or a ground terminal on the CR9000. The tri-axis accelerometers have a red and black wire for excitation, like the single-axis, along with three other wires for the input of each axis. The input wires coming from the gages are white, yellow, and green and refer to the x, y, and z axis, respectively. Three-conductor wire was used for excitation, ground, and the x-axis input wire. Then two-conductor wire was used to connect the additional input wire for the y-axis reading.

Thermocouples require only two-conductor wire since they are only reading the resistance between two different types of wire. However, since there is only three and six conductor wire, the three-conductor was used for the wire run from the gage to the junction box. Unlike any of the other gage types, thermocouples require thermocouple wire at the gage site and at the connection to the logger box. Therefore, a small length (~10 inches) of thermocouple wire was soldered to the trunk cable wire at the data logger box and inserted in the appropriate channels.

The vibrating wire gages require a four-conductor wire that comes pre-attached to the gage when it is shipped from the supplier. Two

of the four wires are input and ground for the thermistor measurement from the gage. The other two wires are the high and low input wires that connect to the filter module for the actual frequency based strain reading from the gage. Jumper wires run from the high and low inputs in the filter module to the designated excitation and ground channels as well to provide excitation to the gage.

Two different size zinc plated steel trays fabricated by McMaster-Carr were used to run the wires in. Four inch wide by two inch deep tray was used for the trunk cables and places where there was a large number of smaller wires running. Two inch wide by two inch deep tray was used in areas where there were not as many wires being run. The four inch wide tray was also encased around the seven trunk cables running out of the box and up the concrete pier. The tray was screwed into the pier with masonry screws and the wires were zip-tied to the tray in order to resist the wires from falling away from the pier. The tray holding the other wires was hung from the bottom flange with steel beam clamps. The wires running in trays from the bottom flanges were also zip-tied to the tray to provide additionally neatness and security to the wires.

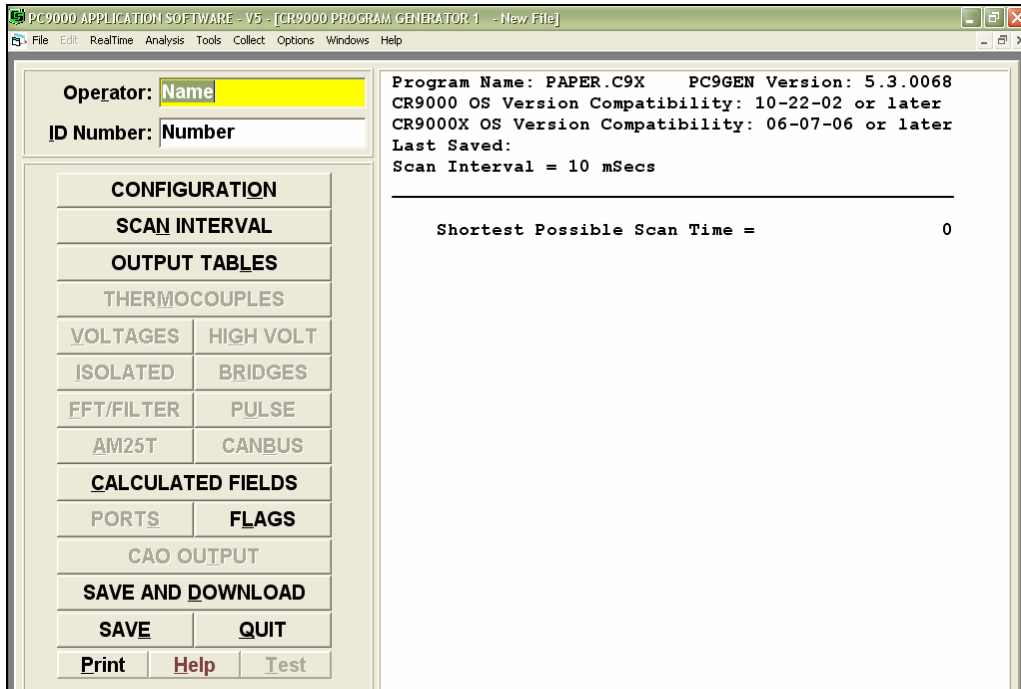
#### **6.4 Data Logger Programming**

The CR9000X data logger data acquisition programs can be written two different ways, through the PC9000 program generator or the CRBasic editor, which serves as the basis behind the PC9000 program. The program generator version is the more user-friendly way to program with easy to use icons and buttons. By using the program generator a

Basic file is created with the actual computer language that the data logger can read. However, PC9000 provides only the basics of programming the logger and does not allow for more complicated programming, such as triggering off multiple gages, triggering every hour for monitored data, and programming of vibrating wire gages. The Basic editor functions on Basic computer language and entering actual code, which allows for more complex data acquisition programs. Once anything is programmed in CRBasic the user cannot revert back to the PC9000 version because PC9000 will restore the program to default settings and erase anything that was entered manually into the Basic editor.

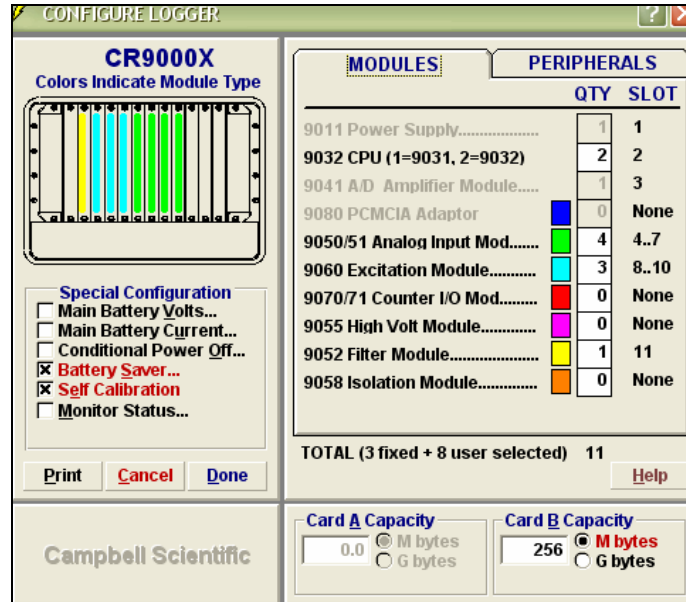
Since the program generator is much easier to use when the user is not fluent in Basic computer language, any thing that could be entered through the generator was. Appropriate module, scan rate, and output table specifications were made through the code generator. All the gages, excluding vibrating wire gages, were programmed through the PC9000 generator as well. Aliases, which were the gage designations, were also specified. The following sections give an overview of programming in the PC9000 program generator. However, specifics and more in depth capabilities are best explained in Campbell Scientific's *CR9000X Measurement & Control System Training Manual* (2002). Everything shown about programming in the following sections is also detailed in the training manual.

The picture in Figure 6.17 shows the main screen of the PC9000 program generator without any specifications made.



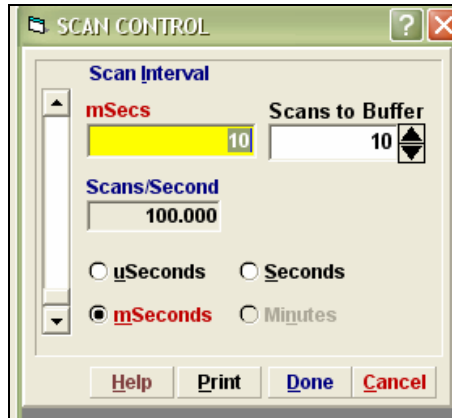
**Figure 6.17 PC9000 program generator main screen**

From the main screen the first step is to set the configuration, which deals with which modules are being used in the data logger. By clicking the configuration icon in the main screen, the screen shown in Figure 6.18 appears. In the configure logger box the number of input, excitation, and filter modules was specified. The program generator then automatically tells the user where to place the individual modules in the CR9000 data logger. The following configure logger box also prompts the user to specify the size of the memory card being used to store output table data.



**Figure 6.18 PC9000 program generator configure logger specification window**

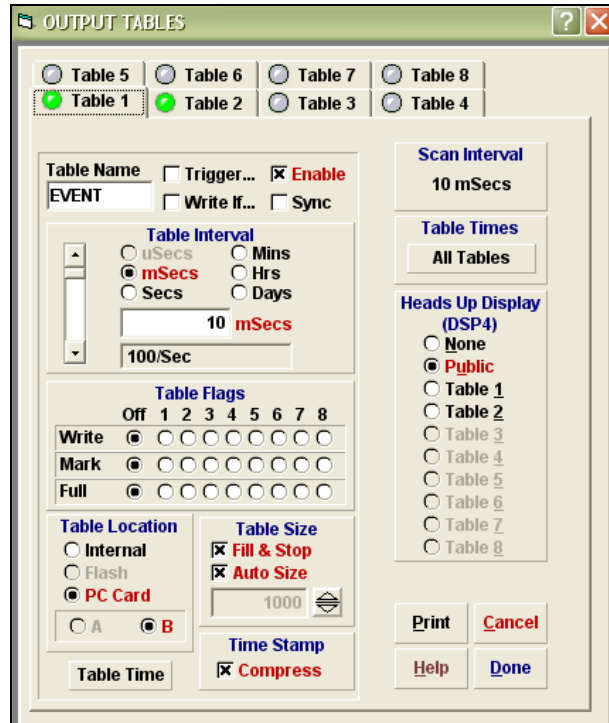
The next step is to set the scan interval. If the "Scan Interval" icon is selected from the main program generator page, the following window, shown in Figure 6.19, will appear.



**Figure 6.19 PC9000 program generator scan control window**

As can be seen in the sample window above, the units and the size of the scan interval can be specified. The user can also set the scans to buffer parameter. The scans to buffer sets the number of scans that processing can lag measurements without having skipped scans (loss of data). Once the scan interval is set the program generator automatically calculates the according amount of scans per second.

The next step in creating the logger program is to create output tables. There were only two output tables needed for the smart bridge application, however, PC9000 can program up to eight tables. If the "Output Tables" icon is selected in the main window of the generator, the specification box shown in Figure 6.20 will appear.



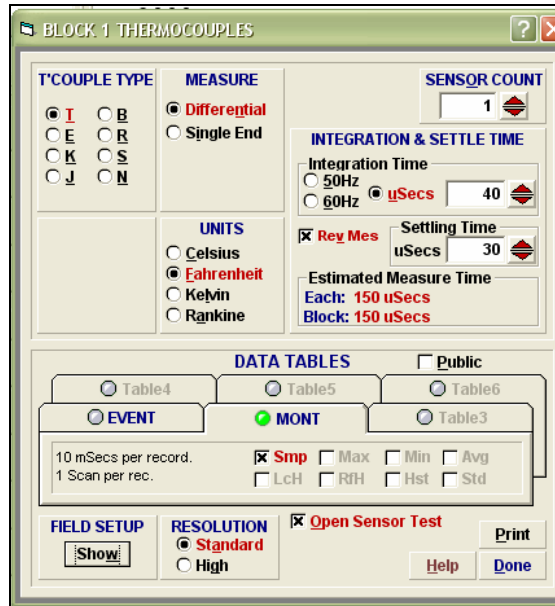
**Figure 6.20 PC9000 program generator output table specification window**

Table names, basic triggers thresholds, and the rate at which the table records scanned data can all be set in this window. A table flag is another way to trigger a table, however, this would be done manually by hitting a flag button. The location, either to the internal memory or the PC card, of where the output table is written to is specified in this window as well. The table can either be set to a certain size or auto sized. When the table is auto sized it will just be sized based on the available memory on the PC card or the internal memory, depending on where it will be written to. If the user wants the PC card or internal memory to fill to the specified amount of data and stop recording, then the fill and stop box shall be

checked. If this box is not checked the logger loops around and continues to write over existing data when the table fills up, which could lead to loss of important data.

The only steps left are programming in the different types of gages that will be read by the data logger. Thermocouples are programmed under the "Thermocouple" icon. Foil strain gages, accelerometers, and RTD's are all programmed in the "Bridge" section. Lastly, string pots are programmed under the section "Voltage". The program generator creates something called a block, which is gages in the same section, of the same type, and programmed with the same specifications. Therefore, within bridges there are multiple blocks since all gages within the bridge section are not of the same type and all strain gages will not be read to the same output table. The majority of the foil gages will be read to the event table. However, the dummy and coupon gages will be read to the monitored data table, so they must be in a separate block. The idea of blocks should become clearer as the different programming of gages is discussed.

Thermocouples are the most straightforward gage to program. The screen that appears when programming a thermocouple is shown in Figure 6.21.



**Figure 6.21 PC9000 program generator thermocouple specification window**

The settings that are shown in the window above are the default setting when the thermocouple icon is chosen. All the defaults remain unchanged for the use of standard and bondable thermocouples unless the user prefers different output units. In the lower portion of the window the output table is specified. In the case of the smart bridge all thermocouples are reading to the monitored data table. This window also allows for the setting of aliases by clicking on the "Show" button under Field Setup.

Foil strain gages, RTD's, and accelerometers, are all programmed under bridges. However, multiple blocks must be created since each gage has different specifications associated with it. When the "Bridge" icon is selected, the window shown in Figure 6.22 appears.

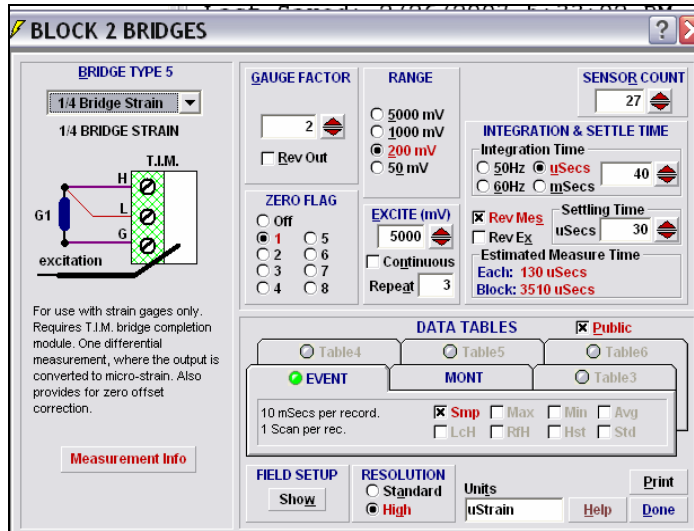


**Figure 6.22 PC9000 program generator bridge specification window for foil strain gages**

The window that is shown above is the setup for a foil gage. The type of gage for the smart bridge application is made up of a quarter bridge completion module, so that is what was chosen in the drop down menu in the top left corner of the window. The integration and settle time were the default values for a quarter bridge type. Due to the number of strain gages that were used on the bridge, three gages shared one excitation channel. This sharing of excitation voltage is accounted for by typing the number three in the "Repeat" box. A zero flag has also been set so that when flag one is up all strain gages in this block will be zeroed. The block above represents the foil gages that will record during an event, therefore the sample box under the event table has been checked. The coupon and dummy gages are located in another bridge block with the same settings as shown above but have the sample box checked under the

monitor table. The coupon and dummy gages were set to zero when flag four is high.

The RTD's are programmed quite similarly to the foil gages since they both function on the principle of resistance. The window in Figure 6.23 shows the settings for programming the RTD's.

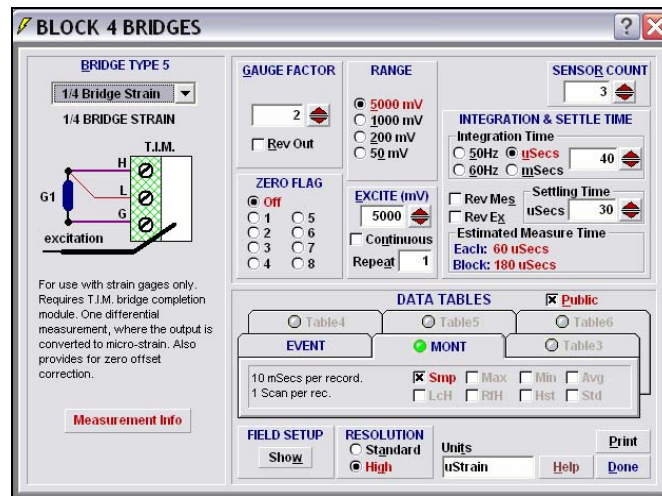


**Figure 6.23 PC9000 program generator bridge specification window for RTD's**

The only differences between programming the RTD's and the foil gages are that the range was set to 5000 mV, there is no reverse measurement, and no zero flag was set. A zero flag is not wanted in this case since the temperature should not be reset to a zero value.

The accelerometers are programmed slightly different than the previous discussed bridges. The window displaying the accelerometer program settings is shown in Figure 6.24.

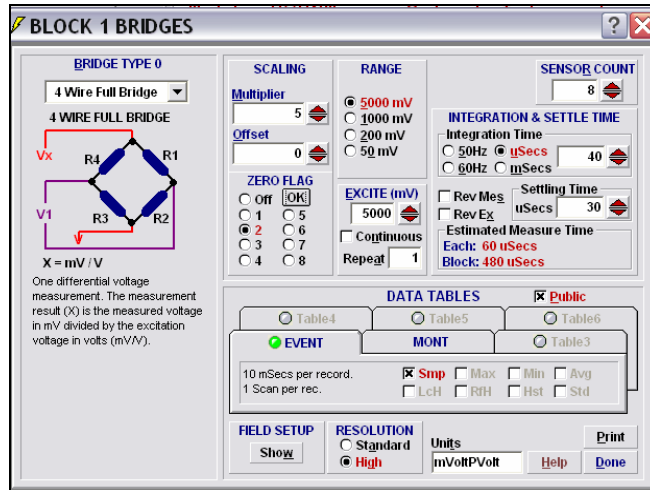


**Figure 6.24 PC9000 program generator bridge specification window for accelerometers**

The accelerometers are programmed as a four wire full bridge and are set with a default scaling multiplier of five. The integration and settling times were left as the default values. The accelerometers were set to be zeroed when flag two is high and were set to output in the event table. As can be seen in the figure above, the sensor count is set at eight, yet, there are only six actual acceleration gages. Since two of the gages are taking lateral and vertical accelerations, the program needs to read two separate outputs. Therefore, gages A35 and A65 have two output aliases each of "A35X" and "A35Y" and "A65X" and "A35Y".

The string pots were programmed as voltages. The window shown in Figure 6.25 appears when the "Voltage" icon is selected in the main screen of the program generator.

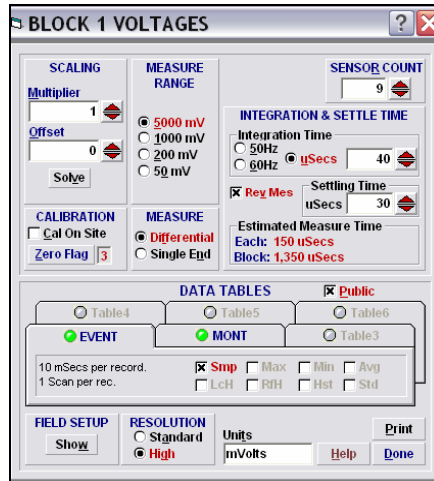


**Figure 6.25 PC9000 program generator voltage specification window for string pots**

The default multiplier for a voltage is one. All the multiplier represents is the slope of the line for the measurement instructions. The integration and settling time settings were left at the PC9000 default values. The string pots were set to zero when flag three is high and to output to both the event and monitored data tables.

If the user was satisfied with the basic specifications available in the PC9000 generator, the save and download icon could be selected in the main screen of the generator and the program would download to the data logger. Once the program downloads to the data logger it begins scanning immediately as long as the "run now" box is selected in the download window. However, due to the use of vibrating wire gages and more complex triggers, programming was extended to the basic code form for the smart bridge application.

Programmers from Campbell Scientific wrote the Basic code for the vibrating wire gages and sent the program to the university via email. The program that was developed allows the data logger to switch between a fast scan rate and a slow scan rate that is necessary for the vibrating wire gages. The program also includes all necessary code for the vibrating wire gages to scan and output data. An additional program, internal to the vibrating wire program, was also developed by the programmers from Campbell. This program was permanently downloaded to the data logger and is called on by the vibrating wire program. The Basic code for all other gages that was created from the program generator was combined with the vibrating wire code. The multiple gage triggers were also set in the Basic code once the two were combined. A copy of the entire Basic code that supports all gages, excluding gages that could not be accommodated by the fifty-six input channels, is located in Appendix C.

## **6.5 Installation**

The first step in the installation was building the platform and installing the fiberglass enclosure and occurred in October of 2006. Gary Wenczel and Danny Richardson performed the installation in roughly two eight hour working days. Shortly after the platform and box were installed DelDOT ran conduit for the DSL and power line.

The AutoCAD drawings of the different gages and their locations provided an organized way of planning wire and tray layout designs and the location of the junction boxes. After the tray and wire layouts were decided, they were also drawn on the plans in CAD. From the drawings

the proper calculations of estimated tray and wire that was needed were made. All measurements were over estimated by about five to ten feet in order to avoid any shortages. Wires and trays were ordered as soon as necessary footages were known.

In mid December of 2006 a 65 foot telescoping boom was rented from a local rental company for a week. The lift was delivered on site December 12 and picked up December 19. Although the lift is rented out for a seven-day week, the company monitors the hours the lift is run during that rental period and limits the allowable running time to forty hours. Anything over forty hours would be considered an overcharge. During that week all the trays were installed, all trunk cables and regular gage wire were run, and the junction boxes were installed. All gage wires received shrink-tube labels corresponding to their particular gage designation. The ends of the trunk cables running into the large fiberglass enclosure were splayed out and combinations of the pairs were assigned to the different gages. The pairs assigned to the individual gages were shrink-tubed together and labeled with the corresponding gage designation. All color combinations and corresponding trunk cable were recorded on site and later put into an Excel spread sheet in order to keep track of which wire pair went to which gage. The table of trunk cable wire pairs is located in Appendix B. Some gage wire ends were soldered inside the junction box to the terminal strips, however due to the time constraint from the lift rental, not all the connecting was completed. During the five working days with the lift there were five different people working in the

field. Not all five people were there at all times during the week. There were usually at least three people present at the bridge working on the installation. Each person's field hours were tracked over the week and a total of 185 man hours were recorded.

In January of 2007 Verizon installed the phone line to the site to allow for DSL communication. Delmarva installed the power line in the beginning of February 2007.

A second phase of installation occurred from mid March to the beginning of April 2007. This time the lift was rented for a month from March 12 until April 9. During this installation phase a lot of time was initially spent wiring the junction boxes and the main box where the data logger is located. All wire ends had to be stripped and soldered in order to prevent the ends from fraying. The DSL internet connection was established and the electrical outlet was also installed. Having a functioning power source was vital at this stage in order to test the gages and other equipment. The majority of the time there was one person in the lift and one person working on the ground. The person in the lift handled all the wiring of the junction boxes and installation and wiring of the gages. The person on the ground wired the main box, controlled the data logger program, and verified the gages were all functioning properly. By having a laptop out at the site and directly connecting to the data logger, the real time data showing the gage readings could be viewed and it was determined if the gages were reading correctly. A third person was

sometimes needed for additional help in the lift or on the ground doing any possible prep work for installation.

Once all the wiring was completed in the junction box, gages were installed at their appropriate locations. All gage locations had to be prepped by grinding the paint off the girder to ensure proper bonding of the gage. The accelerometers were bonded with epoxy directly to the girder and the protective plastic case was placed over top and sealed with RTV. The foil gages were spot welded to the girder and wires were soldered to the bridge completion modules at the gage location. The gages and bridge completion modules were covered with the plastic protection and also sealed with RTV. Bondable thermocouples and RTD's were attached to the beams in the proper locations with epoxy. A small hole was drilled into the underside of the deck and a thermocouple was grouted in the hole for reading deck temperature. The string pots were the last portion of the installation. The installation of the unit to the beam was straight forward; however, the stationary cable system was not as simple. The cable that was strung from the piers to serve as a base point for the string pots seemed to not be strong enough. This issue is further discussed in Chapter 7 in the current status section.

The foil gages consumed a large portion of the gage installation time since that was the type gage there was most of. The vibrating gages were the most time consuming per gage since they required the most in depth installation procedure. A lot of time was spent trying to make the string pot cable work, but this installation time can be reduced once a

solution to the problem is made. As stated before, there were usually two people at the site during this phase, and sometimes a third person was needed. The hours were tracked and a total of about 245 man-hours were recorded for the second portion of the installation.

Based on the experiences with this instrumentation project, an anticipated schedule for an entire instrumentation project was created. The first permanent instrumented bridge in Delaware was part of a master's thesis and the majority of work was performed by a graduate student. The anticipated schedule assumes that future work will be done by a full time specialist that is already skilled in the necessary areas to carry out the required tasks. The schedule is shown in Table 6.2.

**Table 6.2 Anticipated Schedule for Future Bridge Instrumentation**

Task	Months from Start of Project											
	1	2	3	4	5	6	7	8	9	10	11	12
1. Bridge Selection & Site Visit*	■											
2. Define SHM Objectives	■											
3. Diagnostic Tests		■	■									
4. FEM Model			■	■								
5. Design SHM System <sup>+</sup>				■	■	■						
6. Gage & Wiring Layouts					■	■						
7. Purchasing & Procurement						■	■					
8. Data Logger Programming							■	■	■			
9. Gage Testing (In-Lab)							■	■	■			
10. Develop Reporting Protocols								■	■			
11. Installation										■		
12. System Validation											■	■
13. Finalize Reporting Protocols												■

**6.6 Costs**

Throughout the project, a running list of what had been purchased and what still needed to be purchased was kept in Microsoft Excel. Some items had set prices, such as known types of instrumentation, and exact future expenditures could be known. However, items such as building materials and unknown accessories to gages were not known exactly and could not always be projected accurately. Therefore, the amount of money that still needed to be spent throughout the project was not always known. Table B.3, located in Appendix B,

\* Step 1 includes obtaining bridge plans, ratings, inspection reports, and the assessment of the structure.

+ Step 5 includes choosing types of gages and data logger for the system and addressing power and internet sources at the bridge site.

summarizes all expenditures, excluding labor and travel costs, necessary for the permanent instrumentation project. If this prototype were to be applied to another bridge the majority of the prices would vary. There would be somewhat of a variance because the majority of the cost is based on the instrumentation, which can vary widely among different bridges. However, this cost summary serves as a basis to project costs for a similar application with any other size or type of bridge.

An entire cost summary including labor and travel costs was created. The labor costs are projected based on an engineering wage rate of \$35.00/ hour. Although the time spent on this project spanned about an eighteen month period, future instrumentations will be more industrialized and the hours will be compressed into a shorter time period. Table 6.3 is a summary of all costs associated with the permanent instrumented bridge

**Table 6.3 Summary of total costs for permanent instrumentation of Bridge 1-821**

**Summary of Costs**

**Hours**

Planning/ Prep/ Site Visits (Estimate of 4 hrs/wk for 18 months)

4 hrs/wk \* 4 wks/mnth \* 18 mnths = 288 hrs → 288 hrs

Instrumentation (From recorded hours)

430 hrs → 430 hrs

**Total Labor = 718 hrs**

Estimated Cost of Labor = \$35.00/ hr

\$35.00/hr \* 718 hrs = \$ 25,130 → \$ 25,130 \* 2.5 = \$ 62,825.00 (labor cost)

**Travel (Fuel Cost)**

All trips to the site (Estimate 10 trips/wk for 4 wks)

10 trips/wk \* 4 wks = 40 trips

40 trips \* 20 miles/trip \* \$.40/mile = \$320 → \$ 320 / vehicle

\*Assume two vehicles travel to the site → \$320 /vehicle \* 2 = \$ 640.00 (travel cost)

**Instrumentation**

Gages & Data Logger → \$ 32,200.00 (instrumentation)

**Materials/ Supplies**

All other materials needed for instrumentation → \$ 12,200.00 (misc. materials)

**Table 6.3 continued**

***Lift/ Access***

Cost of lift rental and fuel for the lift

→

**\$ 4,700.00** (*lift/ access*)

---

**Total Cost = \$112,565.00** / *61 gages*

→ **\$1,845.33** **per gage**

\*\*Note: Phone/ Internet/ Power will also be an incurred charge

The hours associated with planning, preparation, and site visits are an estimate and relate to a graduate student's schedule, as well as instrumentation hours. As stated before, these hours will essentially be the same, but just compressed over a shorter amount of time. However, the cost associated with these hours is based on an engineering rate so it would remain the same if this instrumentation was performed by a company. Travel cost for site visits is based on assuming two vehicles travel to the site and the bridge is only 20 miles away. It also assumes a fuel cost of \$0.40 per mile. Instrumentation costs, including gages, data logger and accessories, and all other miscellaneous materials, are rather accurate since it is based on the cost record that was kept over the course of the project. The cost of access to the bridge is based on two separate lift rentals of one week and one month. This cost could change slightly if the week long rental was excluded and the instrumentation was compressed into one month. If the installation process was consistent with 40 hour work weeks, it is possible that instrumentation could be completed in one month.

The total cost of \$112,565.00 divided by 61 gages results in a cost of roughly \$1850.00 per gage. This price is slightly under the LTBPP's estimation of \$2000.00 per gage. DelDOT's cost of highway bridges is \$300.00 per square foot. The cost of Bridge 1-821, based on a deck area of 14,000 sq. ft. (200 ft x 70 ft), is \$4.2 million. Therefore, instrumentation costs represent about 2.7 percent of the total cost of the

bridge. This percentage is minimal to the total cost and can benefit the bridge owner by redirecting their costs more efficiently.

## Chapter 7

### **CURRENT STATUS & FUTURE WORK**

As of April 2007, all sixty one gages have been installed on the bridge and all fifty six gages that were chosen to initially be connected into the system are wired in. The planning and installation took 18 months to complete. Based on total hours of effort (at an assumed engineering rate) and equipment costs the entire cost of the project was estimated to be \$112,565. The cost translates into an average cost of about \$1,850 per gage. The total cost of the installation represents approximately 3% of the cost of the bridge.

All accelerometers and strain gages have the necessary gage protection and have been protected from the environment with RTV. All gages are calibrated and functioning properly except for the potentiometers (string pots). The cable that was run from the piers to provide a stationary reference point for the potentiometer seems to be too flexible. The real time event data recorded by the potentiometers does not show any deflections in the girders from ambient traffic. The occurrence of an event was clear from mid span strain gages peaking, and at the corresponding time there was no response from the displacement gages. In order to verify that the string pots were themselves functioning properly, one string pot with a cable referencing ground was placed next to a string pot that was connected to the cable strung from the piers. The

string pot referencing ground displayed deflections that occurred simultaneously with mid-span strain gage peaks. The original connection at one side of the pier included a large spring in order to account for any change in length due to temperature effects. The spring was removed to see whether it was relieving the tension in the cable when the beam would deflect and the potentiometer would pull up on the cable. Unfortunately, when the spring was removed, the string pots were still not reading any deflections.

Although a large portion of the project has been completed, there is still future work to be done. Due to power lines located near the bridge, there is a considerable amount of noise in the data. This problem needs to be addressed by either filtering the post-processed data or by installing low pass filters on the CR9000 data acquisition system to filter the data as it is recorded. The triggers that signal an event and the initiation of recording data still need to be set. The trigger must be set to a threshold that is high enough to skip random data and low enough to actually catch the event. Therefore, study of the ambient traffic data needs to be done to figure out the data trends and what a reasonable trigger value would be. The area of data processing also needs to be handled. There needs to be an organized system of retrieving the data from the acquisition system, storing it to a permanent location, and then analyzing the data. The analysis of the data should result in summary reports of key components of the bridge's behavior and integrity that would be important to bridge owners. An ultimate goal associated with the

project is to have a web interface that can be accessed by the DOT that will display real time data from the bridge and key information about the bridge's health and status. Another future goal is the installation of a weigh-in-motion (WIM) system on the bridge. It is important to know associated weights of vehicles that cause large strains or displacements in the bridge. Another way to characterize the loads would be to install a camera at the bridge. However, a camera only gives a picture of the vehicle crossing and not the actual weight. One other aspect that was not addressed entirely was the installation of environmental gages. There are thermocouples and RTD's to measure air and surface temperature. However, the LTBPP recommends measuring other environmental factors like UV, humidity, precipitation, and wind speed. One solution to this problem may be to just record these environmental factors from a local weather station. Although the recordings would not be directly from the bridge location, the conditions at the bridge would most likely be very similar.

Having gone through the planning and instrumentation process, many lessons have been learned. One lesson learned was from the string pot setup. It would have been useful to have simulated the cable setup planned for the field in the laboratory. In this way, an appropriate cable and attachment method could have been validated. Another recommendation is to select a bridge that is not located near high-tension power lines. The noise problem created by the lines, and the need for additional filtering, can be avoided by choosing a bridge that is not located

close to power lines. Prior to installing, the entire field system should be set up and tested. While each individual gage type was tested one at a time, it would have been useful to connect all the gages to be installed in the field to the system in house and to have tested the functional capability of the entire system.

In summary, although there may have been some minor set backs during the project, a large portion of the work has been completed. A calibrated finite element model was created and compared to diagnostic test results, which is a key element in the process. As discussed in the introduction, the LTBPP has recommendations on which types of gages will be used on permanently instrumented bridges. The recommendations were followed and the majority of the gages were installed on the prototypical bridge. Only WIM sensors and weather related gages were not included in the Delaware bridge. Detailed records of instrumentation costs and hours of work associated with installation were recorded and presented. All work completed in this portion of the first permanent instrumented Delaware bridge can be replicated and used on future long term instrumented bridges.

## **APPENDIX A. SAMPLE POWER AND CROSS SPECTRA**

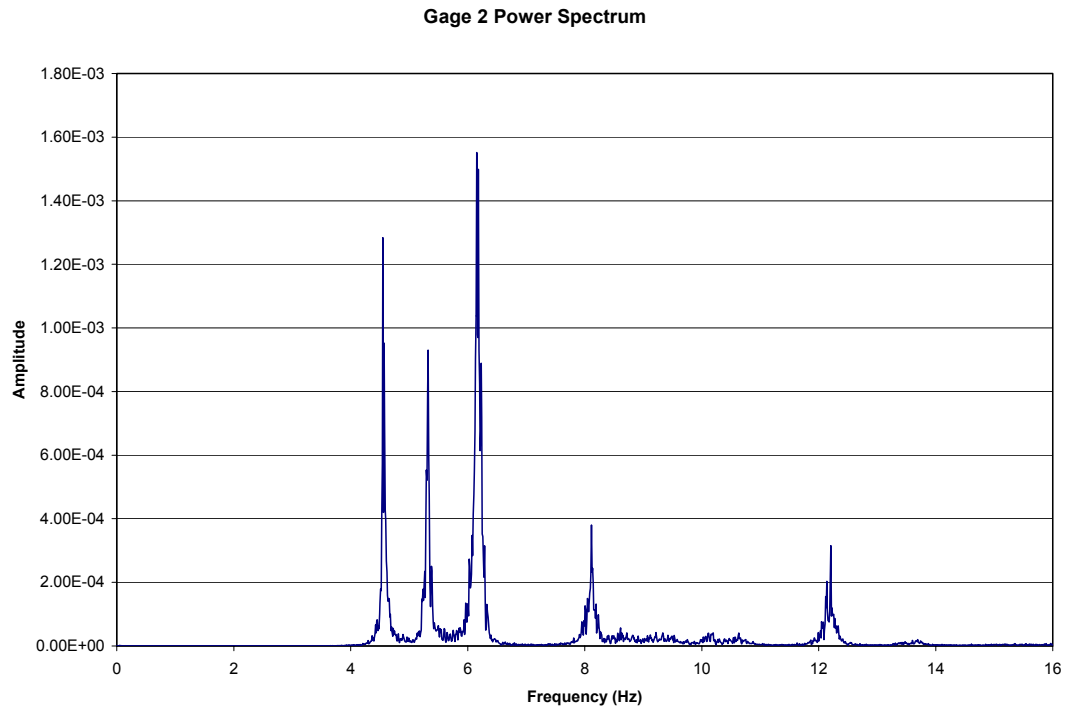


**Figure A.1 Gage (2) power spectrum**

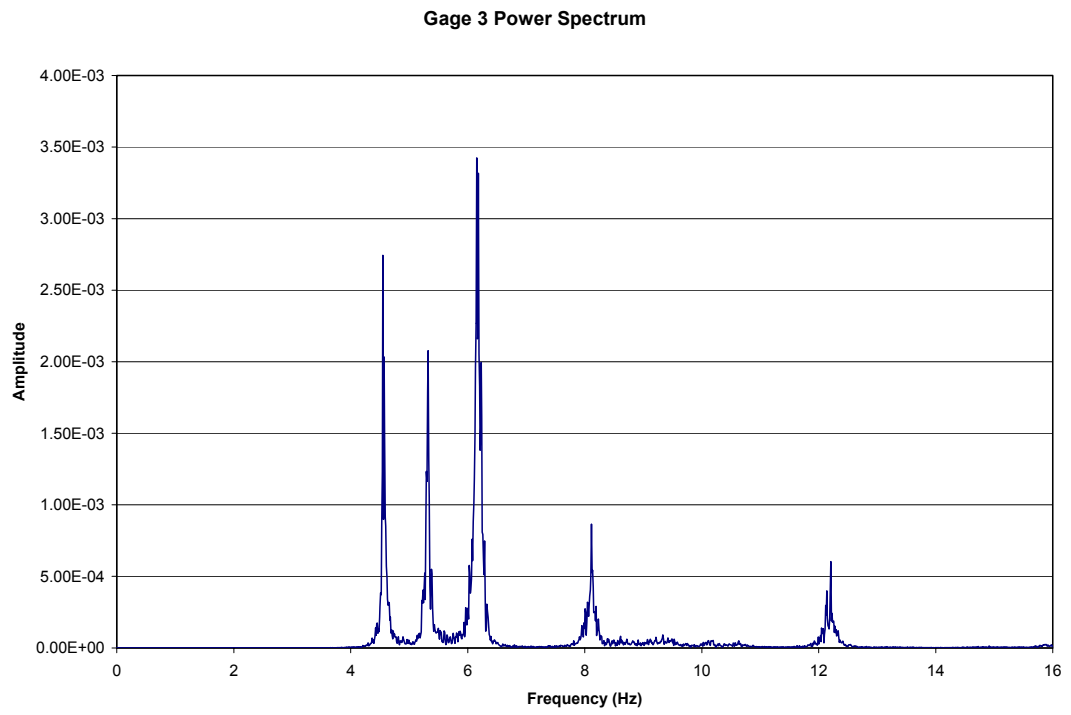


**Figure A.2 Gage (3) power spectrum**

Gage 4 Power Spectrum

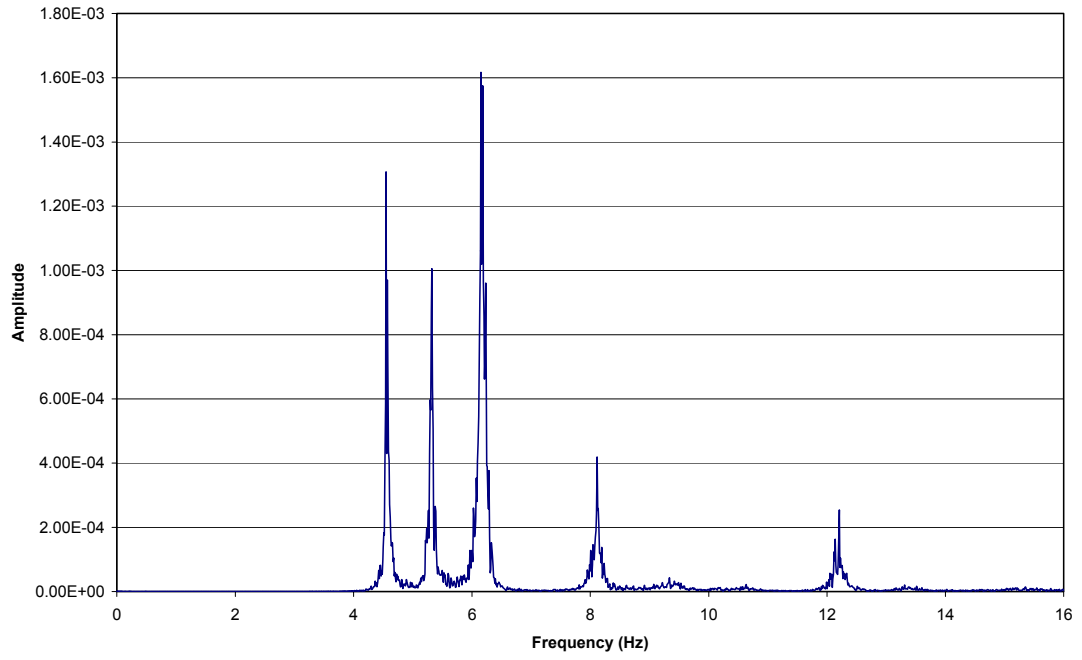


Figure A.3 Gage (4) power spectrum

Gage 5 Power Spectrum

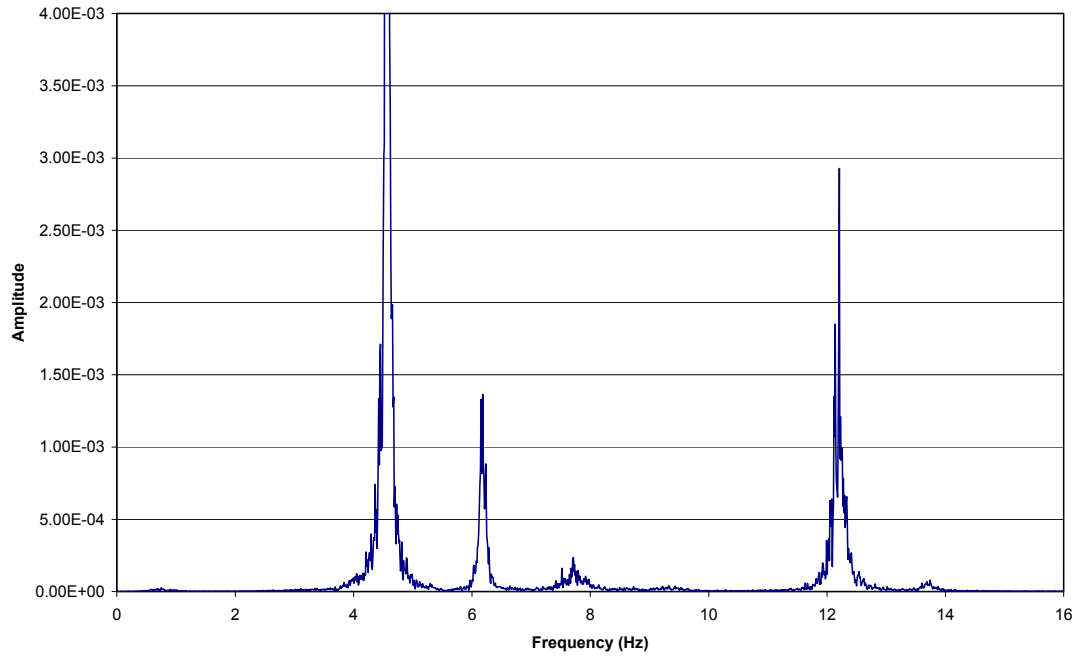


Figure A.4 Gage (5) power spectrum

Gage 6 Power Spectrum

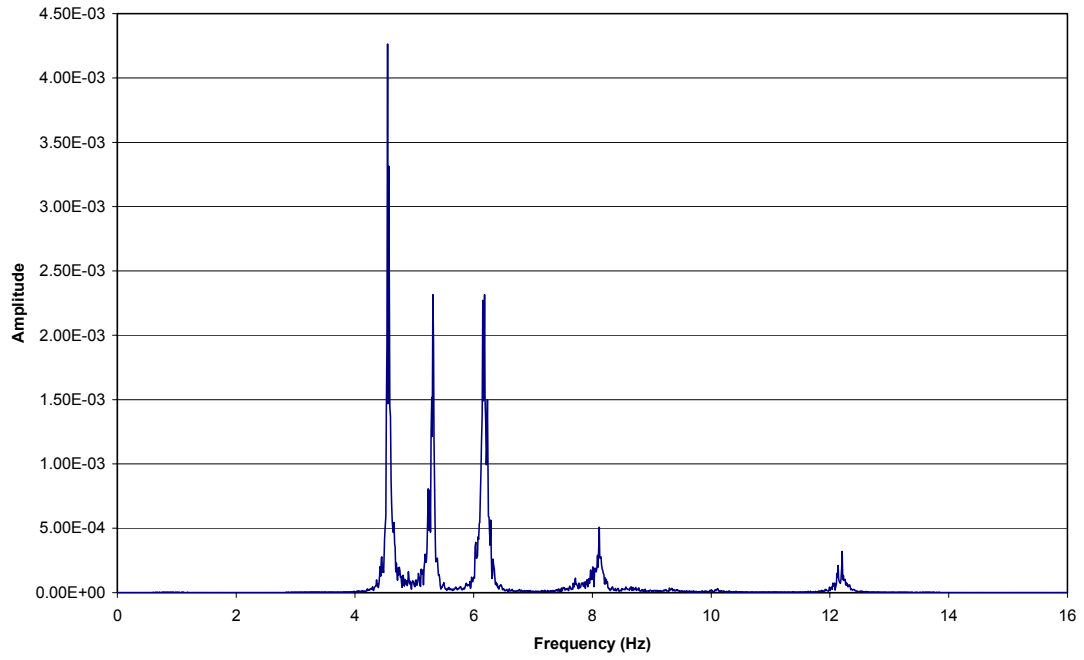
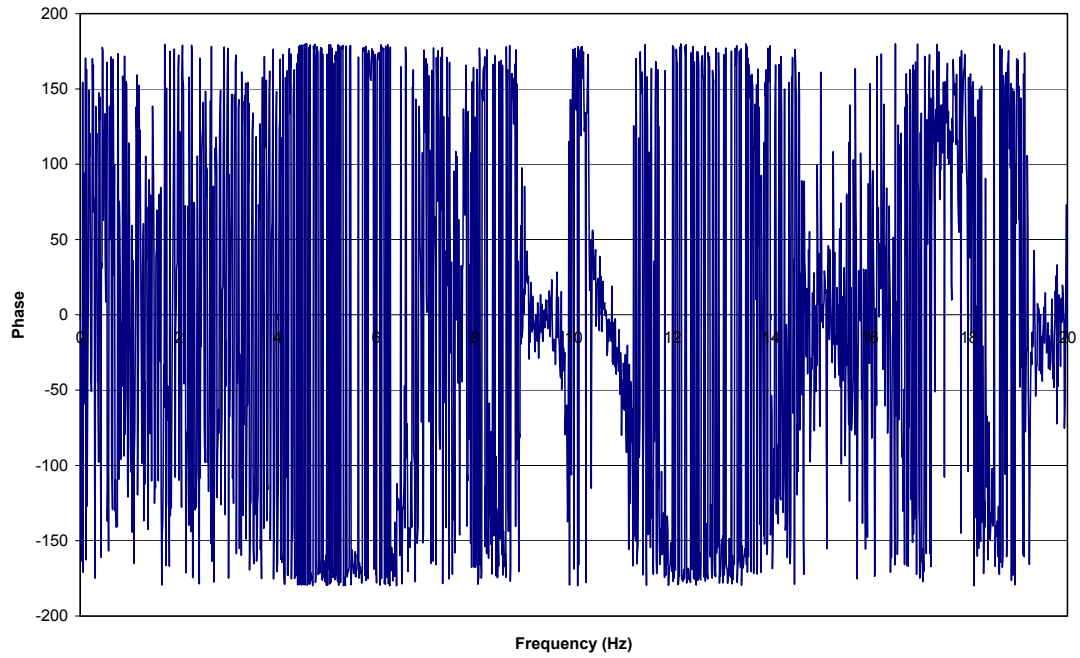


Figure A.5 Gage (6) power spectrum

Cross Spectra of Gage 1 w.r.t. Gage 3



**Figure A.6 Cross spectrum for gage (1) with respect to gage (3)**

Cross Spectra of Gage 2 w.r.t. Gage 3

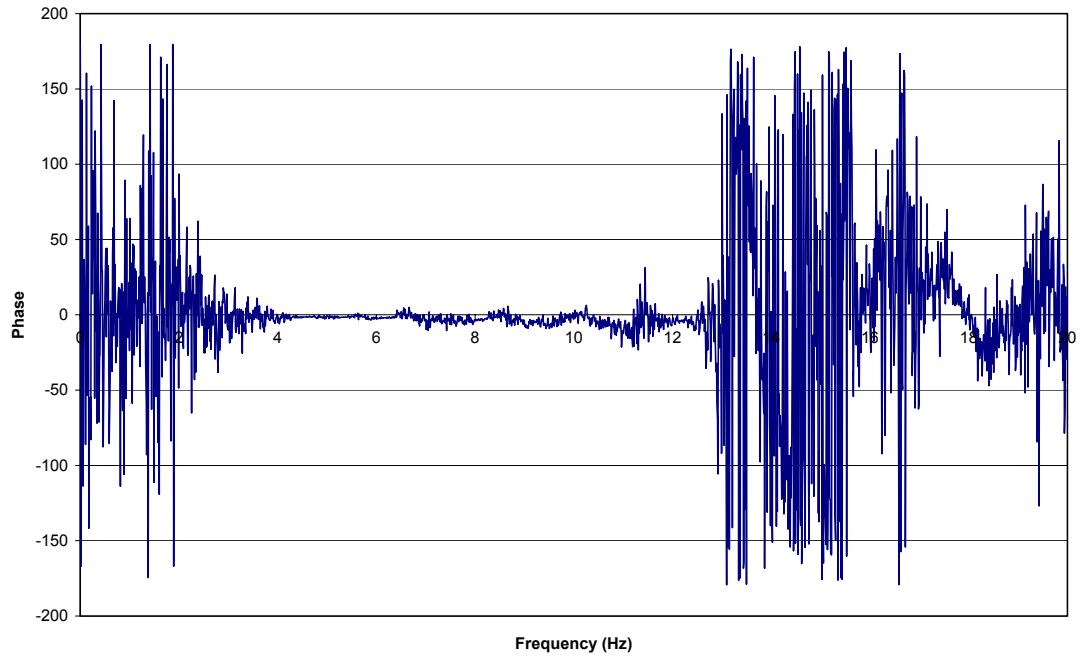


**Figure A.7 Cross spectrum for gage (2) with respect to gage (3)**

Cross Spectra of Gage 4 w.r.t. Gage 3

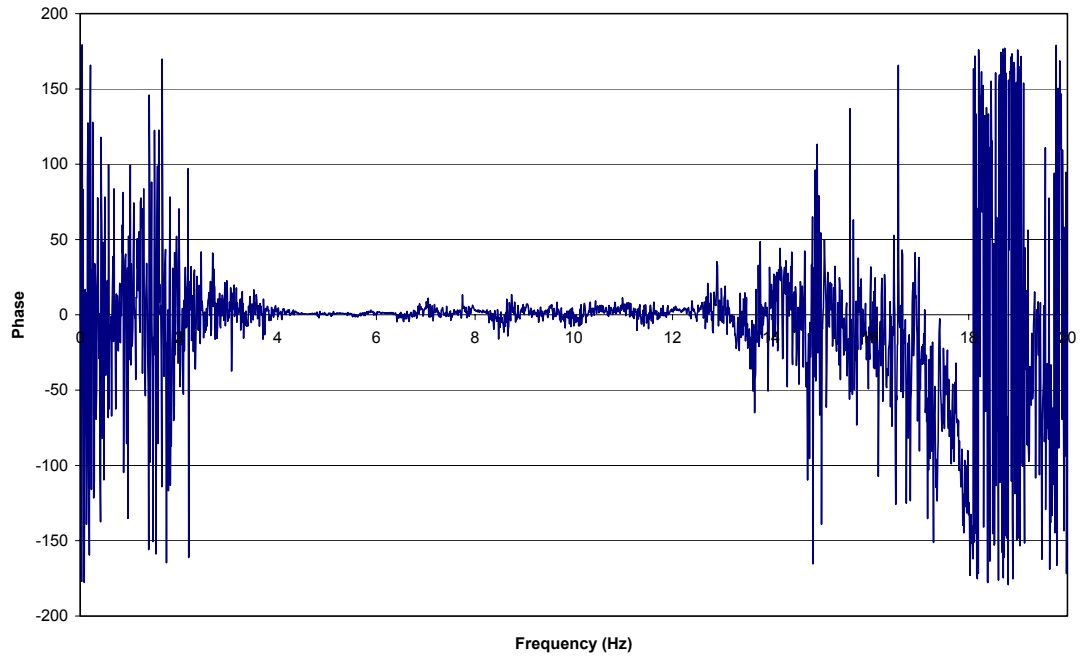


**Figure A.8 Cross spectrum for gage (4) with respect to gage (3)**

Cross Spectra of Gage 6 w.r.t. Gage 3

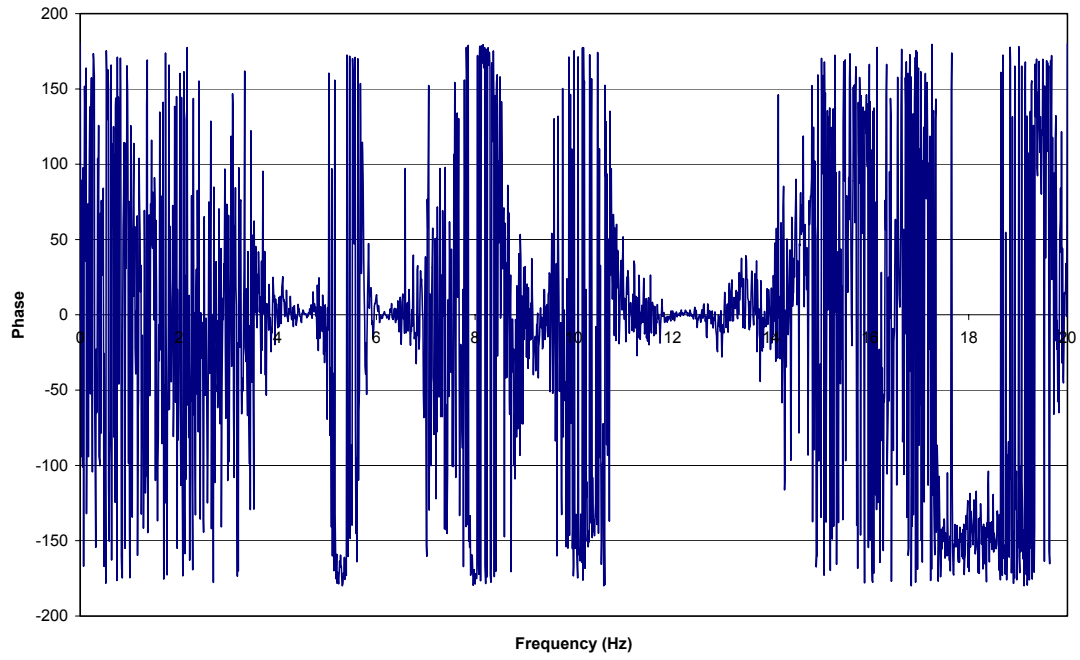


**Figure A.9 Cross spectrum for gage (6) with respect to gage (3)**

## **APENDIX B**

**Table B.1 South Junction Box Trunk Cable Wire Pair Designations**

**South Junction Box Trunk Cables**

<b>TS1</b>	<b>Gage</b>	<b>Pair Excit/Grnd</b>	<b>Input Pair (H/L)</b>	<b>Pair Shunt Cal.</b>
	S15T	BK G	W G	R O
	S15B	Y G	G O	BR G
	S19T	R W	BK O	BK W
	S19B	BK BR	W BL	R G
	S31B	Y BK	R Y	R BR
	SDUM	BL BK	Y W	R BK
	S32B	O BL	Y BL	BL BR
	S33B	R BL	G BL	O W
<b>TS2</b>	<b>Gage</b>	<b>Pair Excit/Grnd</b>	<b>Input Pair (H/L)</b>	<b>Pair Shunt Cal.</b>
	S34B	G BL	W G	R O
	S35T	O G	G Y	BR G
	S35B	W BL	W Y	BR W
	SCOU	BR BK	R BR	R Y
	S36B	O W	BL Y	BL BR
	S37B	BK G	O BL	BL BK
	S38B	BK Y	R BK	BK W
	S39T	R G	R BL	O BK
<b>TS3</b>	<b>Gage</b>	<b>Pair Excit/Grnd</b>	<b>Input Pair (H/L)</b>	<b>Pair Shunt Cal.</b>
	S39B	BK W	W Y	BR W
	V35T	O G	BR G	N/A
	V35B	BL G	Y G	N/A
	D15	G W	R f R W	N/A
	D31	O BK	W f RW	N/A
	D33	R O	BR f R BR	N/A
	D35	BK BR	R f R BR	N/A
	D37	R Y	BL f O BL	N/A
	D39	BK Y	O f O BL	N/A
	A25	R G	BL f BL W	N/A
	A31	R BK	W f BL W	N/A
	A35X	BL BR	Y f BL Y	N/A
	A39	O W	BL f BL Y	N/A
	A45	BK G	R f BL R	N/A
T35	N/A	BL BK	N/A	

<i>Wire Pair Color Legend</i>	
<b>R - red</b>	<b>BK - black</b>
<b>BL - blue</b>	<b>O - orange</b>
<b>BR - brown</b>	<b>W - white</b>
<b>Y - yellow</b>	<b>G - green</b>

**Table B.1 continued**

<b>TS4</b>	<b>Gage</b>	<b>Pair Excit/Grnd</b>	<b>Input Pair (H/L)</b>	<b>Pair Shunt Cal.</b>
	TCOU	N/A	Y W	N/A
	TD35	N/A	BR BL	N/A
	T39	N/A	Y BL	N/A
	A35Y	Shared	G f G BR	N/A
	RCOU	BK G	BK R	N/A
	R35	BL BK	O W	N/A
	R39	BL O	Y R	N/A

**Table B.2 North Junction Box Trunk Cable Wire Pair Designations**

**North Junction Box Trunk Cables**

<b>TN1</b>	<b>Gage</b>	<b>Pair Excit/Grnd</b>	<b>Input Pair (H/L)</b>	<b>Pair Shunt Cal.</b>
	S55T	W O	W BR	Y BL
	S55B	Y W	BL W	BL BR
	S59T	R G	R BR	R BK
	S59B	G O	BL BK	G BK
	S61B	BK W	W R	G BR
	S63B	O BK	G W	Y BK
	S65T	O BL	Y R	R BR
	S65B	BL G	BK BR	Y G
	T65	N/A	R O	N/A
<b>TN2</b>	<b>Gage</b>	<b>Pair Excit/Grnd</b>	<b>Input Pair (H/L)</b>	<b>Pair Shunt Cal.</b>
	S67B	Y BL	W O	W BR
	S69T	O BL	BL BR	R Y
	S69B	G O	W Y	W BL
	S75T	Y G	G W	BL G
	S75B	BK BL	Y BK	W BK
	S79T	BL R	BR G	R G
	S79B	O BK	W R	BK R
	V55	R O	BR R	N/A
	V65	G BK	BR BK	N/A

<i>Wire Pair Color Legend</i>	
<b>R - red</b>	<b>BK - black</b>
<b>BL - blue</b>	<b>O - orange</b>
<b>BR - brown</b>	<b>W - white</b>
<b>Y - yellow</b>	<b>G - green</b>

**Table B.2 continued**

<b>TN3</b>	<b>Gage</b>	<b>Pair Excit/Grnd</b>	<b>Input Pair (H/L)</b>	<b>Pair Shunt Cal.</b>
	D55	R O	BL f BL W	N/A
	D65	R G	W f BL W	N/A
	D75	G Y	O f G O	N/A
	A65X	Y W	G f G O	N/A
	A65Y	Shared	BL f BL O	N/A

**Table B.3 Cost of Instrumentation**

**Boards & Gages**

Item	Cost	Quantity	Total Cost	Quantity Purchased	Remaining Cost	Comments
CR9000X Base System	\$10,080.00	1	\$10,080.00	1	\$0.00	
CR9000X Enclosure	\$844.80	1	\$844.80	1	\$0.00	
Voltage Divider Time Module	\$43.20	2	\$86.40	2	\$0.00	
256 MB Memory Card	\$168.00	1	\$168.00	1	\$0.00	
Compact Flash Adapter	\$19.20	1	\$19.20	1	\$0.00	
9060 Excitation Board	\$1,270.00	3	\$3,810.00	3	\$0.00	
9050 Input Board	\$1,104.00	4	\$4,416.00	4	\$0.00	
Antialias Board	\$3,315.00	1	\$3,315.00	1	\$0.00	
Standard Strain Gages	\$19.35	40	\$774.00	40	\$0.00	
Bridge Completion Module	\$30.00	35	\$1,050.00	35	\$0.00	
Precision Resistors	\$12.15	16	\$194.40	16	\$0.00	
Vibrating Wire Gages	\$125.00	4	\$500.00	4	\$0.00	
String Pots	\$475.00	9	\$4,275.00	9	\$0.00	
Weldable Temp. Sensor (RTD)	\$17.96	5	\$89.81	5	\$0.00	
LST Network (RTD)	\$48.15	5	\$240.75	5	\$0.00	
Bondable Thermocouples	\$17.00	3	\$51.00	3	\$0.00	
Accelerometers (Uni-Axial)	\$249.00	4	\$996.00	4	\$0.00	
Accelerometers (Bi-Axial)	\$499.00	2	\$998.00	2	\$0.00	

**Table B.3 continued**

**Wires & Trays**

Item	Cost / ft	Feet of Wire/Tray	Total Cost	Quantity Purchased (ft)	Remaining Cost	Comments
Vibrating Wire Cable	\$0.51	95	\$48.45	95	\$0.00	
Trunk Cable (Type I)	\$2.59	990	\$2,564.10	990	\$0.00	
General Cable (3 Pair)	\$0.30	1200	\$360.00	1200	\$0.00	
General Cable (3 Conductor)	\$0.10	60	\$6.00	60	\$0.00	already in lab
Narrow Tray (2")	\$6.92	255	\$1,764.60	255	\$0.00	Includes Fasteners & Hangers
Wide Tray (4")	\$6.93	200	\$1,386.00	200	\$0.00	Includes Fasteners & Hangers

**Additional Costs**

Item	Cost	Quantity	Total Cost	Quantity Purchased	Remaining Cost	Comments
Gage Protection (VW)	\$105.00	1	\$105.00	1	\$0.00	One kit for all gages
Gage Protection (Foil)	\$2.72	45	\$122.40	45	\$0.00	
RTV - Silicon Protectant	\$52.55	5	\$262.75	5	\$0.00	
Epoxy	\$76.60	1	\$76.60	1	\$0.00	
Fiberglass Enclosure	\$695.08	1	\$695.08	1	\$0.00	Includes box & mounting panel
Junction Boxes	\$643.57	2	\$1,287.14	2	\$0.00	Includes mounting materials & seals
Platform	\$760.00	1	\$760.00	1	\$0.00	Includes lumber & new drill
Miscellaneous Tools	\$615.82	1	\$615.82	1	\$0.00	
Labeling	\$653.36	1	\$653.36	1	\$0.00	
Battery Backup / Voltage Regualtor	\$214.00	1	\$214.00	1	\$0.00	
12 Volt Power Supply	\$52.00	1	\$52.00	1	\$0.00	
String Pot Mount	\$1,159.28	1	\$1,159.28	1	\$0.00	Gage mount and steel cables

**Table B.3 continued**

**Lift Costs (45' Articulated Boom)**

<b>Item</b>	<b>Cost</b>	<b>Quantity</b>	<b>Total Cost</b>	<b>Quantity Purchased</b>	<b>Remaining Cost</b>	<b>Comments</b>
Week Rental (5 days)	\$1,361.00	1	\$1,361.00	1	\$0.00	without fuel
Month Rental (20 days)	\$3,025.00	1	\$3,025.00	1	\$0.00	
Lift Fuel Cost	\$284.24	1	\$284.24	1	\$0.00	
<b>Total =</b>			<b>\$48,711.18</b>		<b>\$0.00</b>	

## **APPENDIX C. SAMPLE CR9000 BASIC CODE**





```

Dim BBlk2ZeroUs (BREP2)                                'Block2 zero uStrain
variable
Units BBlk2ZeroMv = mVperV                             'Block2 default units
(mVperV)
Units BBlk2ZeroUs = uStrain                             'Block2 default units
(uStrain)
Units BBlk2 = uStrain                                  'Block2 default units
(uStrain)
' _____ Bridge Block 3 _____
Const BRNG3 = 1                                         'Block3 measurement range (T)
Const BREP3 = 2                                         'Block3 repetitions
Const BEXCIT3 = 5000                                   'Block3 excitation mVolts
Const BSETL3 = 30                                       'Block3 settling time
(usecs)
Const BINT3 = 40                                       'Block3 integration time
(usecs)
Const BGF3 = 2                                         'Block3 gauge factor
Const BCODE3 = -1                                       'Block3 gauge code for 1/4
bridge strain
Const BMULT3 = 1                                       'Block3 default multiplier
Const BOSET3 = 0                                       'Block3 default offset
Public BBlk3 (BREP3)                                   'Block3 dimensioned source
Dim GBlk3 (BREP3)                                       'Block3 dimensioned gauge
factor
Dim BBlk3ZeroMv (BREP3)                                'Block3 zero mV variable
Dim BBlk3ZeroUs (BREP3)                                'Block3 zero uStrain
variable
Units BBlk3ZeroMv = mVperV                             'Block3 default units
(mVperV)
Units BBlk3ZeroUs = uStrain                             'Block3 default units
(uStrain)
Units BBlk3 = uStrain                                  'Block3 default units
(uStrain)
' _____ Bridge Block 4 _____
Const BRNG4 = 0                                         'Block4 measurement range
(T)
Const BREP4 = 3                                         'Block4 repetitions
Const BEXCIT4 = 5000                                   'Block4 excitation mVolts
Const BSETL4 = 30                                       'Block4 settling time
(usecs)
Const BINT4 = 40                                       'Block4 integration time
(usecs)
Const BGF4 = 2                                         'Block4 gauge factor
Const BCODE4 = -1                                       'Block4 gauge code for 1/4
bridge strain
Const BMULT4 = 1                                       'Block4 default multiplier
Const BOSET4 = 0                                       'Block4 default offset
Public BBlk4 (BREP4)                                   'Block4 dimensioned source
Units BBlk4 = uStrain                                  'Block4 default units
(uStrain)

' _____ Vibrating Wire Constants _____

const CR9060_slot = 10                                ' Slot for CR9060 used in vbw
(coil and thermistor) excitations

```

```

' User selectable
' vbw #1 coil excitation is Switched Excitation ch 8
' vbw #2 coil excitation is Switched Excitation ch 9
' vbw #3 coil excitation is Switched Excitation ch 10
' vbw #4 coil excitation is Switched Excitation ch 11
' vbw #1 thermistor excitation is Switched Excitation ch 12
' vbw #2 thermistor excitation is Switched Excitation ch 13
' vbw #3 thermistor excitation is Switched Excitation ch 14
' vbw #4 thermistor excitation is Switched Excitation ch 15

const CR9052_slot = 11          ' Slot for CR9052 used in vbw
coil measurements

' User selectable
' vbw #1 is channel 1
' vbw #2 is channel 2
' vbw #3 is channel 3
' vbw #4 is channel 4

const CR9050_slot = 7          ' Slot for CR9050 used
in vbw thermistor measurement

' User selectable
' vbw #1 is single-ended channel 21
' vbw #2 is single-ended channel 23
' vbw #3 is single-ended channel 25
' vbw #4 is single-ended channel 27

' Scan and timing constants.
' This program alternates between slow (typically a 2.1 sec interval)
vbw measurements made in
' the vbw scan and fast measurements (typically a 250 Hz rate)
made in the fast scan.
' To determine the vbw coil resonant frequency, the vbw scan makes
very fast

```

```

'      (typically 16.667 kHz), raw measurements of the coil response
in a subscan
'      within the vbw scan.
'
'      Switching between the vbw scan and the fast scan is as follows.
'      First, N_vbw_scan consecutive vbw measurements are performed at a
rate equal to 1/T_vbw_scan.
'      T_vbw_scan is determined from lower-level parameters that set
the rate at which
'      the raw vbw responses are sampled (typically 16.667 kHz, or
1/60 usec).
'      Next, N_fast_scan consecutive fast measurements are performed at
a rate equal to 1/T_fast_scan.
'      Then, the program reverts back to the vbw scan, performing
N_vbw_scan consecutive vbw measurements.
'      Then, the program reverts back to the fast scan, performing
N_fast_scan consecutive fast measurements.
'      The process repeats until stopped by the user.

'      The time between blocks of vbw measurements (equivalently, blocks
of fast measurements) is
'      T_vbw_scan*(N_vbw_scan + N_overhead) +
T_fast_scan*(N_fast_scan + N_overhead)
'      Depending on the scan configuration, N_overhead will vary
between 0 and 3.

```

```

const T_vbw_subscan = 60      ' CR9052 measurement period of vbw
responses in usec.

```

```

'      Top of CR9052 passband = 1e6/(2.0*T_vbw_subscan)*(2.0/2.5)
'      60 usec allows vbw_f_hi up to 6.667 kHz
'      Do not change this unless lower-frequency vbw sensors are used.

```

```

const N_vbw_subscan = 35000
'      Number of vbw subscans/scan. This parameter determines T_vbw_scan.
const T_vbw_scan = T_vbw_subscan*N_vbw_subscan
'      VBW scan period in usec. Determines the time between consecutive
vbw
'      measurements while in the vbw scan.
'      Do not edit this directly!
'      Instead, modify N_vbw_subscan to give the desired vbw scan
rate.
const N_vbw_scan = 50

```

```

'const N_vbw_scan = 5                                ' Number of vbw
frequency measurements to perform before switching to

'   to the fast scan

' Hint: for debug, set to 0 to stay in vbw scan without switching to

'   to the fast scan.

' constants for vbw measurement #1
const vbw1_Vex_02p = 5000                            ' The zero-to-peak vibrating wire
excitation level in mV.

'   Suggested value: 5000 (giving 10 V peak to peak).
const vbw1_f_lo = 1400                               ' The minimum vbw coil
frequency in Hz.

'   The best performance is achieved by matching this parameter

'   to the expected frequency range of a particular vbw sensor.

'   Values below 450 Hz are not recommended.
const vbw1_f_hi = 3500                               ' The maximum vbw coil frequency in
Hz.

'   The best performance is achieved by matching this parameter

'   to the expected frequency range of a particular vbw sensor.

'   Values above 6.5 kHz are not recommended.

' If you are unsure of the frequency range for your specific

'   vbw sensor, then set

'   vbw_f_lo = 450

'   vbw_f_hi = 6500

' You will get unexpected results if vbw1_f_lo >= vbw1_f_hi
const vbw1_range = mV200 ' Analog range for CR9052 vbw measurements

'   Suggested value: mV200.

' Diagnostic thresholds, these are user-definable.
const vbw1_min_amp = 0.1                             ' vbw coil responses, in mV rms,
below this amplitude will turn on warning flag
const vbw1_max_amp = 40.0 ' vbw coil responses, in mV rms, above
this amplitude will turn on warning flag

'   responses above this limit may be the result of a noise source

```

```

const vbw1_min_snr = 1.5          ' vbw signal-to-maximum-noise
ratios below this limit will turn on warning flag
const vbw1_min_t_res = 1000      ' vbw thermistor measurements, in Ohms,
below this value will turn on warning flag
const vbw1_max_t_res = 4000      ' vbw thermistor measurements, in Ohms,
above this value will turn on warning flag

' constants for vbw measurement #2
' see above for full documentation
const vbw2_Vex_02p = 5000        ' zero-to-peak vbw
excitation in mV
const vbw2_f_lo = 1400           ' vbw low-frequency limit
in Hz
const vbw2_f_hi = 3500           ' vbw high-frequency limit
in Hz
const vbw2_range = mV200         ' input range to measure vbw
response
const vbw2_min_amp = 0.1         ' diagnostic threshold:
min vbw response in mV rms
const vbw2_max_amp = 40.0        ' diagnostic threshold:
max vbw response in mV rms
const vbw2_min_snr = 1.5         ' diagnostic threshold: min
signal-to-maximum-noise ratio
const vbw2_min_t_res = 1000      ' diagnostic threshold:
min thermistor resistance in Ohms
const vbw2_max_t_res = 4000      ' diagnostic threshold:
max thermistor resistance in Ohms

' constants for vbw measurement #3
' see above for documentation
const vbw3_Vex_02p = 5000        ' zero-to-peak vbw
excitation in mV
const vbw3_f_lo = 1400           ' vbw low-frequency limit
in Hz
const vbw3_f_hi = 3500           ' vbw high-frequency limit in Hz
const vbw3_range = mV200         ' input range to measure vbw
response
const vbw3_min_amp = 0.1         ' diagnostic threshold:
min vbw response in mV rms
const vbw3_max_amp = 40.0        ' diagnostic threshold: max vbw
response in mV rms
const vbw3_min_snr = 1.5         ' diagnostic threshold: min
signal-to-maximum-noise ratio
const vbw3_min_t_res = 1000      ' diagnostic threshold:
min thermistor resistance in Ohms
const vbw3_max_t_res = 4000      ' diagnostic threshold:
max thermistor resistance in Ohms

' constants for vbw measurement #4
' see above for documentation
const vbw4_Vex_02p = 5000        ' zero-to-peak vbw
excitation in mV
const vbw4_f_lo = 1400           ' vbw low-frequency limit
in Hz

```

```

const vbw4_f_hi      = 3500          ' vbw high-frequency limit
in Hz
const vbw4_range     = mV200        ' input range to measure vbw
response
const vbw4_min_amp   = 0.1          ' diagnostic threshold:
min vbw response in mV rms
const vbw4_max_amp   = 40.0         ' diagnostic threshold:
max vbw response in mV rms
const vbw4_min_snr   = 1.5          ' diagnostic threshold: min
signal-to-maximum-noise ratio
const vbw4_min_t_res = 1000         ' diagnostic threshold:
min thermistor resistance in Ohms
const vbw4_max_t_res = 4000         ' diagnostic threshold:
max thermistor resistance in Ohms

const ts_len = 4096          ' Vbw time-series length of vbw response
to sample and analyze.

'
'          Suggested value: 4096.
'May be increased for improved frequency precision or
'decreased for faster processing speed.
'Bechmarked performance with 1 mV rms vibrating wire response:

'      ts_len          frq precision
'      1024           1.6e-3 Hz
'      2048           0.8e-3 Hz
'      4096           0.4e-3 Hz

' _____ Vibrating Wire Variables _____

' variables to hold vbw measurements
public vbw_f_peak (4)          ' measured vbw coil
frequency, 4 channels
units vbw_f_peak = Hz          ' typical coil
frequencies are between 450 and 6500 Hz

public vbw_sig_str (4)        ' diagnostic: measured vbw
coil signal strength, 4 channels
units vbw_sig_str = mV rms     ' typical response
amplitudes are between 0.5 and 10 mV

public vbw_snr (4)            '
diagnostic: the ratio of the measured vbw signal strength to
units vbw_snr = no_units      ' the maximum noise (or
harmonic) component, 4 channels.

' Typical values are 3 to 60 (higher is better).

' Optimizing f_lo and f_hi will improve the measured f_peak and
' increase the snr.

public vbw_t_res (4)          '
measured vbw thermistor resistance

```

```

units vbw_t_res = Ohms                                     ' see vbw
manufacturer data sheets for typical values

public vbw_warning (4)                                    ' Warning
flags, 4 channels.
units vbw_warning = no_units                               ' Bit-wise OR of

' 1: measured vbw coil amplitude too low

' 2: measured vbw coil amplitude too high (likely an external
noise source)

' 4: measured vbw coil frequency "pegged" at low limit

' 8: measured vbw coil frequency "pegged" at high limit

' 16: saturated CR9052 input (likely an open coil or open coil
leads)

' 32: measured vbw signal-to-maximum-noise ratio (smnr) too low

'      (may be a noise source encroaching on the vbw response,
'      or f_lo and f_hi are poorly matched to the vbw sensor,
'      or the vbw sensor has excessive harmonic response)

' 64: measured thermistor resistance out of range

'      (likely an open or shorted thermistor or thermistor leads)

' housekeeping
public battv
units battv = V

'\\\\\\\\\\\\\\\\\\\\\\\\\\\\\\\\\\\\\\\\ ALIASES & OTHER VARIABLES //////////////////////////////////

Alias TBlk1(1) = TD35                                     'Assign alias name "TD35" to
TBlk1(1)
Alias TBlk1(2) = T65                                     'Assign alias name "T65" to
TBlk1(2)
Alias TBlk1(3) = TCOU                                    'Assign alias name "TCOU" to
TBlk1(3)
Alias VBlk1(1) = D15                                     'Assign alias name "D15" to
VBlk1(1)
Alias VBlk1(2) = D31                                     'Assign alias name "D31" to
VBlk1(2)
Alias VBlk1(3) = D33                                     'Assign alias name "D33" to
VBlk1(3)
Alias VBlk1(4) = D35                                     'Assign alias name "D35" to
VBlk1(4)
Alias VBlk1(5) = D37                                     'Assign alias name "D37" to
VBlk1(5)

```

Alias VBlk1 (6) = D39	'Assign alias name "D39" to
VBlk1 (6)	
Alias VBlk1 (7) = D55	'Assign alias name "D55" to
VBlk1 (7)	
Alias VBlk1 (8) = D65	'Assign alias name "D65" to
VBlk1 (8)	
Alias VBlk1 (9) = D75	'Assign alias name "D75" to
VBlk1 (9)	
Alias BBlk1 (1) = A25	'Assign alias name "A25" to
BBlk1 (1)	
Alias BBlk1 (2) = A31	'Assign alias name "A31" to
BBlk1 (2)	
Alias BBlk1 (3) = A35X	'Assign alias name "A35X" to
BBlk1 (3)	
Alias BBlk1 (4) = A35Y	'Assign alias name "A35Y" to
BBlk1 (4)	
Alias BBlk1 (5) = A39	'Assign alias name "A39" to
BBlk1 (5)	
Alias BBlk1 (6) = A45	'Assign alias name "A45" to
BBlk1 (6)	
Alias BBlk1 (7) = A65X	'Assign alias name "A65X" to
BBlk1 (7)	
Alias BBlk1 (8) = A65Y	'Assign alias name "A65Y" to
BBlk1 (8)	
Alias BBlk2 (1) = S15T	'Assign alias name "S15T" to
BBlk2 (1)	
Alias BBlk2 (2) = S15B	'Assign alias name "S15B" to
BBlk2 (2)	
Alias BBlk2 (3) = S19T	'Assign alias name "S19T" to
BBlk2 (3)	
Alias BBlk2 (4) = S19B	'Assign alias name "S19B" to
BBlk2 (4)	
Alias BBlk2 (5) = S31B	'Assign alias name "S31B" to
BBlk2 (5)	
Alias BBlk2 (6) = S32B	'Assign alias name "S32B" to
BBlk2 (6)	
Alias BBlk2 (7) = S33B	'Assign alias name "S33B" to
BBlk2 (7)	
Alias BBlk2 (8) = S34B	'Assign alias name "S34B" to
BBlk2 (8)	
Alias BBlk2 (9) = S35T	'Assign alias name "S35T" to
BBlk2 (9)	
Alias BBlk2 (10) = S35B	'Assign alias name "S35B" to
BBlk2 (10)	
Alias BBlk2 (11) = S36B	'Assign alias name "S36B" to
BBlk2 (11)	
Alias BBlk2 (12) = S37B	'Assign alias name "S37B" to
BBlk2 (12)	
Alias BBlk2 (13) = S38B	'Assign alias name "S38B" to
BBlk2 (13)	
Alias BBlk2 (14) = S39T	'Assign alias name "S39T" to
BBlk2 (14)	
Alias BBlk2 (15) = S39B	'Assign alias name "S39B" to
BBlk2 (15)	





```

        CallTable ZERO_1                'Go up and run Table ZERO_1
    Next Scan                          'Loop up for the next scan
    For I = 1 To BREP2                  'Do this 27 times
        BBlk2ZeroMv(I) = ZERO_1.BBlk2ZeroMv_Avg(I,1)
    Next I                              'Do it again
    Flag(1) = False                    'Reset Flag(1)
End Sub                                'End gauge zero measure
routine

Sub Zero2                              'Begin zero measure routine
    Count = 0                          'Set Count to zero
    Scan(PERIOD,P_UNITS,100,100)      'Scan 100 times. 1.00
Seconds.

BrFull(BBlk1ZeroMv(),BREP1,BRNG1,4,13,8,7,1,BEXCIT1,False,False,BSETL
1,BINT1,BMULT1,0)
    Count = Count + 1                 'Increment Count
    CallTable ZERO_2                  'Go up and run Table ZERO_2
    Next Scan                          'Loop up for the next scan
    For I = 1 To BREP1                'Do this 8 times
        OBlk1(I) = -ZERO_2.BBlk1ZeroMv_Avg(I,1)
    Next I                              'Do it again
    Flag(2) = False                  'Reset Flag(2)
End Sub                                'End gauge zero measure
routine

Sub Zero3                              'Begin zero measure routine
    Count = 0                          'Set Count to zero
    Scan(PERIOD,P_UNITS,100,100)      'Scan 100 times. 1.00
Seconds.

VoltDiff(VBlk1Zero(),VREP1,VRNG1,4,4,True,VSETL1,VINT1,MVBlk1(),0)
    Count = Count + 1                 'Increment Count
    CallTable ZERO_3                  'Go up and run Table ZERO_3
    Next Scan                          'Loop up for the next scan
    For I = 1 To VREP1                'Do this 9 times
        OVBk1(I) = -ZERO_3.VBlk1Zero_Avg(I,1)
    Next I                              'Do it again
    Flag(3) = False                  'Reset Flag(3)
End Sub                                'End gauge zero measure
routine

Sub Zero4                              'Begin zero measure routine
    Count = 0                          'Set Count to zero
    Scan(PERIOD,P_UNITS,100,100)      'Scan 100 times. 1.00
Seconds.

BrFull(BBlk3ZeroMv(),BREP3,BRNG3,7,6,9,14,2,BEXCIT3,False,True,BSETL3
,BINT3,BMULT3,BOSET3) 'Strain

StrainCalc(BBlk3ZeroUs(),BREP3,BBlk3ZeroMv(),0,BCODE3,GBBlk3(),0)
    Count = Count + 1                 'Increment Count
    CallTable ZERO_4                  'Go up and run Table ZERO_4
    Next Scan                          'Loop up for the next scan
    For I = 1 To BREP3                'Do this 2 times

```



```

' The vbw scan
  Scan (T_vbw_scan, uSec, 20, N_vbw_scan)

                                ' IMPORTANT! Do not put any executable code
here.
                                ' The next "include ..." line of code must
immediately follow the Scan instruction.

                                ' The code in vbwinc_4 excites the vbws and
measures the frequency of their peak response,
                                ' placing the result in vbw_f_peak. The
code in vbwinc_4 also measures the amplitude
                                ' of the vbw response and the signal-to-
maximum-noise ratio (used as diagnostics)
                                include "cpu:incnew.c9x"
                                'filemanage ("cpu:vbwinc_4.c9x", 32)

' _____ Flag Control _____
  If Status.MeasureTime(1,1) >= 20 Then 'Test measurement
    Flag(8) = True                      'Flag(8) if test condition
is true
  ElseIf Status.MeasureTime(1,1) > 30 Then 'Other condition
    Flag(8) = False                    'Flag(8) if test condition
is true
  End If                                'End of If
'-----
--
' vbw thermistor measurements
  BrHalf (vbw_t_res (1), 1, mV5000, CR9050_slot, 21, CR9060_slot,
12, 1, 5000, False, 1000, 16667, 1.0, 0.0)
  'vbw_t_res (1) = vbw_t_res (1) * 10e3/(1 - vbw_t_res (1))
' convert to ohms using 10k-ohm fixed resistor
  vbw_t_res (1) = vbw_t_res (1) * 350/(1 - vbw_t_res (1))
' convert to ohms using 350-ohm resistor

  BrHalf (vbw_t_res (2), 1, mV5000, CR9050_slot, 23, CR9060_slot,
13, 1, 5000, False, 1000, 16667, 1.0, 0.0)
  vbw_t_res (2) = vbw_t_res (2) * 10e3/(1 - vbw_t_res (2))
' convert to ohms using 10k-ohm fixed resistor

  BrHalf (vbw_t_res (3), 1, mV5000, CR9050_slot, 25, CR9060_slot,
14, 1, 5000, False, 1000, 16667, 1.0, 0.0)
  vbw_t_res (3) = vbw_t_res (3) * 10e3/(1 - vbw_t_res (3))
' convert to ohms using 10k-ohm fixed resistor

  BrHalf (vbw_t_res (4), 1, mV5000, CR9050_slot, 27, CR9060_slot,
15, 1, 5000, False, 1000, 16667, 1.0, 0.0)
  vbw_t_res (4) = vbw_t_res (4) * 10e3/(1 - vbw_t_res (4))
' convert to ohms using 10k-ohm fixed resistor

' _____ Temp Blocks _____
  ModuleTemp (TRef(), 1, 4, 20)
'RefTemp, CardCount, StartCard, Integrate

```

```
TCDiff (TBlk1 (), TREP1, TRNG1, 4, 1, TTYPE1, TRef (1), True, TSETL1, TINT1, TMULT  
1, TOSET1)
```

```
' _____ Foil Gages & RTD's _____
```

```
BrFull (BBlk3 (), BREP3, BRNG3, 7, 6, 9, 14, 2, BEXCIT3, False, True, BSETL3, BINT3  
, BMULT3, BOSET3) 'Strain  
StrainCalc (BBlk3 (), BREP3, BBlk3 (), BBlk3ZeroMv (), BCODE3, BGF3, 0)  
'Strain calculation
```

```
BrFull (BBlk4 (), BREP4, BRNG4, 7, 8, 9, 15, 1, BEXCIT4, False, False, BSETL4, BINT  
4, BMULT4, BOSET4) 'Strain  
StrainCalc (BBlk4 (), BREP4, BBlk4 (), 0, BCODE4, BGF4, 0) 'Strain  
calculation
```

```
' _____ String Pots _____
```

```
VoltDiff (VBlk1 (), VREP1, VRNG1, 4, 4, True, VSETL1, VINT1, MVBlk1 (), OVBlk1 ())
```

```
If Flag (3) Then Zero3 'Go do Zero3 subroutine  
If Flag (4) Then Zero4 'Go do Zero4 subroutine
```

```
' Conditionally set warning flags (this code is not  
required) to give "quick check" on measurements.
```

```
vbw_warning (1) = 0  
if (vbw_sig_str (1) < vbw1_min_amp) then vbw_warning (1) =  
1 or vbw_warning (1)  
if (vbw_sig_str (1) > vbw1_max_amp) then vbw_warning (1) =  
2 or vbw_warning (1)  
if (vbw_f_peak (1) = vbw1_f_lo) then vbw_warning (1) =  
4 or vbw_warning (1)  
if (vbw_f_peak (1) = vbw1_f_hi) then vbw_warning (1) =  
8 or vbw_warning (1)  
if (vbw_smnr (1) < vbw1_min_smnr) then vbw_warning (1) =  
16 or vbw_warning (1)  
if (vbw_f_peak (1) = nan) then vbw_warning (1) =  
32 or vbw_warning (1)
```

```
if ((vbw_t_res (1) < vbw1_min_t_res) or (vbw_t_res (1) >  
vbw1_max_t_res) or (vbw_t_res (1) = nan)) then  
vbw_warning (1) = 64 or vbw_warning (1)  
endif
```

```
vbw_warning (2) = 0  
if (vbw_sig_str (2) < vbw2_min_amp) then vbw_warning (2) =  
1 or vbw_warning (2)  
if (vbw_sig_str (2) > vbw2_max_amp) then vbw_warning (2) =  
2 or vbw_warning (2)  
if (vbw_f_peak (2) = vbw2_f_lo) then vbw_warning (2) =  
4 or vbw_warning (2)  
if (vbw_f_peak (2) = vbw2_f_hi) then vbw_warning (2) =  
8 or vbw_warning (2)
```

```

        if (vbw_smnr    (2) < vbw2_min_smnr) then vbw_warning (2) =
16 or vbw_warning (2)
        if (vbw_f_peak (2) = nan)           then vbw_warning (2) =
32 or vbw_warning (2)

        if ((vbw_t_res (2) < vbw2_min_t_res) or (vbw_t_res (2) >
vbw2_max_t_res) or (vbw_t_res (2) = nan)) then
            vbw_warning (2) = 64 or vbw_warning (2)
        endif

        vbw_warning (3) = 0
        if (vbw_sig_str (3) < vbw3_min_amp) then vbw_warning (3) =
1 or vbw_warning (3)
        if (vbw_sig_str (3) > vbw3_max_amp) then vbw_warning (3) =
2 or vbw_warning (3)
        if (vbw_f_peak  (3) = vbw3_f_lo)   then vbw_warning (3) =
4 or vbw_warning (3)
        if (vbw_f_peak  (3) = vbw3_f_hi)   then vbw_warning (3) =
8 or vbw_warning (3)
        if (vbw_smnr    (3) < vbw3_min_smnr) then vbw_warning (3) =
16 or vbw_warning (3)
        if (vbw_f_peak  (3) = nan)         then vbw_warning (3) =
32 or vbw_warning (3)

        if ((vbw_t_res (3) < vbw3_min_t_res) or (vbw_t_res (3) >
vbw3_max_t_res) or (vbw_t_res (3) = nan)) then
            vbw_warning (3) = 64 or vbw_warning (3)
        endif

        vbw_warning (4) = 0
        if (vbw_sig_str (4) < vbw4_min_amp) then vbw_warning (4) =
1 or vbw_warning (4)
        if (vbw_sig_str (4) > vbw4_max_amp) then vbw_warning (4) =
2 or vbw_warning (4)
        if (vbw_f_peak  (4) = vbw4_f_lo)   then vbw_warning (4) =
4 or vbw_warning (4)
        if (vbw_f_peak  (4) = vbw4_f_hi)   then vbw_warning (4) =
8 or vbw_warning (4)
        if (vbw_smnr    (4) < vbw4_min_smnr) then vbw_warning (4) =
16 or vbw_warning (4)
        if (vbw_f_peak  (4) = nan)         then vbw_warning (4) =
32 or vbw_warning (4)

        if ((vbw_t_res (4) < vbw4_min_t_res) or (vbw_t_res (4) >
vbw4_max_t_res) or (vbw_t_res (4) = nan)) then
            vbw_warning (4) = 64 or vbw_warning (4)
        endif

        ' fix me: convert vbw_f_peak (currently in Hz) to desired
engineering units.
        ' fix me: convert vbw_t_res (currently in Ohms) to temperature.

```

```

        calltable MONT                                ' store vbw results in output
table
        NextScan                                    ' end of the vbw
scan

    'Fast Scan Program

    Scan(PERIOD,P_UNITS,10,800000)                  'Scan once every 10
mSecs, non-burst
    '
    '----- Flag Control -----
    If Status.MeasureTime(1,1) >= 20 Then 'Test measurement
        Flag(8) = True                          'Flag(8) if test condition
is true
    ElseIf Status.MeasureTime(1,1) > 30 Then 'Other condition
        Flag(8) = False                          'Flag(8) if test condition
is true
    End If                                        'End of If
    '-----
    '----- Volt Blocks -----
    VoltDiff(VBlk1(),VREP1,VRNG1,4,4,True,VSETL1,VINT1,MVBlk1(),OVBlk1())
    '----- Bridge Blocks -----
    '-----
    'Channels 13 & 14 on Module # 4 Single Axis accels, Excitation
channels 7 and 8.

    BrFull(BBlk1(1),2,BRNG1,4,13,8,7,1,BEXCIT1,False,False,BSETL1,BINT1,B
MULT1,OBBlk1(1))
    '*****First Tri-axial Accel *****
    'Channels 1 and 2 on module # 5 (Tri-axial) ** Uses Continuous
Excitation 1 for both measurements.

    BrFull(BBlk1(3),2,BRNG1,5,1,8,1,2,BEXCIT1,False,False,BSETL1,BINT1,BM
ULT1,OBBlk1(3))

    *****
    'Channels 3 and 4 on module # 5 (single Axis), Excitation
channels 11 and 12.

    BrFull(BBlk1(5),2,BRNG1,5,3,8,11,1,BEXCIT1,False,False,BSETL1,BINT1,B
MULT1,OBBlk1(5))
    'Channels 5 and 6 on Module # 5 (Tri-Axial). Uses Continuous
excitation channel 2 for both measurements.

    BrFull(BBlk1(7),2,BRNG1,5,5,8,2,2,BEXCIT1,False,False,BSETL1,BINT1,BM
ULT1,OBBlk1(7))

    BrFull(BBlk2(),BREP2,BRNG2,5,7,8,15,3,BEXCIT2,False,True,BSETL2,BINT2
,BMULT2,BOSET2) 'Strain
    StrainCalc(BBlk2(),BREP2,BBlk2(),BBlk2ZeroMv(),BCODE2,BGF2,0)
    'Strain calculation

```



**APPENDIX D. ADDITIONAL PHOTOGRAPHS**





**Figure D.1 Interior of main fiberglass box**



**Figure D.2 Laptop with field monitor**



**Figure D.3 Foil strain gage with bridge completion module**



**Figure D.4 Protective gage enclosure**



**Figure D.5 Steel coupon with attached gages**

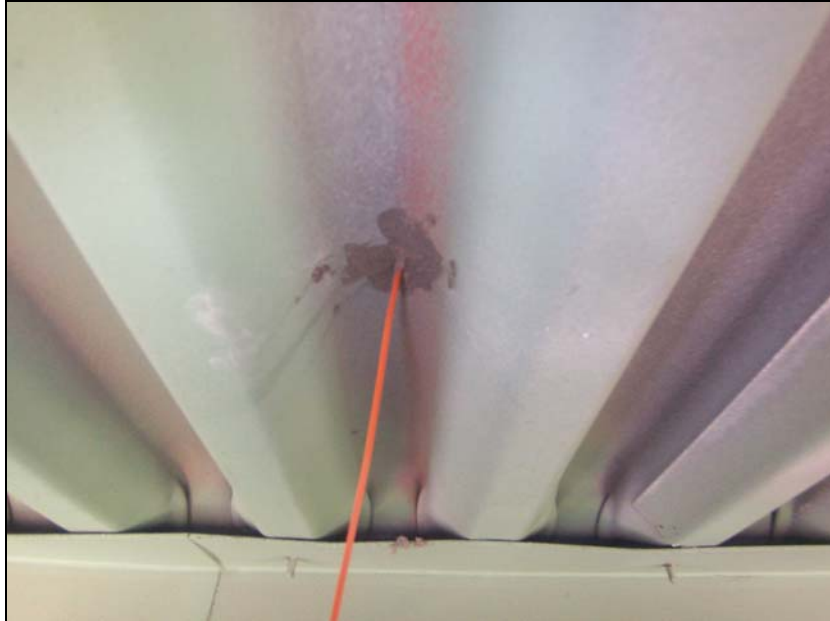


**Figure D.6 Thermocouple (TD35) grouted into deck**



**Figure D.7 Accelerometer epoxied to beam**



**Figure D.8 Enclosed vibrating wire and foil strain gages**



**Figure D.7 String pot mount**

## REFERENCES

- "AASHTO Standard Specifications for Highway Bridges, 17<sup>th</sup> Edition."  
(2002). American Association of State Highway and Transportation  
Officials.
- ABAQUS, (2006) Version 6.6-1. Providence, Rhode Island. ABAQUS, Inc.
- Aktan, E. A., Catbas, N. F., Grimmelsman, K. A., and Pervizpour, M.  
(2002) "Development of a Model Health Monitoring Guide for Major  
Bridges." Drexel Intelligent Infrastructure and Transportation  
Safety Institute.
- Burrell, Geoff. (2004) "Delaware's Smart Bridge Diagnostic Test." Research  
Experience for Undergraduates in Bridge Engineering. University of  
Delaware.
- Chajes, M. J., Shenton, H. W., Weston, D. F., Stuffle, T. J., and West, J.  
(2006) "Structural Health Monitoring of Delaware's Indian River Inlet  
Bridge." Proceedings of the 3<sup>rd</sup> International Conference on Bridge  
Maintenance, Safety and Management, IABMAS, Porto, Portugal.
- Chajes, M. J., McNeil, S., Shenton, H. W., Mertz, D. R., Attoh-Okine, N.,  
Kukich, D. S., Williams, M. R. (2006) "Long-Term Bridge  
Performance Program." The Center for Innovative Bridge  
Engineering.
- "CR9000X Measurement & Control System Training Manual." (2004)  
Revision 060204. Campbell Scientific Inc.
- FEMAP-Finite Element Modeling and Postprocessing. (2006) Version 9.2.0.  
UGS Corp.
- Lauzon, R. G. and DeWolf, J. T. (2003) "Connecticut's Bridge Monitoring  
Program; Making Important Connections Last." TR News 224  
January – February.

Liu, J. (2006) "Understanding Bridge Performance Through Integrated Modeling and Monitoring." Dissertation at University of Delaware.

Lynch, Mamie. (2003) "Delaware's First Smart Bridge." Research Experience for Undergraduates in Bridge Engineering. University of Delaware.

Nassif, H., Suksawang, N., Davis, J., Gindy, M., and Abu-Amra, T. (2006) "Field-Testing and Structural Monitoring of Doremus Avenue Bridge." Center for Advanced Infrastructure and Transportation, Rutgers University.

Wherum, Katie. (2006) "Dynamic Analysis of Delaware's Smart Bridge." Research Experience for Undergraduates in Bridge Engineering. University of Delaware.

# Delaware Center for Transportation University of Delaware Newark, Delaware 19716

## **AN EQUAL OPPORTUNITY/AFFIRMATIVE ACTION EMPLOYER**

The University of Delaware is committed to assuring equal opportunity to all persons and does not discriminate on the basis of race, creed, color, gender, age, religion, national origin, veteran or handicapped status, or sexual orientation in its educational programs, activities, admissions or employment practices as required by Title IX of the Educational Amendments of 1972, Section 504 of the Rehabilitation Act of 1973, Title VII of the Civil Rights Act of 1964, and other applicable statutes. Inquiries concerning Section 504 compliance and information regarding campus accessibility should be referred to the Americans with Disabilities Act (ADA) Coordinator, 831-4643, located at 413 Academy Street. Inquiries concerning Title VII and Title IX should be referred to the Office of the Assistant Vice President for Affirmative Action, 831-8735, located at 124 Hullihen Hall.

